EXTENDING THE ADJUSTING KINEMATIC PARAMETER APPROACH TO SPATIAL ROBOTIC MECHANISMS

A Thesis Submitted to the College of

Graduate Studies and Postdoctoral Studies

in Partial Fulfillment of the Requirements

for the Degree of Master of Science

in the Department of Mechanical Engineering

University of Saskatchewan

Saskatoon

By

ANIL BORUGADDA

Permission to Use

In presenting this thesis in partial fulfillment of the requirements for a Postgraduate degree from the University of Saskatchewan, I agree that the Libraries of this University may make it freely available for inspection. I further agree that permission for copying of this thesis in any manner, in whole or in part, for scholarly purposes may be granted by the professor or professors who supervised my thesis work or, in their absence, by the Head of the Department or the Dean of the College in which my thesis work was done. It is understood that any copying or publication or use of this thesis or parts thereof for financial gain shall not be allowed without my written permission. It is also understood that due recognition shall be given to me and to the University of Saskatchewan in any scholarly use which may be made of any material in my thesis.

Requests for permission to copy or to make other uses of materials in this thesis in whole or part should be addressed to:

Head of the Department of Mechanical Engineering

Engineering Building, University of Saskatchewan

57 Campus Drive, Saskatoon, Saskatchewan S7N5A9 Canada

OR

Dean of the College of Graduate and Postdoctoral Studies

116 Thorvaldson Building

110 Science Place

University of Saskatchewan

Saskatoon, Saskatchewan S7N5C9 Canada

Abstract

Robotic mechanisms refer to mechanisms that include at least one varying speed motor (servomotor). Dynamic balancing is a critical issue in designing robotic mechanisms, which affects their accuracy and efficiency. The force and moment from robotic mechanisms can cause vibration motions on the base, which is called the shaking force and shaking moment (including torque), while at the same time causes "small" vibration motions on the body of the mechanism. Several well-known methods are available for decades for balancing the shaking force and shaking moment, including the counter-weight (**CW**) method, add-of-spring (**AOS**) method, add-of-linkage (**AOL**), and adjusting kinematic parameter (**AKP**). AKP was developed in our group in 1990s; however, it is only applicable to planar robotic mechanisms.

The primary objective of this thesis was to extend AKP to spatial robotic mechanisms. A spherical parallel robotic mechanism, which is a type of spatial robotic mechanisms, was chosen as a study vehicle due to their relatively simple kinematics and dynamics. The mechanism is symmetrical consisting of three legs and one mobile platform, where the end effector (e.g., camera orienting device) is mounted. Each leg contains a lower link and an upper link. The equations for force balancing using AKP were derived by (1) writing the position vectors of the COM of mechanisms with respect to the reference point 'O', (2) writing the expression of the COM into a form that includes the time-dependent term (B_i) and the non time-dependent term (A_i), and (3) letting all B_i be zero, i.e., $B_i=0$, which are the equations for force balancing. Simulation was performed by the software called SPACAR developed at TU Delft. The simulation results showed the effectiveness of the AKP approach

to spatial spherical mechanisms for force balancing.

Another objective of this thesis was to use a combination of AKP and CW to dynamic balance a spherical mechanism. Dynamic balancing includes both force and moment balancing. The condition of moment balancing is that the total angular momentum of the mechanism with respect to a reference point remains zero. The equations for moment balancing were derived with three steps: (1) letting the angular momentum of the mechanism with respect to the center point to zero, which results into an equation; (2) writing this equation into a format that the time-dependent term (B_i) and the term (A_i) that includes the dimension and mass distribution are separate, like $A_0 + A_1B_1+A_2B_2+\ldots+A_nB_n$; (3) letting all A_i be zero. Using SPACAR as the simulation tool, the results again showed the effectiveness of the AKP approach to dynamic balancing for spatial mechanisms.

The final objective was to optimize the mechanism which has been force balanced for the minimal shaking moment; this problem is also called partial shaking moment balancing. The problem was formulated by considering the minimization of shaking moment as an objective function while the force balancing equation as a constraint equation. The variables in the optimization problem are the masses and lengths of the links. The function 'fmincon' from the MATLAB optimization toolbox was employed for solving this optimization problem. Using the SPACAR software, a simulation was conducted to show the effectiveness of the approach to partial dynamic balancing of spherical mechanisms.

The main contributions of this thesis lie in the field of balancing of robotic mechanisms.

Specifically, the thesis extends the AKP approach to spatial robotic mechanisms, which provides more means to balancing of spatial robotic mechanisms. It is noted that each method has its pros and cons, and a combined use of several methods is a strategy for improvement of the quality of balancing. For the first time, the thesis provides a combined AKP and CW approach to fully dynamic balancing a spatial mechanism. Finally, the thesis demonstrates the feasibility of optimal moment balancing when the mechanism has already been force balanced with the combined AKP and CW approach.

Acknowledgements

I thank my Supervisor Professor W.J. (Chris) Zhang for his motivation and unconditional support during my research work. He has been a source of inspiration encouraging me in accepting challenging work and reviewing literature with critical thinking. His discussions, reviews and comments helped me in completing meaningful research work. I also thank him for encouraging me to take up a short visiting research in China (sponsored by Mitacs), which had been a most memorable experience.

I also thank my advisory committee members Professor Travis Wiens, Chair and Professor Reza Fotouhi, member and the external examiner Professor Mohamed Boulfiza for their guidance and support. I thank them for their patience in reviewing my research work. I thank Prof. Changli Liu, Dr. Bing Zhang and the graduate students at the Complex systems research center laboratory at East China University of Science and Technology, Shanghai, for supporting my research work in China.

Financial support for this project was provided by the University of Saskatchewan in awarding the Robert R. Moffat Memorial Scholarship and John Spencer Middleton & Jack Spencer Gordon Middleton bursary. I acknowledge Mitacs-Canada and China-Scholarship-Council for awarding the Globalink research award and Canada-150-Study-Abroad-Graduate-Scholarship in supporting my research work in China. I thank my wife Krupa and daughter Avina for their help, patience, encouragement and many sacrifices made during my period of study. Lastly, I thank my mother for her support and encouragement till date.

Table of Contents

List of Tables

List of Figures

Nomenclature

Symbols

$\boldsymbol{c_i}$	Center of mass coordinates
I	Moment of inertia
$\boldsymbol{k}$	Radius of gyration
$\boldsymbol{L_i}$	Angular momentum
$\mathbf{l_i}$	Unit vector along axis
$\mathbf{l_{il}}$	Lower link length
$\boldsymbol{l^{\circ}_{1l}}$	Lower link unbalanced length
$\mathbf{l_{iu}}$	Upper link length
$\boldsymbol{l^{\circ}_{iu}}$	Upper link unbalanced length
M	Moment
m	Mass
$\mathbf{m_i}$	Unit vector along axis
$\mathbf{m_{il}}$	Lower link mass
$\boldsymbol{m_p}$	Mobile Platform mass
$\mathbf{m_{iu}}$	Upper link mass
$\mathbf{n_i}$	Unit vector along axis
$\boldsymbol{P_i}$	Point coordinates
$\mathbf{r_i}$	Position vector
$\mathbf{R_i}$	Rotation matrix
v	Velocity
$\boldsymbol{v_{iu}}$	AKP length adjustment

$\boldsymbol{\omega}$	Angular velocity
$\boldsymbol{\gamma_i}$	Semi-cone angle
$\boldsymbol{\beta_i}$	Driving link angle
$\boldsymbol{\theta_i}$	Joint angle
$\boldsymbol{\delta_i}$	Rotation angle
$\boldsymbol{\varphi}$	Tilt and torsion angle
$\boldsymbol{\sigma}$	Tilt and torsion angle
$\boldsymbol{\psi}$	Tilt and torsion angle

Abbreviations

ACRCM	Active counter-rotary counter-mass
AD	Auxiliary device
AKP	Adjusting kinematic parameter
AM	Angular momentum
COM	Center of mass
CRCW	Counter-rotary counterweight
CW	Counterweight
D-H	Denavit and Hartenberg
DOF	Degree of freedom
LIV	Linearly independent vectors
PRSM	Partially redundant servomotor
RDP	Redundancy design principle
RH	Right hand

RTC	Real-time controllable
RRR	Three revolute joints
SPR	Spherical parallel robot
T&T	Tilt and Torsion

Chapter 1

Introduction

1.1. Concept of Balancing

A machine or mechanism is composed of moving components. A mechanism is driven by a motor and is subjected to a load. A mechanism is a device that performs motion and force transfer (Zhang, 1994). Shaking force is defined as the force that is transmitted to the ground from the mechanism with its inertia only (Herder, 2001), and shaking moment is defined as the moment that is transmitted to the ground from the mechanism with its inertia only (Wijk, 2014). Force balancing is a process that cancels the shaking force (Ouyang, 2002), and dynamic balancing is a process that cancels both the shaking force and shaking moment (Wijk, 2014). When a mechanism is in operation, there is a driving torque on the motor. If the motor runs at constant speed, the torque has fluctuation, and vice versa. Torque balancing is a process to reduce the fluctuation (Sun, Zhang, Huang & Zhang, 2010; Sun, Zhang, Cheng & Zhang, 2011). In the following, the word 'balanced' refers to 'fully balanced' otherwise the word 'partially balanced' will be used.

Based on Newtonian dynamics, a force balanced mechanism will have a constant linear momentum (mv, where m is the mass, and v is velocity), and a dynamic balanced mechanism will have both a constant linear momentum and a constant angular momentum (I_ω, where I is the moment of inertia, and ω is the angular velocity) (Wijk, 2014).

There is another balancing situation, that is, the gravity of a mechanism does not contribute to the relative motion among components, or a mechanism can be at rest in any position or the gravity of a mechanism does not create any additional force or torque on linear motor or rotary motor. In

this situation, we say that a mechanism is static balanced (Wijk, 2014). It can be proved that a force balanced mechanism must be a static balanced mechanism, but reverse may not be correct. A narrative proof can be outlined as follows.

Proof: according to the definition of static balance, the gravitational potential energy is constant. This implies that the linear momentum in the y-direction is constant. Notice that a force-balanced mechanism has a constant linear momentum, that is, the linear moment in the y-direction is constant. However, a constant linear momentum in the y-direction does not imply a constant linear momentum in the x-direction. Hence, a static balanced mechanism may not be a force-balanced mechanism. **End of Proof**.

It is noted that a balance may be partial in that there are still shaking force, shaking moment on the ground but they are very small. A *partial balance* is thus defined as the minimization of shaking force, shaking moment, or torque fluctuation (Sun, Zhang, Cheng & Zhang, 2011).

1.2. Principle of Balancing

The principle of balance refers to the knowledge that explains why a mechanism is balanced. For force-balanced mechanisms, there are three principles and they are outlined below:

- ***Principle I****: the total shaking force is zero.*
- ***Principle II****: the total linear momentum is constant.*
- ***Principle III****: the total center of mass (COM) is stationery.*

In the above, Principle I drives Principle II, and Principle II derives Principle III. We denote these principles as **Principle I (II, III)-F** for brevity (where F: force) for subsequent discussions in this thesis. For dynamic balanced mechanisms, we denote the principle as **Principle I (II, III)-D**. There are three principles for dynamic-balanced mechanisms, and they are as follows:

- ***Principle I-D****: Principle I-F plus the total shaking moment being zero.*
- ***Principle II-D****: Principle II-F plus the total angular momentum being constant.*
- ***Principle III-D****: Principle III-F plus the total shaking moment being zero.*

1.3. Methods of Balancing

1.3.1. The Principle of Method

The method of balancing refers to how an unbalanced mechanism can be balanced by both external and internal means with a minimum effort. The minimum effort refers to the least number of interventions to be imposed on a mechanism. In literature, in most of the cases, the external means make sense except the work of Wijk (2014) in which they proposed a concept that is to design a mechanism which is balanced at the design stage and they called such a mechanism the inherent balanced mechanism. In this thesis, only the external means were concerned. The well-known methods that need some external means are:

- Counterweight (**CW**) approach,
- Adjusting kinematic parameter (**AKP**) approach,
- Auxiliary devices (**AD**) approach, and
- Hybrid approach (**CW and AKP**, **CW-AKP** for short).

The CW approach was first proposed using a four-bar linkage as an illustrative (Talbourdet & Shepler, 1941). The method was termed as 'static balancing method' but was used for the complete force balancing of linkage. It was proposed as a mathematical solution applicable to four-bar linkage. In this approach masses or counterweights were added to the linkage to make the center of mass of mechanism stationary (see Principle III-F before). However, many problems were associated with this approach. Based on the contour theorem proposed by Tepper and Lowen (1972), this method was used for the complete force balancing of planar mechanisms with revolute joints only.

The AKP approach was first proposed for real-time controllable (**RTC**) mechanisms (Wang, 2000). This approach was developed for a five-bar planar mechanism which has two degrees of freedom (**DOF**) but the approach is suitable to any mechanism with DOF greater than one and with one servomotor or programmable or varying speed motor. The force balance conditions were derived with the links, where their COM is located on its kinematic axis (Wang, 2000). Later, this approach was improved by Ouyang (2002) as the extended AKP approach, where links with their COM are possibly off their kinematic axis. In the extended AKP or just AKP without confusion in this document, the masses of revolute joints were also considered (Ouyang, 2002). It is noted that with the AKP approach, when the force balance condition is applied, the task specification (e.g., the end-effector trajectory following) will be changed, but using the controller of the servomotor this change can be annulled (Ouyang & Zhang, 2005). For this reason, this approach is suitable for the mechanism which has programmable motors or actuators. Further, using this approach both the reaction forces in revolute joints and the task performance (e.g., trajectory tracking) can be

improved (Ouyang, Zhang & Wu, 2002). The AKP approach will be explained in detail in Section 2.3 of this document.

A combined CW and AKP approach (called hybrid approach and CW-AKP for short) was reported in literature (Huang, Ouyang, Cheng & Zhang, 2010). The applicability of this approach is the same as that of the AKP approach. By hybrid, it is meant that the combination of CW and AKP makes them complimentary to each other (Ouyang, Zhang & Huang, 2016). A more detailed explanation of the CW-AKP approach will be provided in Section 2.3 of this document.

The AD approach is to add additional devices (instead of masses) to the original unbalanced mechanism. The devices may be passive or active. The latter case means a device that has its own actuator along with its controller. The AD approach can balance shaking force, shaking moment and driving torque fluctuation. The first method of the AD approach is to add a servomotor to the original unbalanced mechanism for complete dynamic balancing as proposed by Kochev (1992) but is not practically tested due to technical problems. The added servomotor is also "on-fly", indicating that it is not on the ground. This will increase the weight of the entire system considerably.

The so-called partially redundant servomotor (**PRSM**) method is another AD approach and was developed with a four-bar linkage driven by a servomotor (Sun, Zhang, Huang & Zhang, 2010; Sun, Zhang, Cheng & Zhang, 2011). The PRSM method does not add any new motor but makes use of the redundant capability (i.e., changing the velocity and thus changing the inertial force of a linkage) of a servomotor to perform partial balancing of mechanisms, which makes sense of

redundancy with the servomotor. Out of the three redundancy design principles (**RDP**) that was proposed by Sun et al. (2010) viz. physical redundancy (**RDP-I**), function redundancy (**RDP-II**) and "good" side role (**RDP-III**), the PRSM approach is based on RDP-III. It is noted that the redundant servomotor concept proposed by Nahon & Angeles (1989) for dynamic balancing is in fact a kind of RDP-II. Various other approaches used a servomotor for dynamic balancing, but they did not use the redundancy concept of RDP as proposed.

Another method of the AD approach is based on the idea of adding a counter-mass device and making it rotate and is called **ACRCM** (active counter-rotary counter-mass) by Wijk and Herder (2008). The counter-mass device is to balance the shaking force while its moment of inertia is used to balance shaking moment by actively controlling its angular velocity. For ACRCM, an additional actuator is needed to be installed on the base to control this angular velocity of the counter-mass device. This device rotates in the opposite direction of the motion of the links in the mechanism to achieve moment balancing.

Using Principle III-F along with the AD approach, a novel force balancing method for serial manipulators was proposed in the literature (Boisclair et al., 2017). In this method, the torque was generated from the Halbach cylinders fitted in the revolute joint between the links. The Halbach cylinders are integrated in the fabrication or retrofitted at a later stage. Some drawbacks with this approach include that building the magnet assembly is expensive, demagnetization is possible over time, and there is a difficulty in predicting the output torque produced by the Halbach cylinder. One benefit of AD is that it can balance mechanisms with loads[1].

[1] In the standard text of mechanisms, balancing only considers the inertia of a mechanism, so no load is considered. However, the load affects the shaking force and moment.

Five design strategies for force-balancing of the serial linkages with revolute joints were reviewed on a 1-DOF/ 3-DOF linkages (De Jong & Herder, 2015).

- **Strategy I**: CWs were re-positioned to match the shifted COM. For 1-DOF one prismatic joint and for 3-DOF linkage four prismatic joints were used for re-positioning. Strategies I, II & III used Principle II-F along with the CW approach.
- **Strategy II**: the revolute joint was re-positioned to match the shifted COM. For 1-DOF, two prismatic joints and for 3-DOF, twelve revolute joints were used.
- **Strategy III**: CWs were added or removed to maintain force balancing. For 3-DOF linkage mass was changed by pumping fluid to CWs from a stationary tank. The flow amount was calculated from the condition equations.
- **Strategy IV**: linkages were added at the base to form a reaction mechanism that moves the mechanism back into its force-balanced position. For 3-DOF mechanism, a 2-DOF reaction mechanism was added at the base. Strategies IV & V used principle II-F along with the AD approach.
- **Strategy V**: In this redundant joint strategy links were added to the mechanism to provide additional DOF. These DOF's were controlled such that COM remains stationary. For 1-DOF and 3-DOF, two additional redundant joints were added.

The main drawback with the AD method, especially active AD methods, includes design complexity, difficulty in implementation and large balancing mass, increased size of the balanced mechanism, and cost increase (due to additional components and operations at the singularity position, causing additional energy consumption).

1.3.2. Balancing Equations

The methods of balancing will need eventually to appear in form of mathematical equations. Such equations are called balancing equations. In the balancing equations, the variables capture the concepts in the methods. For instance, for the CW approach to force balancing, the added mass and its location need to be determined given a force-unbalanced mechanism, and thus variables are needed to represent the added mass and its location. By determining these variables in the balancing equations, one finds what and where to put an added mass. In short, the balancing equation describes the balancing method mathematically.

For example, it makes sense to develop the balancing equation for the CW approach along with the principle of balancing P-III-F. It is noted that the general goal of deriving the balancing equation is to make a minimum effort toward balancing. For instance, the minimal effort of the CW approach refers to the minimal number of links of a mechanism (force-unbalanced), on which external masses are added. Techniques can be developed to derive such a minimal number of equations, e.g., the technique called LIV (linearly independent vectors) method (Berkof & Lowen, 1969; Tepper & Lowen, 1972; Lowen, Tepper & Berkof, 1983). Details of the LIV technique can be found in Appendix A of this report. The minimal number of balancing equations is also called the sufficient balancing equation (Gosselin, 2008).

1.4. Research Motivation

The research motivation was represented by raising questions and why the raised questions make sense to the reduction of vibration of a machinery in general. A preliminary literature review (see

later for a more detailed discussion) has made the author with the following observations along with the questions.

Observation 1*: The AKP approach for force balancing is only for planar mechanisms*. A question (***Question 1***) thus arises whether the AKP approach can be extended to force balancing for spatial mechanisms.

Observation 2*: The AKP and hybrid approaches are currently valid only for force-balanced mechanisms.* A question (***Question 2***) is therefore raised whether AKP and hybrid AKP-CW can contribute to the moment balancing or partially moment balancing.

This thesis was motivated to answer the above two questions.

1.5. Research Objectives

Objective 1*: to develop the balancing equations for AKP for the force balancing of spherical mechanisms. It is noted that the spherical mechanism is chosen because it has a relatively simple kinematics and dynamics yet without missing the characteristics of spatial configurations. It is also noted that one servo-motor must be among the motors.*

Objective 2*: to develop the balancing equations for AKP-CW for dynamic balancing of spatial spherical mechanisms.*

Objective 3*: to extend the AKP-CW approach to optimizing the force-balancing of mechanisms with the goal that the shaking moment is made as minimum.*

Research with Objective 1 will answer Question 1, and research with Objectives 2-3 will answer Question 2.

1.6. Research Methodology for Objective 1

This thesis took the special Agile Eye manipulator as a case for the study. This is a parallel 3-RRR spherical mechanism with 3-DoF as shown in figure 1-1. The mechanism contains nine revolute joints in total and operates by using three servomotors fixed at its base. The end effector is a triangular plate with three ends, where each end is attached by one RRR linkage[2]. In this linkage all nine revolute joint axes meet at a common point which is its center of rotation (Gosselin & Hamel, 1994; Gosselin, Pierre & Gagne, 1996).

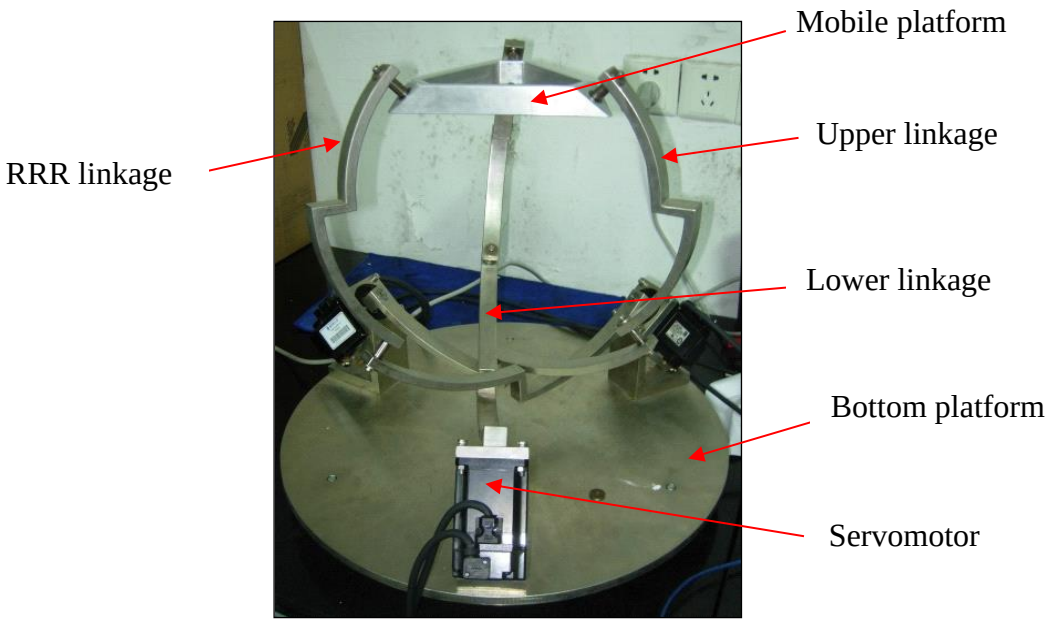

Figure 1-1. 3-RRR 3-DOF SPR mechanism at ECUST lab, China.

[2] In this thesis, the term 'mechanism' and the term 'linkage' are used interchangeably.

The AKP developed by Ouyang (2002) was taken as a starting point. The same procedure as derived for planar mechanisms was employed to develop the balancing equations for spatial spherical mechanisms.

1.7. Research Methodology for Objective 2

The CW-AKP developed by Huang (2010) was taken as a starting point. This approach was applied to derive the force balancing condition equations by writing the position vectors of the mechanism and its links and kinematic loop equation of the mechanism. For the moment balance condition equations, the angular momentum at the base point was considered and equations were written down. For verification, simulation was taken by using the CAD model of the spherical mechanism. The CAD model is similar to the model at the ECUST laboratory and is shown in figure 1-2. The simulation using SPACAR[3] was carried out to verify the approach by combining AKP and CW.

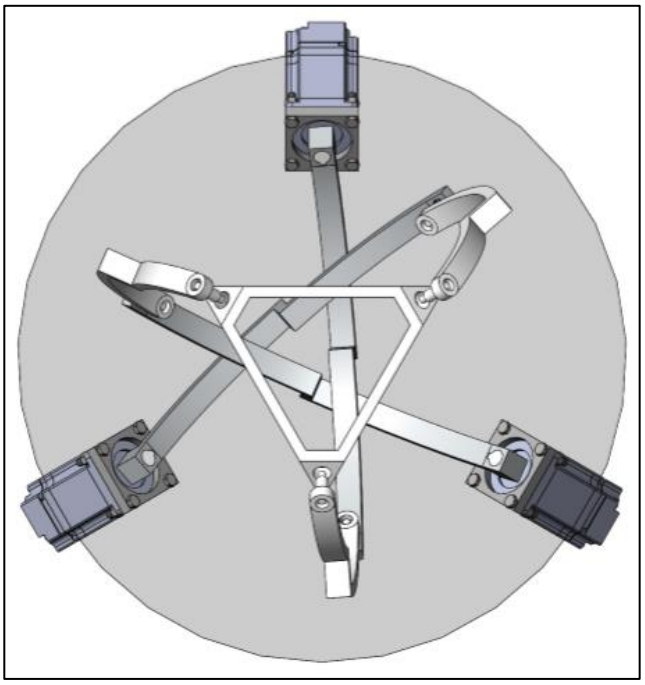

Figure 1-2. SPR top view using Solidworks v2015 CAD model.

[3] SPACAR is software for modeling and simulation of multi flexible body dynamics, developed at TU Delft.

1.8. Research Methodology for Objective 3

The CW-AKP developed by Huang (2010) was taken as a starting point; however, Huang (2010) did not perform optimization for moment balancing, which was performed in this thesis. The objective function in the optimization model was the shaking moment. The optimal variables were those in the balancing equation of the combined CW and AKP, e.g., the added masses along with their locations. For validation, the simulation by SPACAR on the spherical mechanism was taken. Figure 1-3 shows the CAD model in another position of the spherical mechanism for a better understanding.

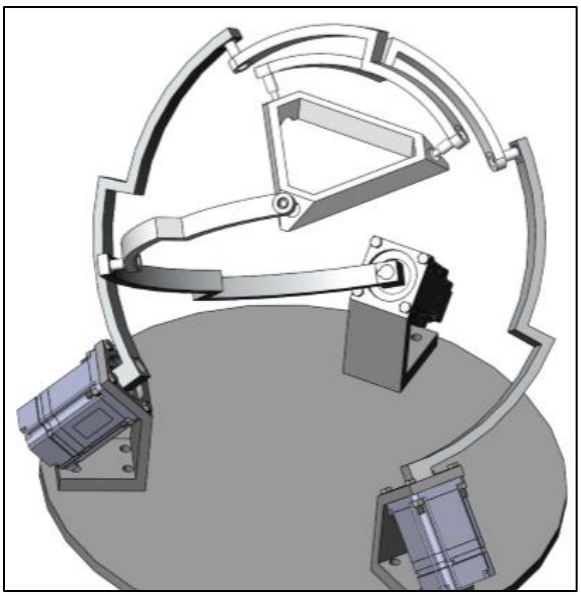

Figure 1-3. SPR CAD model in another orientation.

1.9. Organization of Thesis

This thesis is organized into six Chapters. Chapter 1 discusses the principles and methods of balancing, along with the research motivation, objectives and methodologies. Chapter 2 summarizes the literature and the preliminary work completed at our research laboratory. In Chapter 3, the force balancing equations for the spatial spherical mechanism are derived for AKP

approach. In Chapter 4, the dynamic balancing equations for the spatial spherical mechanism are derived for the combined AKP and CW approach. In Chapter 5, the force-balanced mechanism is optimised for minimizing the shaking moment. Finally, in Chapter 6 conclusions, contributions and future work are presented.

Chapter 2

Background and Literature Review

2.1. Introduction

In this chapter, the literature review of balancing of robotic mechanisms is presented. This also includes the previous work on the subject of force balancing of planar mechanisms in our research laboratory at the University of Saskatchewan. Finally, the literature review on the spherical parallel robotic mechanism is discussed.

2.2. Balancing of Spatial Mechanisms

In literature, there have been many methods developed for force balancing of spatial mechanisms. However, the situation remains to be that no one method can achieve the total balancing (i.e., dynamic balancing plus torque balancing) in a cost effective and power effective manner. A reasonable strategy may thus be to combine different methods by following the engineering hybridization principle (Zhang, Ouyang & Sun, 2010).

AKP has never been explored for dynamic balancing. As mentioned before, dynamic balancing of spatial mechanisms or robots is still based on the additional components to an unbalanced mechanism, which is costly (owing to the additional components).

A novel spatial mechanism called reactionless parallelepiped 3-DOF mechanism was designed using revolute joints, spherical joints, counter-rotating-gears and concentric multi-link spherical joints (Wu & Gosselin, 2005). A 6-DOF parallelepiped mechanism was also designed using three

3-DOF parallelepiped mechanisms as legs and limiting 1-DOF from each mechanism (Wu & Gosselin, 2005). Using Principle I-F along with the CW approach, force-balancing conditions were derived. The moment-balancing conditions were derived using Principle II-D along with the AD approach (counter-rotating gear mechanism was added). The mechanism was dynamic balanced for two case studies involving three rotary actuators. The first case study involves two actuators rotating along the z-axis and the third actuator along the x-axis. In the second case study, the three actuators rotate along the x, y and z axes, respectively. The balanced conditions were derived in both cases. Based on the balanced condition equations, optimization was performed, which takes the minimum of the weight of the link including the counterweight and its position vector as an objective function.

However, there are few drawbacks in the approach of (Wu & Gosselin, 2005). First, the weight of the mechanism increases still significantly, which may subsequently increase the driving torque. Second, the concentric multi-link spherical joint used in the mechanism is of distinctive design (Hamlin & Sanderson, 1994). The joints and driving motors will experience large payloads after balancing. The speed and the workspace of the mechanism will thus reduce. Finally, additional components added to form a parallelepiped structure increase the complexity of the whole mechanism, which challenges the practicality of the mechanism.

2.3. Previous Work in Our Research Laboratory

The AKP force balancing approach was proposed by Wang (2000) and Ouyang (2002) in the advanced engineering design laboratory (AEDL) at the University of Saskatchewan. The AKP approach is applicable to RTC (real time controllable) mechanisms with 2-DOF or more and with

one of them being a controllable varying speed motor. Using the AKP approach, force balancing can be achieved by adjusting the kinematic parameters (link length) of the RTC mechanism. The AKP approach is currently only applicable to planar robotic mechanisms.

A combined CW-AKP approach to force balancing of a five-bar closed-loop mechanism with 2-DOF (Huang, Ouyang, Cheng & Zhang, 2010) was developed. This hybrid approach used Principle I-F. This novel approach is based on the notion of intelligent mechatronics systems, specifically the hybrid engineering design principle (Zhang, Ouyang, Gupta & Sun, 2010). Using this approach, the trajectory tracking performance and workspace area are both improved as compared to using the AKP approach or CW approach alone.

For the five-bar mechanism, using the CW-AKP approach, two links out of five do not need to undergo any change, namely the base link and one of the coupler links. The remaining three links, two cranks and the remaining coupler need to be modified for force balancing. The modifications are based on the equations for force balancing, picked up from both the equation for AKP and equation for CW, accordingly. If a particular link is modified with the CW approach, mass re-distribution to this link will follow the corresponding equation for CW, and otherwise will follow the corresponding equation for AKP. In case study I, the first crank link was modified using the CW approach and the remaining crank and coupler links were modified using the AKP approach. This balancing scheme was represented as 1CW+3/4AKP. In case study II, the first crank link was modified using the AKP approach and remaining crank and coupler links were modified using the CW approach. This balancing scheme was represented as 1AKP+3/4CW. SPACAR / MATLAB

software was used for evaluation of different balancing schemes through simulation. The simulation results showed that the case I performed better than the case II.

A future study on the AKP approach was expected to apply it to spatial mechanisms and to examine its usefulness by combining with other balancing approaches for dynamic balancing. The optimization of the balancing parameters for partial moment balancing was also expected as a future study (Ouyang, Zhang & Huang, 2016).

2.4. Previous Work on Spherical Parallel Robot (SPR)

2.4.1. Kinematic Model and Workspace

Studies on kinematic modeling of SPR have been extensively reported. A solution for a SPR based on its direct or forward kinematics was studied by Innocenti (1993) and an eighth order polynomial equation was proposed as a solution. Eight positions of the SPR are possible for the given lengths of the links. The main drawback of the proposed solution is that it cannot be used in the real-time applications. Gosselin et al. (1996) studied the kinematics of a SPR named as the agile eye. This mechanism has a special geometry with 3-DOF. A closed form solution was found that can work for real-time applications. (Appendix B gives the relationship between curved link and straight link).

Another work on kinematic analysis of a SPR was proposed by Bai et al. (2009) and about the forward displacement analysis of SPR in particular. A closed-loop four-bar-linkage was formed with two upper links and one mobile platform. Using two such loops, the input-output trigonometric equations with joint angles were derived and solved using a semi graphical method.

Zhang et al. (2014) studied kinematic analysis of a SPR with a novel design. In this new design, on the fixed base platform, the three revolute joint axes are orthogonal to each other. Again on the mobile platform the three revolute joint axes were orthogonal to each other. Using this method, a shoulder joint design was proposed. More studies are required to further analyze this new design.

For research on SPR workspace, Bai (2010) studied the optimum design for a given workspace. The design parameters are its link dimensions and other constraints. A SPR that has the maximum rotational mobility was proposed using a numerical method of optimization but involved generalization of its equations. SPR embodiment design for maximum workspace using a novel approach was presented by Gao et al. (2015). Three principles for the embodiment design were proposed to reduce the interference between parts (or links) on a common motion plane, common plane with and without joint consideration. The embodiment design parameters considered are the link sizes, SPR radius and links layout. The proposed design showed that the loss in system workspace was less.

2.4.2. Force and Dynamic Balancing

Studies on force balancing of the parallel mechanisms have been reported. Arakelian et al. (2015) studied the force balancing of planar 3-RRR parallel manipulator using principle III-F and CW approach. Instead of complete force balancing the system using multiple CWs, only three CWs were added, resulting in the partial balancing of the system. The location of the counterweights is adjustable that makes this system adaptive in nature. Between an unbalanced and a partially balanced system, the shaking forces are shown to be reduced by 35%.

Acevedo et al. (2012) studied the dynamic balancing of 3-DOF spatial parallel manipulator using a combined CW and AD approach and principle III-D. A total of six counter-rotating-counterweights (CRCW) and three counterweights were added to the system. Results showed that complete force balance and partial moment balance were achieved. However, increase in the total mass of the balanced mechanism was not reported.

Gosselin (2008) studied dynamic balancing of the spatial parallel mechanism with six legs. The mechanism consists of six lower links, six upper links, a mobile platform and eighteen revolute joints. The links were straight and not curved. A total of thirty-six balancing conditions were derived and the force balancing was achieved by using the principle III-F and the CW approach.

Chapter 3

Force Balancing of the SPR using the AKP Approach

3.1. Introduction

In this chapter the first objective is set to derive the force balance equations for SPR using AKP. Ouyang (2002) derived the force balance equations for a planar closed-loop five bar mechanism using AKP and this will be extended to spatial mechanisms. SPACAR software will be used as simulation tool for the verification of the balancing.

3.2. Kinematic Model

Figure 3-1 shows the 3D CAD model of the mechanism using the software called Solidworks. The mechanism is symmetrical consisting of three legs and a mobile platform, where the end effector is mounted. Each leg contains a lower link and an upper link, where the lower link is driven by a servomotor, and the upper link is connected to the mobile platform. At each connection, the revolute joint provides rotation between two respective components about the joint axis, and all these axes intersect to one point (i.e., the center O of the sphere). In total, the mechanism consists of three servomotors, three lower links, three upper links, a mobile platform, nine revolute joints and a ground bottom platform. The three legs (each consisting of the lower link and upper link) are identical. The three servomotors are mounted on the bottom platform and distributed by an angle δ_i=120°. According to the definition of the spherical mechanism, there is a center point of spherical surface, denoted as O, and this point is stationery, acting as the common intersecting point for all the axes.

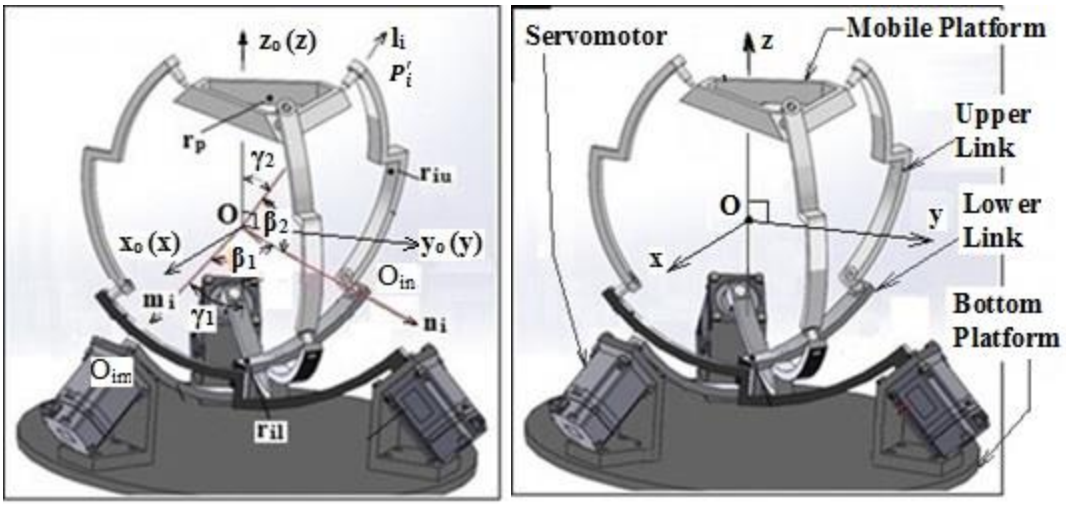

(a) (b)

Figure 3-1. SPR Mechanism (a) Kinematic Model (b) Components.

Now let us define the coordinate system for each link of the mechanism based on the D-H notation (see Appendix C). Denote *i* for the *i-th* leg (i=1-3), *u* for the upper link, *l* for the lower link, $\mathbf{l_i}$ for the joint axis between the upper link and the mobile platform, $\mathbf{n_i}$ for the joint between the upper link and lower link, and $\mathbf{m_i}$ for the joint axis between the lower link and bottom platform (figure 3-1a). Note that $\mathbf{l_i}$, $\mathbf{m_i}$, and $\mathbf{n_i}$ are unit vector, but no bold face is written for them in the following discussion for simplicity but without any confusion. Since all three legs are identical and they are symmetrical to the point O, it is sufficient to take one particular leg as an example to define the coordinate system for the mechanism. Consider initially the mobile platform is in a horizontal state. Define Z_o towards the mobile platform and perpendicular to it when it is at the initial time. Define X_o as perpendicular to Z_o and parallel to one of the three edges that connect three motors on the bottom platform. Define Y_o by following the right-hand rule to X_o and Z_o. The coordinate system O-$X_o(Y_o)Z_o$ is fixed to the ground and taken as a global reference coordinate system (figure 3-1b, O-X(Y)Z). A note is taken of that in the following only Z and X are defined, as Y can always be defined after X and Z.

Now let us define a local coordinate system to each moving link (lower link, upper link, and mobile platform). Define Z_{il} along the l_i axis, Z_{im} on the m_i axis, and Z_{in} on the n_i axis. X_{im} is defined as common perpendicular to Z_{im} and Z_{in}, and the origin of the frame[4] $X_{im}(Y_{im})Z_{im}$ is located at O, denoted as O_{im}. X_{in} is defined as common perpendicular to Z_{in} (n_i) and Z_{il} (l_i), and the origin of the frame $X_{in}(Y_{in})Z_{in}$ located at O, denoted as $O_{in.}$ θ_i is defined as the angle about Z_{i0} as well as Z_{im} (m_i), rotating from X_{i0} and X_{im} as shown in figure 3-2. Define X_{i0} such that it makes θ_i be zero initially (which corresponds that the mobile platform is at the horizontal state). The origin of the frame $X_{i0}(Y_{i0})Z_{i0}$ is O_{i0}, which is located at O.

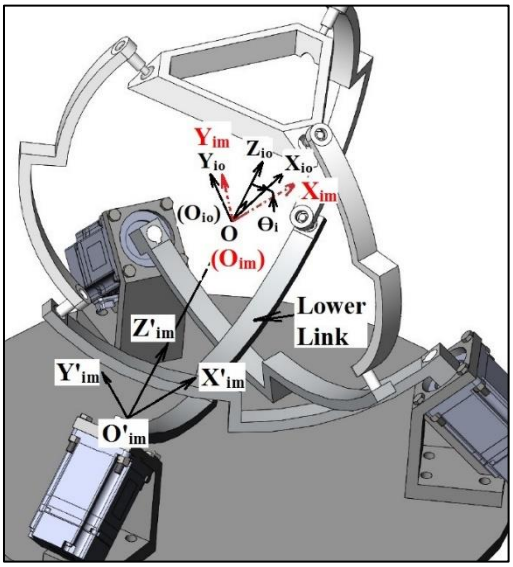

Figure 3-2. For SPR Mechanism defining Θ_i for lower link.

Define μ_i as the angle about Z_{in}, rotating from X_{im} to X_{in} as shown in figure 3-3. From the foregoing discussion, it can be seen that the frame O_{im}-$X_{im}Y_{im}Z_{im}$ is fixed on the lower link, and O_{in}-$X_{in}Y_{in}Z_{in}$ is fixed on the upper link. Both frames are moving frames, while the frame $X_{i0}Y_{i0}Z_{i0}$ is fixed to the ground, or stationary. For the convenience of later discussions, denote the frame O_{im}-$X_{im}Y_{im}Z_{im}$

[4] Frame means coordinate system in this document.

Frame L (moving frame), the frame O_{in}-$X_{in}Y_{in}Z_{in}$ **Frame U** (moving frame), and the frame O_{i0}-$X_{i0}Y_{i0}Z_{i0}$ **Frame O** (fixed frame).

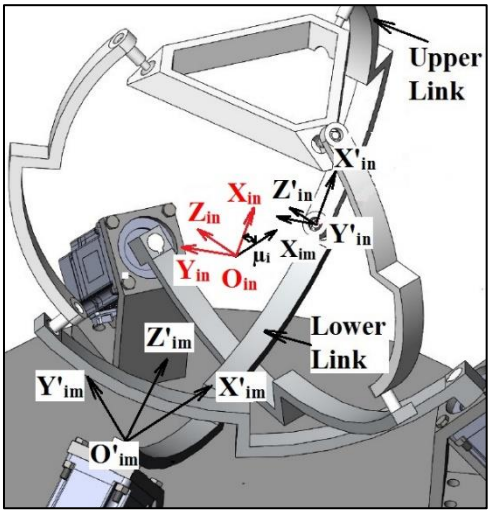

Figure 3-3. For SPR Mechanism defining μ_i for upper link.

Note that for each leg i, there are the foregoing three frames corresponding to it. Define a local coordinate system O'-X'Y'Z' on the mobile platform as shown in figure 3-4.

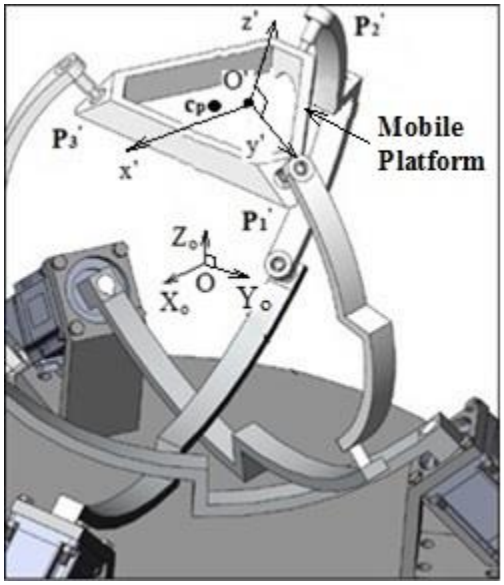

Figure 3-4. SPR Mechanism with mobile platform details.

Specifically, O' is on the center of the platform. The axis Z' is defined as perpendicular to the mobile platform. The Y' axis is defined as perpendicular to Z' axis and passes through the point P_i' of the mobile platform. For the convenience of later discussions, let us call this local coordinate system **Frame M** (moving frame). Let β_1 stand for the angle between the m_i (Z_{i0}) and n_i (Z_{in}); β_2 for the angle between n_i (Z_{in}) and l_i (Z_i); γ_1 for the angle between the Z_0 and m_i (Z_{i0}); γ_2 for the angle between Z' and l_i, as shown in figure 3-1. It is noted that these four angles are identical to each leg (containing the lower link and the upper link).

Table 3-1 shows the D-H parameters of the lower link and upper link (respectively), which are associated with the three coordinate systems: O_{i0}-$X_{i0}Y_{i0}Z_{i0}$ (**Frame O**), O_{im}-$X_{im}Y_{im}Z_{im}$ (**Frame L**) and O_{in}-$X_{in}Y_{in}Z_{in}$ (**Frame U**). Finally, there are additional three parameters that need to be mentioned, that is, d_{i0} (the distance between O_{il} and O_0), d_0 (the distance between the O and O' at the initial time), and θ_{i0} (the angle between the X_{im} and X_{i0}). It is noted that the local coordinate system (O'-X'Y'Z') on the mobile platform does not follow the D-H notation, and for this reason, the parameters that describe the relation of the frame O'-X'Y'Z' with respect to the other moving links are not included in Table 3-1.

Table 3-1. D-H parameters for the i^{th} lower and upper links (i: *i-th* leg, i = 1, 2 & 3)

	$\boldsymbol{\alpha_i}$	$\mathbf{a_i}$	$\mathbf{d_i}$	$\boldsymbol{\Theta_i}$
Lower Link	$\boldsymbol{\beta_1}$	0	0	$\boldsymbol{\Theta_i}$
Upper Link	$\boldsymbol{\beta_2}$	0	0	$\boldsymbol{\mu_i}$

3.3. Transformation Matrix

The transformation matrix for the lower link (i.e. from Frame O to Frame L) using the parameters from Table 1-1 can be written as

$$T_{li} = \begin{bmatrix} c\theta_i & -s\theta_i c\beta_1 & s\theta_i s\beta_1 & 0 \\ s\theta_i & c\theta_i c\beta_1 & -c\theta_i s\beta_1 & 0 \\ 0 & s\beta_1 & c\beta_1 & 0 \\ 0 & 0 & 0 & 1 \end{bmatrix} \tag{3.1}$$

The transformation matrix for the upper link (i.e. from Frame L to Frame U) using parameters from Table 1-1 can be written as

$$T_{ui} = \begin{bmatrix} c\mu_i & -s\mu_i c\beta_2 & s\mu_i s\beta_2 & 0 \\ s\mu_i & c\mu_i c\beta_2 & -c\mu_i s\beta_2 & 0 \\ 0 & s\beta_2 & c\beta_2 & 0 \\ 0 & 0 & 0 & 1 \end{bmatrix} \tag{3.2}$$

3.4. COM of SPR

In this section the COM of the SPR is written using the position vector and mass of the lower link, upper link and mobile platform.

3.4.1 Position Vector Representation

Lower Link:

- Using the lower link transformation matrix T_{li}, the rotation matrix (3×3), which is a subset of T_{li}, is formed by eliminating the fourth row and fourth column. The rotation matrix is denoted as $\boldsymbol{R_{li}}$.
- $^{o}\mathbf{r}_{il}$ represents the position of the COM of the lower link with respect to the global reference frame ($O\text{-}x_o y_o z_o$), see figure 3-5.

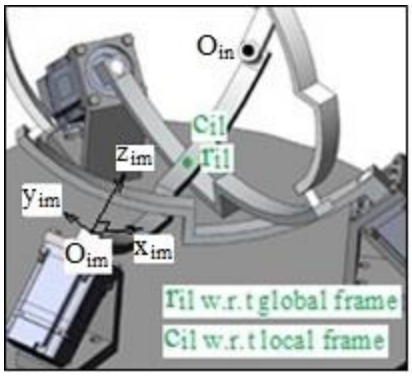

Figure 3-5. SPR Mechanism with lower link details.

Upper Link:

- Using the upper link transformation matrix T_{ui}, the rotational matrix (3×3), which is a subset of T_{ui}, is formed by eliminating the fourth row and fourth column. The rotational matrix is denoted as $\boldsymbol{R_{ui}}$.
- ${}^{o}\mathbf{r}_{iu}$ represents the position of the COM of the lower link with respect to the global reference frame ($O\text{-}x_o y_o z_o$), see figure 3-6.

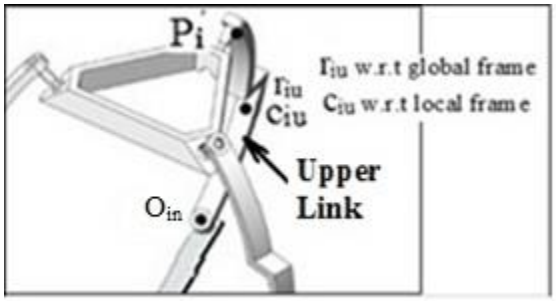

Figure 3-6. SPR Mechanism with upper link details.

Mobile Platform:

- The rotation matrix R_{li} represents the relationship of the mobile platform with reference to the global reference frame and is determined by the angles δ_i and γ_2. The details of R_{li} will be given later.

- The tilt and torsion rotation matrix R_{TT} used to represent the orientation of the mobile platform with respect to the global reference frame is determined by the angles φ, σ & ψ.
- The point ${}^{M}c_p$ represents the COM of the mobile platform w.r.t. its local coordinate frame (MP); see the previous discussion and figure 3.3.
- $^{O}\mathbf{r_p}$ represents the position of the COM of the mobile platform w.r.t. the global reference frame.

Equation for the Global COM of the mechanism:

- The global COM equation of the mechanism w.r.t. the reference frame $O\text{-}X_o(Y_o)Z_o$ is written using the position vectors $^{O}\mathbf{r_{il}}$, $^{O}\mathbf{r_{iu}}$ & $^{O}\mathbf{r_p}$ and its respective masses.
- Using principle III-F, the total center of mass (COM) remains stationery if all time dependent terms vanish.
- The force balance conditions are derived by equating the coefficients of the time dependent terms to be zero.
- The non-time-dependent terms r_x, r_y and r_z defines the stationary COM of the mechanism making the mechanism force balanced (Principle III-F).
- The masses of the nine revolute joints in the mechanism are ignored.

3.4.2 COM of the Lower Link

The rotation matrix for the lower link considering angle δ_i and equation (3.1) is given as

$$R_{li} = \begin{bmatrix} c\theta_i c\delta_i - s\theta_i s\delta_i & -s\theta_i c\beta_1 c\delta_i - c\theta_i c\beta_1 s\delta_i & s\theta_i s\beta_1 c\delta_i + c\theta_i s\beta_1 s\delta_i \\ c\theta_i s\delta_i + s\theta_i c\delta_i & -s\theta_i c\beta_1 s\delta_i + c\theta_i c\beta_1 c\delta_i & s\theta_i s\beta_1 s\delta_i - c\theta_i s\beta_1 c\delta_i \\ 0 & s\beta_1 & c\beta_1 \end{bmatrix} \quad (3.3)$$

where $\delta_i = \frac{2(i-1)\pi}{3}$ implies that the three motor axes are separated by 120°.

Let $^{O}\mathbf{r_{il}}$ be the position vector of the COM of the lower link with respect to the global reference frame (for i=1, 2 & 3) and l_{i1} represent link length, then $^{O}\mathbf{r_{il}}$ can be written as

$$\boldsymbol{^{o}r_{il}} = {}^{O}O_{im} + R_{mi}\ {}^{L}c_{i1} \tag{3.4}$$

$${}^{O}O_{im} = \begin{bmatrix} x_{io} \\ y_{io} \\ z_{io} \end{bmatrix} \qquad {}^{L}c_{i1} = \begin{bmatrix} x_{ic} \\ y_{ic} \\ z_{ic} \end{bmatrix} \quad \text{i=1, 2 \& 3} \tag{3.5}$$

where

- ${}^{O}O_{im}$ is the point of O_{im} (figure 3-1) w.r.t. the global reference frame;
- R_{li} is the rotation matrix of the local frame on the lower link w.r.t. the global reference frame;
- ${}^{L}c_{i1}$ represents the COM of the lower link with respect to the local frame (L).

By combining equations (3.3) (3.4) and (3.5), we can write

$$\boldsymbol{^{o}r_{il}} =$$

$$\begin{bmatrix} x_{io} + x_{ic}(c\theta_i c\delta_i - s\theta_i s\delta_i) - y_{ic}(s\theta_i c\beta_1 c\delta_i + c\theta_i c\beta_1 s\delta_i) + z_{ic}(s\theta_i s\beta_1 c\delta_i + c\theta_i s\beta_1 s\delta_i) \\ y_{io} + x_{ic}(c\theta_i s\delta_i + s\theta_i c\delta_i) - y_{ic}(s\theta_i c\beta_1 s\delta_i - c\theta_i c\beta_1 c\delta_i) + z_{ic}(s\theta_i s\beta_1 s\delta_i - c\theta_i s\beta_1 c\delta_i) \\ z_{io} + y_{ic}s\beta_1 + z_{ic}c\beta_1 \end{bmatrix} \tag{3.6}$$

Equation (3.6) represents the position vector of the COM of the lower link w.r.t. the global reference frame.

3.4.3. COM of the Upper Link

The rotation matrix for the upper link is given as

$$R_{ui} = \begin{bmatrix} c\mu_i & -s\mu_i c\beta_2 & s\mu_i s\beta_2 \\ s\mu_i & c\mu_i c\beta_2 & -c\mu_i s\beta_2 \\ 0 & s\beta_2 & c\beta_2 \end{bmatrix} \tag{3.7}$$

Let $\mathbf{^{O}O_{in}}$ be the intersecting point between lower link and upper link (for i=1, 2 & 3), see figure 3-1, and l_{iu} represent link length of the upper link, then $\mathbf{^{O}O_{in}}$ can be written as

$${}^{O}O_{in} = {}^{O}O_{im} + R_{li}I_{il} \tag{3.8}$$

where $I_{il} = \begin{bmatrix} 0 \\ 0 \\ l_{i1} \end{bmatrix}$ and l_{i1} is the distance between points O_{im} and O_{in} of the lower link. (3.9)

$$ {}^{O}O_{in} = \begin{bmatrix} x_{io} \\ y_{io} \\ z_{io} \end{bmatrix} + \begin{bmatrix} c\theta_i c\delta_i - s\theta_i s\delta_i & -s\theta_i c\beta_1 c\delta_i - c\theta_i c\beta_1 s\delta_i & s\theta_i s\beta_1 c\delta_i + c\theta_i s\beta_1 s\delta_i \\ c\theta_i s\delta_i + s\theta_i c\delta_i & -s\theta_i c\beta_1 s\delta_i + c\theta_i c\beta_1 c\delta_i & s\theta_i s\beta_1 s\delta_i - c\theta_i s\beta_1 c\delta_i \\ 0 & s\beta_1 & c\beta_1 \end{bmatrix} \begin{bmatrix} 0 \\ 0 \\ l_{i1} \end{bmatrix} $$

$$ = \begin{bmatrix} x_{io} + l_{i1}(s\theta_i s\beta_1 c\delta_i + c\theta_i s\beta_1 s\delta_i) \\ y_{io} + l_{i1}(s\theta_i s\beta_1 s\delta_i - c\theta_i s\beta_1 c\delta_i) \\ z_{io} + l_{i1} c\beta_1 \end{bmatrix} \quad (3.10) $$

Let $^{O}\mathbf{r_{iu}}$ be the position vector of the COM of the upper link with respect to the global reference frame (for i=1, 2 & 3) and l_{iu} represents the link length of the upper link, then $^{O}\mathbf{r_{iu}}$ can be written as

$$ \boldsymbol{^{o}r_{iu}} = {}^{O}O_{in} + R_{ui}\, {}^{L}c_{iu} \quad (3.11) $$

$$ {}^{L}c_{iu} = \begin{bmatrix} x_{iuc} \\ y_{iuc} \\ z_{iuc} \end{bmatrix} \quad \text{i=1, 2 \& 3} \quad (3.12) $$

where

- R_{ui} is the rotation matrix w.r.t. the global reference frame;
- ${}^{L}c_{iu}$ represents the COM of the upper link with respect to its local frame U.

By combining equations (3.7) (3.10) (3.11) and (3.12), we can obtain

$$ \boldsymbol{^{o}r_{iu}} = \begin{bmatrix} x_{io} + l_{i1}(s\theta_i s\beta_1 c\delta_i + c\theta_i s\beta_1 s\delta_i) + x_{iuc} c\mu_i - y_{iuc} s\mu_i c\beta_2 + z_{iuc} s\mu_i s\beta_2 \\ y_{io} + l_{i1}(s\theta_i s\beta_1 s\delta_i - c\theta_i s\beta_1 c\delta_i) + x_{iuc} s\mu_i + y_{iuc} c\mu_i c\beta_2 - z_{iuc} c\mu_i s\beta_2 \\ z_{io} + l_{i1} c\beta_1 + y_{iuc} s\beta_2 + z_{iuc} c\beta_2 \end{bmatrix} \quad (3.13) $$

Equation (3.13) represents the position vector of the COM of the upper link w.r.t. the global reference frame.

3.4.4. COM of the Mobile Platform

Point P_i' is the joint point between the upper link and the mobile platform. The joint is a revolute joint, and its joint axis is represented by the unit vector l_i and γ_2 is the semi-cone angle formed by the mobile platform (Gao et al., 2015).

The rotation matrix for the mobile platform considering angle δ_i is given as

$$R_{li} = \begin{bmatrix} c\delta_i & -s\delta_i c\gamma_2 & -s\delta_i s\gamma_2 \\ s\delta_i & c\delta_i c\gamma_2 & c\delta_i s\gamma_2 \\ 0 & -s\gamma_2 & c\gamma_2 \end{bmatrix} \tag{3.14}$$

where $\delta_i = \frac{2(i-1)\pi}{3}$ implies that the three motor axes are separated by 120°. (3.15)

Calculating Rotation Matrix R_{TT} using Tilt &Torsion (T&T) Angles (φ, σ, ψ)

Angles φ, σ & ψ are used to interpret the orientation of mobile platform (Bonev, 2002) with respect to the global reference frame at 'O'.

T&T rotation $R_{TT} = R_{TTz}(\varphi)R_{TTy}(\sigma)\, R_{TTz}(-\varphi)\, R_{TTz}(\psi)$

$$= R_{TTz}(\varphi)R_{TTy}(\sigma)\, R_{TTz}(\psi - \varphi) \tag{3.16}$$

Along the z-axis, the rotation (anticlockwise direction) is φ

$$R_{TTz}(\varphi) = \begin{bmatrix} cos\varphi & -sin\varphi & 0 \\ sin\varphi & \cos\varphi & 0 \\ 0 & 0 & 1 \end{bmatrix} \tag{3.17}$$

Along the y-axis, the rotation (clockwise direction) is σ

$$R_{TTy}(\sigma) = \begin{bmatrix} cos\sigma & 0 & sin\sigma \\ 0 & 1 & 0 \\ -sin\sigma & 0 & cos\sigma \end{bmatrix} \tag{3.18}$$

Along the z-axis along, φ & ψ (anticlockwise direction)

$$R_{TTz}(\psi - \varphi) = \begin{bmatrix} cos\,(\varphi - \psi) & -sin\,(\varphi - \psi) & 0 \\ sin\,(\varphi - \psi) & cos\,(\varphi - \psi) & 0 \\ 0 & 0 & 1 \end{bmatrix} \tag{3.19}$$

Combining equations (3.17), (3.18) & (3.19) yields to

$$R_{TT} = \begin{bmatrix} c\varphi c\sigma\, c(\varphi-\psi) - s\varphi s(\varphi-\psi) & -c\varphi c\sigma s(\varphi-\psi) - s\varphi c(\varphi-\psi) & c\varphi s\sigma \\ s\varphi c\sigma\, c(\varphi-\psi) + c\varphi s(\varphi-\psi) & -s\varphi c\sigma\, s(\varphi-\psi) + c\varphi c\,(\varphi-\psi) & s\varphi s\sigma \\ -s\sigma c(\varphi-\psi) & s\sigma s(\varphi-\psi) & c\sigma \end{bmatrix} \quad (3.20)$$

Let $^{O}\mathbf{r_p}$ be the position vector of the COM of the mobile platform with respect to the global reference frame and for i=1, 2 & 3

$$^{o}\boldsymbol{r_p} = {}^{O}O' + R_{li}\, R_{TT}\, {}^{M}c_p \quad (3.21)$$

$${}^{M}c_p = \begin{bmatrix} x_p \\ y_p \\ z_p \end{bmatrix}, \quad {}^{O}O' = \begin{bmatrix} x \\ y \\ z \end{bmatrix} \quad (3.22)$$

where

- ${}^{O}O'$ represents the origin of the frame M with respect to the global reference frame;
- $R_{li}R_{TT}$ represent the orientation of the mobile platform with respect to the global reference frame;
- ${}^{M}c_p$ represents the COM of the mobile platform with respect to Frame M.

Combining equations (3.14) & (3.19) yields to

$$R_{li}R_{TT} = \begin{bmatrix} c\delta_i & -s\delta_i c\gamma_2 & -s\delta_i s\gamma_2 \\ s\delta_i & c\delta_i c\gamma_2 & c\delta_i s\gamma_2 \\ 0 & -s\gamma_2 & c\gamma_2 \end{bmatrix}$$

$$\begin{bmatrix} c\varphi c\sigma\, c(\varphi-\psi) - s\varphi s(\varphi-\psi) & -c\varphi c\sigma si\, n(\varphi-\psi) - s\varphi c(\varphi-\psi) & c\varphi s\sigma \\ s\varphi c\sigma\, c(\varphi-\psi) + c\varphi s(\varphi-\psi) & -s\varphi c\sigma\, s(\varphi-\psi) + c\varphi c\,(\varphi-\psi) & s\varphi s\sigma \\ -s\sigma c(\varphi-\psi) & s\sigma s(\varphi-\psi) & c\sigma \end{bmatrix} \quad (3.23)$$

$$= \begin{bmatrix} R_{11} & R_{12} & R_{13} \\ R_{21} & R_{22} & R_{23} \\ R_{31} & R_{32} & R_{33} \end{bmatrix} \quad (3.24)$$

where

$$R_{11} = c\delta_i\big(c\varphi c\sigma\, c(\varphi-\psi) - s\varphi s(\varphi-\psi)\big) - s\delta_i c\gamma_2\big(s\varphi c\sigma\, c(\varphi-\psi) + c\varphi s(\varphi-\psi)\big) + s\delta_i s\gamma_2\, s\sigma c(\varphi-\psi)$$

$$R_{21} = s\delta_i\big(c\varphi c\sigma\, c(\varphi-\psi) - s\varphi s(\varphi-\psi)\big) + c\delta_i c\gamma_2\big(s\varphi c\sigma\, c(\varphi-\psi) + c\varphi s(\varphi-\psi)\big) - c\delta_i s\gamma_2(s\sigma c(\varphi-\psi))$$

$$R_{31} = -s\gamma_2\big(s\varphi c\sigma\, c(\varphi-\psi) + c\varphi s(\varphi-\psi)\big) - c\gamma_2(s\sigma c(\varphi-\psi))$$

$$R_{12} = -c\delta_i\big(c\varphi c\sigma si\, n(\varphi-\psi) - s\varphi c(\varphi-\psi)\big) + s\delta_i c\gamma_2(s\varphi c\sigma\, s(\varphi-\psi) + c\varphi c\,(\varphi-\psi)) - s\delta_i s\gamma_2(s\sigma s(\varphi-\psi))$$

$$R_{22} = -s\delta_i\big(c\varphi c\sigma si\, n(\varphi-\psi) - s\varphi c(\varphi-\psi)\big) - c\delta_i c\gamma_2(s\varphi c\sigma\, s(\varphi-\psi) + c\varphi c\,(\varphi-\psi)) + c\delta_i s\gamma_2(s\sigma s(\varphi-\psi))$$

$$R_{32} = s\gamma_2(s\varphi c\sigma\, s(\varphi-\psi) + c\varphi c\,(\varphi-\psi)\,) + c\gamma_2(s\sigma s(\varphi-\psi))$$

$$R_{13} = c\delta_i(c\varphi s\sigma) - s\delta_i c\gamma_2(s\varphi s\sigma) - s\delta_i s\gamma_2(c\sigma)$$

$$R_{23} = s\delta_i(c\varphi s\sigma) + c\delta_i c\gamma_2(s\varphi s\sigma) + c\delta_i s\gamma_2(c\sigma)$$

$$R_{33} = -s\gamma_2(s\varphi s\sigma) + c\gamma_2(c\sigma) \tag{3.25}$$

Combining equations (3.21), (3.22) & (3.23) yields to

$$\boldsymbol{{}^{o}r_{p}} = \sum_{i=1}^{3}\begin{bmatrix} x + R_{11}x_p + R_{12}y_p + R_{13}z_p \\ y + R_{21}x_p + R_{22}y_p + R_{23}z_p \\ z + R_{31}x_p + R_{32}y_p + R_{33}z_p \end{bmatrix} \tag{3.26}$$

Equation (3.26) represents the position vector of the COM of the mobile platform w.r.t. the global reference frame.

3.4.5 COM of the SPR

The global COM of the SPR w.r.t. the global reference frame is

$$\boldsymbol{Mr} = \boldsymbol{m_p\,{}^{o}r_p} + \sum_{i=1}^{3}(\boldsymbol{m_{il}\,{}^{o}r_{il}} + \boldsymbol{m_{iu}\,{}^{o}r_{iu}}) \tag{3.27}$$

where

- M is the total mass of SPR;
- m_p is the mass of the mobile platform;
- m_{iu} is the mass of the upper link of the ith leg;

- m_{il} is the mass of the lower link of the *i*th leg;
- $^{o}\boldsymbol{r_p}$ is the position vector of the COM of the mobile platform w.r.t. the global reference frame;
- $^{o}\boldsymbol{r_{iu}}$ is position vector of the COM of the upper link of the *i*th leg w.r.t. the global reference frame;
- $^{o}\boldsymbol{r_{il}}$ is position vector of the COM of the lower link of the *i*th leg w.r.t. the global reference frame.

and

$$M = m_p + \sum_{i=1}^{3}(m_{il} + m_{iu}) \tag{3.28}$$

Combining equations (3.6), (3.12), (3.26) and (3.27) and for i=1, 2 &3 yields to

$$\begin{aligned}
\mathrm{Mr} = \\
&[m_p \begin{bmatrix} x + R_{11}x_p + R_{12}y_p + R_{13}z_p \\ y + R_{21}x_p + R_{22}y_p + R_{23}z_p \\ z + R_{31}x_p + R_{32}y_p + R_{33}z_p \end{bmatrix} + \\
&m_{il} \begin{bmatrix} x_{io} + x_{ic}(c\theta_i c\delta_i - s\theta_i s\delta_i) - y_{ic}(s\theta_i c\beta_1 c\delta_i + c\theta_i c\beta_1 s\delta_i) + z_{ic}(s\theta_i s\beta_1 c\delta_i + c\theta_i s\beta_1 s\delta_i) \\ y_{io} + x_{ic}(c\theta_i s\delta_i + s\theta_i c\delta_i) - y_{ic}(s\theta_i c\beta_1 s\delta_i - c\theta_i c\beta_1 c\delta_i) + z_{ic}(s\theta_i s\beta_1 s\delta_i - c\theta_i s\beta_1 c\delta_i) \\ z_{io} + y_{ic}s\beta_1 + z_{ic}c\beta_1 \end{bmatrix} + \\
&m_{iu} \begin{bmatrix} x_{io} + l_{i1}(s\theta_i s\beta_1 c\delta_i + c\theta_i s\beta_1 s\delta_i) + x_{iuc}c\mu_i - y_{iuc}s\mu_i c\beta_2 + z_{iuc}s\mu_i s\beta_2 \\ y_{io} + l_{i1}(s\theta_i s\beta_1 s\delta_i - c\theta_i s\beta_1 c\delta_i) + x_{iuc}s\mu_i + y_{iuc}c\mu_i c\beta_2 - z_{iuc}c\mu_i s\beta_2 \\ z_{io} + l_{i1}c\beta_1 + y_{iuc}s\beta_2 + z_{iuc}c\beta_2 \end{bmatrix}]
\end{aligned} \tag{3.29}$$

Let $r = \begin{bmatrix} r_x \\ r_y \\ r_z \end{bmatrix}$ (3.30)

$$\begin{aligned}
Mr_x = \sum_{i=1}^{3}(m_p\big(x + R_{11}x_p + R_{12}y_p + R_{13}z_p\big) + m_{il}(x_{io} + x_{ic}(c\theta_i c\delta_i - s\theta_i s\delta_i) - \\
y_{ic}(s\theta_i c\beta_1 c\delta_i + c\theta_i c\beta_1 s\delta_i) + z_{ic}(s\theta_i s\beta_1 c\delta_i + c\theta_i s\beta_1 s\delta_i)) + m_{iu}(x_{io} + l_{i1}(s\theta_i s\beta_1 c\delta_i + \\
c\theta_i s\beta_1 s\delta_i) + x_{iuc}c\mu_i - y_{iuc}s\mu_i c\beta_2 + z_{iuc}s\mu_i s\beta_2)))
\end{aligned} \tag{3.31}$$

$$Mr_y = \sum_{i=1}^{3}(m_p(y + R_{21}x_p + R_{22}y_p + R_{23}z_p) + m_{il}(y_{io} + x_{ic}(c\theta_i s\delta_i + s\theta_i c\delta_i) - y_{ic}(s\theta_i c\beta_1 s\delta_i - c\theta_i c\beta_1 c\delta_i) + z_{ic}(s\theta_i s\beta_1 s\delta_i - c\theta_i s\beta_1 c\delta_i)) + m_{iu}(y_{io} + l_{i1}(s\theta_i s\beta_1 s\delta_i - c\theta_i s\beta_1 c\delta_i) + x_{iuc}s\mu_i + y_{iuc}c\mu_i c\beta_2 - z_{iuc}c\mu_i s\beta_2))) \quad (3.32)$$

$$Mr_z = \sum_{i=1}^{3}(m_p(z + R_{31}x_p + R_{32}y_p + R_{33}z_p) + m_{il}(z_{io} + y_{ic}s\beta_1 + z_{ic}c\beta_1) + m_{iu}(z_{io} + l_{i1}c\beta_1 + y_{iuc}s\beta_2 + z_{iuc}c\beta_2)) \quad (3.33)$$

Using Principle III-F, the global centre of mass of the mechanism is stationary (fixed) for any configuration of the mechanism if the coefficients of the time dependent terms are equated to zero. From equation (3.31), along the X-direction, equating the time dependent terms to zero leads to

$$\sum_{i=1}^{3}(m_p(x + R_{11}x_p + R_{12}y_p + R_{13}z_p) + m_{il}(x_{ic}(c\theta_i c\delta_i - s\theta_i s\delta_i) - y_{ic}(s\theta_i c\beta_1 c\delta_i + c\theta_i c\beta_1 s\delta_i) + z_{ic}(s\theta_i s\beta_1 c\delta_i + c\theta_i s\beta_1 s\delta_i))) + m_{iu}(l_{i1}(s\theta_i s\beta_1 c\delta_i + c\theta_i s\beta_1 s\delta_i) + x_{iuc}c\mu_i - y_{iuc}s\mu_i c\beta_2 + z_{iuc}s\mu_i s\beta_2) = 0 \quad (3.34)$$

Rearranging the terms,

$$\sum_{i=1}^{3}\big[xm_p + x_p m_p R_{11} + y_p m_p R_{12} + z_p m_p R_{13} + c\theta_i(m_{il}x_{ic}c\delta_i - m_{il}y_{ic}c\beta_1 s\delta_i + m_{il}z_{ic}s\beta_1 s\delta_i + m_{iu}l_{i1}s\beta_1 s\delta_i) - s\theta_i(m_{il}x_{ic}s\delta_i + m_{il}y_{ic}c\beta_1 c\delta_i - m_{il}z_{ic}s\beta_1 c\delta_i - m_{iu}l_{i1}s\beta_1 c\delta_i) + c\mu_i(x_{iuc}m_{iu}) - s\mu_i(y_{iuc}m_{iu}c\beta_2 - z_{iuc}m_{iu}s\beta_2)\big] = 0 \quad (3.35)$$

From equation (3.32), along the Y-direction, equating the time dependent terms to zero

$$\sum_{i=1}^{3}(ym_p + x_p m_p R_{21} + y_p m_p R_{22} + z_p m_p R_{23} + m_{il}(x_{ic}(c\theta_i s\delta_i + s\theta_i c\delta_i) - y_{ic}(s\theta_i c\beta_1 s\delta_i - c\theta_i c\beta_1 c\delta_i) + z_{ic}(s\theta_i s\beta_1 s\delta_i - c\theta_i s\beta_1 c\delta_i)) + m_{iu}(l_{i1}(s\theta_i s\beta_1 s\delta_i - c\theta_i s\beta_1 c\delta_i) + x_{iuc}m_{iu}s\mu_i + y_{iuc}m_{iu}c\mu_i c\beta_2 - z_{iuc}m_{iu}c\mu_i s\beta_2)) = 0 \quad (3.36)$$

Rearranging the terms

$$\sum_{i=1}^{3}\Big[ym_p + x_p m_p R_{21} + y_p m_p R_{22} + z_p m_p R_{23} + c\theta_i(m_{il}x_{ic}s\delta_i + m_{il}y_{ic}c\beta_1 c\delta_i - m_{il}z_{ic}s\beta_1 c\delta_i - m_{iu}l_{i1}s\beta_1 c\delta_i) + s\theta_i(m_{il}x_{ic}c\delta_i - m_{il}y_{ic}c\beta_1 s\delta_i + m_{il}z_{ic}s\beta_1 s\delta_i + m_{iu}l_{i1}s\beta_1 s\delta_i) + x_{iuc}m_{iu}s\mu_i + c\mu_i m_{iu}(y_{iuc}c\beta_2 - z_{iuc}s\beta_2)\Big] = 0 \tag{3.37}$$

From equation (3.33), along the Z-direction, equating the time dependent terms to zero

$$r_z = \sum_{i=1}^{3}(\, m_p\big(z + R_{31}x_p + R_{32}y_p + R_{33}z_p\big)) = 0 \tag{3.38}$$

Rearranging the terms

$$\sum_{i=1}^{3}\Big[zm_p + x_p m_p R_{31} + y_p m_p R_{32} + z_p m_p R_{33}\Big] = 0 \tag{3.39}$$

Gathering all the non-time dependent terms from equations (3.31), (3.32) & (3.33)

$$Mr_x = \sum_{i=1}^{3}(m_{il}x_{io} + m_{iu}\, x_{io}) \tag{3.40}$$

$$Mr_y = \sum_{i=1}^{3}(m_{il}y_{io} + m_{iu}y_{io}) \tag{3.41}$$

$$Mr_z = \sum_{i=1}^{3}(m_{il}(z_{io} + y_{ic}s\beta_1 + z_{ic}c\beta_1) + m_{iu}(z_{io} + l_{i1}c\beta_1 + y_{iuc}s\beta_2 + z_{iuc}c\beta_2)) \tag{3.42}$$

From equations (3.40), (3.41) & (3.42) the global COM will be stationary when

$$Mr_x = m_{1l}x_{1o} + m_{1u}x_{1o} + m_{2l}x_{2o} + m_{2u}x_{2o} + m_{3l}x_{3o} + m_{3u}x_{3o} \tag{3.43}$$

$$Mr_y = m_{1l}y_{1o} + m_{1u}y_{1o} + m_{2l}y_{2o} + m_{2u}y_{2o} + m_{3l}y_{3o} + m_{3u}y_{3o} \tag{3.44}$$

$$\begin{aligned} Mr_z = {} & m_{1l}(z_{1o} + y_{1c}s\beta_1 + z_{1c}c\beta_1) + m_{1u}(z_{1o} + l_{11}c\beta_1 + y_{1uc}s\beta_2 + z_{1uc}c\beta_2) \\ & + m_{2l}(z_{2o} + y_{2c}s\beta_1 + z_{2c}c\beta_1) + m_{2u}(z_{2o} + l_{21}c\beta_1 + y_{2uc}s\beta_2 + z_{2uc}c\beta_2) \\ & + m_{3l}(z_{3o} + y_{3c}s\beta_1 + z_{3c}c\beta_1) + m_{3u}(z_{3o} + l_{31}c\beta_1 + y_{3uc}s\beta_2 + z_{3uc}c\beta_2) \end{aligned} \tag{3.45}$$

From equations (3.43), (3.44) & (3.45), the global COM is stationary at the point (r_x, r_y & r_z)

$$r_x = \frac{m_{1l}x_{1o} + m_{1u}x_{1o} + m_{2l}x_{2o} + m_{2u}x_{2o} + m_{3l}x_{3o} + m_{3u}x_{3o}}{M} \tag{3.46}$$

$$r_y = \frac{m_{1l}y_{1o} + m_{1u}y_{1o} + m_{2l}y_{2o} + m_{2u}y_{2o} + m_{3l}y_{3o} + m_{3u}y_{3o}}{M} \tag{3.47}$$

$$\begin{aligned} r_z = {} & \frac{m_{1l}}{M}(z_{1o} + y_{1c}s\beta_1 + z_{1c}c\beta_1) + \frac{m_{1u}}{M}(z_{1o} + l_{11}c\beta_1 + y_{1uc}s\beta_2 + z_{1uc}c\beta_2) \\ & + \frac{m_{2l}}{M}(z_{2o} + y_{2c}s\beta_1 + z_{2c}c\beta_1) + \frac{m_{2u}}{M}(z_{2o} + l_{21}c\beta_1 + y_{2uc}s\beta_2 + z_{2uc}c\beta_2) \\ & + \frac{m_{3l}}{M}(z_{3o} + y_{3c}s\beta_1 + z_{3c}c\beta_1) + \frac{m_{3u}}{M}(z_{3o} + l_{31}c\beta_1 + y_{3uc}s\beta_2 + z_{3uc}c\beta_2) \end{aligned} \tag{3.48}$$

3.5 Loop Equation

It is noted that the above derived equations for force balancing is only the necessary condition. To reach both the necessary and sufficient condition, the loop equation for the mechanism needs to

be derived. There are two independent loop equations for the SPR according to the literature (Basu & Ghosal, 1997; Wang & Gosselin, 1999). The two loop equations are:

$$^{O}O_{im} + R_{li}l_{i1} + R_{ui}l_{iu} + R_{li}R_{TT}l_p = {}^{O}O_{3m} + R_{l3}l_{31} + R_{u3}l_{32} \quad \text{(For i=1 \& 2)} \tag{3.49}$$

The lengths of the lower link, upper link and mobile platform are

$I_{il} = \begin{bmatrix} 0 \\ 0 \\ l_{i1} \end{bmatrix}$ and l_{i1} is the length of the lower link (3.50)

$I_{iu} = \begin{bmatrix} 0 \\ 0 \\ l_{iu} \end{bmatrix}$ and l_{iu} is the length of the upper link (3.51)

$I_p = \begin{bmatrix} 0 \\ 0 \\ l_p \end{bmatrix}$ and l_p is the length of the mobile platform (3.52)

The two loops (loop-I, loop II) equations are:

$$^{O}O_{1m} + R_{l1}l_{11} + R_{u1}l_{12} + R_{mp1}R_{TT}l_p = {}^{O}O_{3m} + R_{l3}l_{31} + R_{u3}l_{32} \tag{3.53}$$

$$^{O}O_{2m} + R_{l2}l_{21} + R_{u2}l_{22} + R_{mp2}R_{TT}l_p = {}^{O}O_{3m} + R_{l3}l_{31} + R_{u3}l_{32} \tag{3.54}$$

For Loop-I, by combining equations (3.6), (3.12), (3.26), (3.50), (3.52), (3.53) & (3.54) and at $\delta_1 = 0, c\delta_1 = 1$ & $s\delta_1 = 0$ and at $\delta_3 = 240°, c\delta_3 = \frac{1}{2}$ & $s\delta_3 = \frac{\sqrt{3}}{2}$, we can obtain

$$^{O}O_{1m} + R_{l1}l_{1l} + R_{u1}l_{1u} + R_{mp1}R_{TT}l_p = \begin{bmatrix} x_{10} + s\theta_1 s\beta_1 l_{1l} + s\mu_1 s\beta_2 l_{1u} + R_{13}l_p \\ y_{10} - c\theta_1 s\beta_1 l_{1l} - c\mu_1 s\beta_2 l_{1u} + R_{23}l_p \\ z_{10} + c\beta_1 l_{1l} + c\beta_2 l_{1u} + R_{33}l_p \end{bmatrix} \tag{3.55}$$

$$^{O}O_{3m} + R_{l3}l_{3l} + R_{u3}l_{3u} = \begin{bmatrix} x_{3o} + \frac{s\theta_3 s\beta_1 l_{3l}}{2} + \frac{\sqrt{3}c\theta_3 s\beta_1 l_{3l}}{2} + s\mu_3 s\beta_2 l_{3u} \\ y_{3o} + \frac{\sqrt{3}s\theta_3 s\beta_1 l_{3l}}{2} - \frac{c\theta_3 s\beta_1 l_{3l}}{2} - c\mu_3 s\beta_2 l_{3u} \\ z_{3o} + c\beta_1 l_{3l} + c\beta_2 l_{3u} \end{bmatrix}$$

(3.56)

By combining equations (3.55) and (3.56) and equating the matrices, we obtain

$$l_{1u} = \frac{2(x_{3o} - x_{10}) + l_{3l}s\beta_1\left(s\theta_3 + \sqrt{3}c\theta_3 - 2s\theta_1\right) - 2R_{13}l_p}{2s\beta_2(s\mu_1 - s\mu_3)}$$

(3.57)

$$l_{1u} = \frac{2(y_{3o} - y_{10}) + l_{3l}s\beta_1\left(\sqrt{3}s\theta_3 - c\theta_3 + 2c\theta_1\right) - 2R_{23}l_p}{2s\beta_2(c\mu_3 - c\mu_1)}$$

(3.58)

$$z_{10} - z_{3o} = -R_{33}l_p \tag{3.59}$$

For Loop-II, by combining equations (3.6), (3.12), (3.26), (3.50), (3.51), (3.53) & (3.54) and at $\delta_2 = 120°, c\delta_2 = -\frac{1}{2}$ & $s\delta_2 = \frac{\sqrt{3}}{2}$ and at $\delta_3 = 240°, c\delta_3 = \frac{1}{2}$ & $s\delta_3 = \frac{\sqrt{3}}{2}$, we can obtain

$$^{o}O_{2m} + R_{l2}l_{2l} + R_{u2}l_{2u} + R_{mp2}R_{TT}l_p$$

$$= \begin{bmatrix} x_{2o} - \frac{s\theta_2 s\beta_1 l_{2l}}{2} + \frac{\sqrt{3}c\theta_2 s\beta_1 l_{2l}}{2} + s\mu_2 s\beta_2 l_{2u} + R_{13}l_p \\ y_{2o} + \frac{\sqrt{3}s\theta_i s\beta_1 l_{2l}}{2} + \frac{c\theta_i s\beta_1 l_{2l}}{2} - c\mu_2 s\beta_2 l_{2u} + R_{23}l_p \\ z_{2o} + c\beta_1 l_{2l} + c\beta_2 l_{2u} + R_{33}l_p \end{bmatrix}$$

(3.60)

By combining equations (3.56) and (3.60) and equating the matrices, we obtain

$$l_{2u} = \frac{2(x_{3o} - x_{2o}) + s\beta_1 l_{3l}\left(s\theta_3 + \sqrt{3}c\theta_3 - \sqrt{3}c\theta_2 + s\theta_2\right) - 2R_{13}l_p}{2s\beta_2(s\mu_2 - s\mu_3)}$$

(3.61)

$$l_{2u} = \frac{2(y_{3o} - y_{2o}) + s\beta_1 l_{3l}\left(c\theta_3 - \sqrt{3}s\theta_3 + \sqrt{3}s\theta_i + c\theta_i\right) + 2R_{23}l_p}{2s\beta_2(c\mu_2 - c\mu_3)}$$

(3.62)

$$z_{2o} - z_{3o} = -R_{33} l_p \tag{3.63}$$

Considering the two loops formed by the SPR's three legs as described above, equations (3.57), (3.58), (3.61), (3.62) give the upper link equation related to the lower link in terms of both time-dependent and non-time dependent terms. This equation is used in the modification of the upper link using the AKP approach.

3.6 Force Balancing Equations

From equations (3.35), (3.37) and (3.39), the force balancing equation are:

Equations 1 to 6

$$m_{1l} x_{1c} = 0 \tag{3.64}$$

$$m_{1l} y_{1c} c\beta_1 - m_{1l} z_{1c} s\beta_1 - m_{1u} l_{11} s\beta_1 = 0 \tag{3.65}$$

$$\sqrt{3} m_{2l} x_{2c} - m_{2l} y_{2c} c\beta_1 + m_{2l} z_{2c} s\beta_1 + m_{2u} l_{21} s\beta_1 = 0 \tag{3.66}$$

$$-m_{2l} x_{2c} - \sqrt{3} m_{2l} y_{2c} c\beta_1 + \sqrt{3} m_{2l} z_{2c} s\beta_1 + \sqrt{3} m_{2u} l_{21} s\beta_1 = 0 \tag{3.67}$$

$$\sqrt{3} m_{3l} x_{3c} + m_{3l} y_{3c} c\beta_1 - m_{3l} z_{3c} s\beta_1 - m_{3u} l_{31} s\beta_1 = 0 \tag{3.68}$$

$$m_{3l} x_{3c} - \sqrt{3} m_{3l} y_{3c} c\beta_1 + \sqrt{3} m_{3l} z_{3c} s\beta_1 + \sqrt{3} m_{3u} l_{31} s\beta_1 = 0 \tag{3.69}$$

Equations 7 to 9

$$x_{1uc} m_{1u} = 0 \tag{3.72}$$

$$x_{2uc} m_{2u} = 0 \tag{3.73}$$

$$x_{3uc} m_{3u} = 0 \tag{3.74}$$

Equations 10 to 12

$$y_{1uc}m_{1u}c\beta_2 - z_{1uc}m_{1u}s\beta_2 = 0 \quad (3.75)$$

$$y_{2uc}m_{2u}c\beta_2 - z_{2uc}m_{2u}s\beta_2 = 0 \quad (3.76)$$

$$y_{3uc}m_{3u}c\beta_2 - z_{3uc}m_{3u}s\beta_2 = 0 \quad (3.77)$$

Equations 13 to 15

$$xm_p = 0 \quad (3.78)$$

$$ym_p = 0 \quad (3.79)$$

$$zm_p = 0 \quad (3.80)$$

Equations 16 to 18

$$x_p m_p = 0 \quad (3.81)$$

$$y_p m_p = 0 \quad (3.82)$$

$$z_p m_p = 0 \quad (3.83)$$

3.7. AKP Approach for Lower and Upper Links

Considering the link shape, the COM of each link lies on its link axis as in the in-line situation as described by Ouyang (2002) and Ouyang & Zhang (2005). In such a case, only one end of the link pivot adjustment is required.

Let the lengths of the unbalanced lower link be $l^{\circ}_{1l}, l^{\circ}_{2l}$& l°_{3l} and that of the balanced lower links be $l_{1l,}l_{2l}$ & l_{3l}. The length of link adjustment is given by v_{il}.

$$l_{il} = l^{\circ}_{il} - v_{il} \quad (3.84)$$

$$v_{il} = l^{\circ}_{il} - l_{il} \quad (3.85)$$

Using equation (3.65), the lower link equation is written as

$$l_{11} = \frac{m_{1l} y_{1c} c\beta_1 - m_{1l} z_{1c} s\beta_1}{m_{1u} s\beta_1} \tag{3.86}$$

The length of link adjustment is given by v_{1l}

$$v_{1l} = l_{1l}^{\circ} - \mathrm{l_{1l}} = l_{1l}^{\circ} - \frac{m_{1l} y_{1c} c\beta_1 - m_{1l} z_{1c} s\beta_1}{m_{1u} s\beta_1} \tag{3.87}$$

Also $v_{1l} = v_{2l} = v_{3l} = v_{il}$ (because of the symmetry of the mechanism) (3.88)

Let the length of the unbalanced upper link be $l_{1u}^{\circ}, l_{2u}^{\circ}$ & l_{3u}° and balanced upper links be $\mathrm{l_{1u}}, \mathrm{l_{2u}}$ & $\mathrm{l_{3u}}$. The length of the link adjustment is given by v_{iu}

$$\mathrm{l_{iu}} = l_{iu}^{\circ} - v_{iu} \tag{3.90}$$

$$v_{iu} = l_{iu}^{\circ} - \mathrm{l_{iu}} \tag{3.91}$$

From equations (3.57) & (3.58), the balanced upper link length after neglecting the time dependent terms is given as

$$l_{3u} = \frac{2(x_{1o} - x_{30})}{2s\beta_2} \; or \; l_{3u} = \frac{2(y_{1o} - y_{30})}{2s\beta_2} \tag{3.92}$$

Using equation

$$l_{1u} = \; l_{2u} = l_{3u} = \frac{y_{1o} - y_{30}}{s\beta_2} \tag{3.93}$$

Using equation (3.93), the upper link length adjustment is given as

$$v_{1u} = v_{2u} = v_{3u} = l_{1u}^{\circ} - \frac{y_{1o} - y_{30}}{s\beta_2}$$

(3.94)

Equations (3.86), (3.87) & (3.88) give the lower link length adjustments and (3.93) & (3.94) give the upper link length adjustments.

3.8. Validation

Validation of the equations for force balancing of SPR with AKP was conducted through the simulation by using SPACAR. The SPACAR is the name of software for flexible multibody dynamics simulation available in MATLAB R2017a environment. The software was developed at the engineering mechanical automation laboratory at the University of Twente and was partly based on the initial development carried out at the Delft University of Technology. It is available for free download from its internet website https://www.utwente.nl/en/et/ms3/research-chairs/WAoud_niets_uit_wissen_aub/software/spacar/2015/download/.

Out of the five modules available in the SPACAR, the INVDYN module that is for the inverse manipulator dynamics module was used, in particular "mode=2 command" was used. The input specification is done at the end-effector, which includes the displacement, velocity and acceleration. The output motion (i.e., the motion at the actuators) is found by the software (Jonker, 2007). The SPR mechanism was defined using a data file (.dat), which is the input file to the software, containing specific SPACAR keywords and parameters (called SPACAR model). The input file was activated in MATLAB using the command 'spacar (mode,'filename') that was written as spacar (2, 'filename'). The elements used in the analysis were spatial HINGE and

BEAM elements. The SPACAR SPR model consists of nine hinge and nine beam elements for SPR.

The input file contains the details of kinematic data, dynamics data, inverse dynamics data, input data and data for SPAVISUAL, which is the visualization tool in SPACAR for displaying the simulation result. In the results file 'fxtot' command determines the reaction forces and moments that need to be examined. Appendix D gives the SPACAR input file. The specific SPR of figure 1-1 was used for this purpose; specifically, $\beta_1 = 90°$, $\beta_2 = 90°$, $\gamma_1 = 45°$ and $\gamma_2 = 60°$ (Guo et al., 2015).

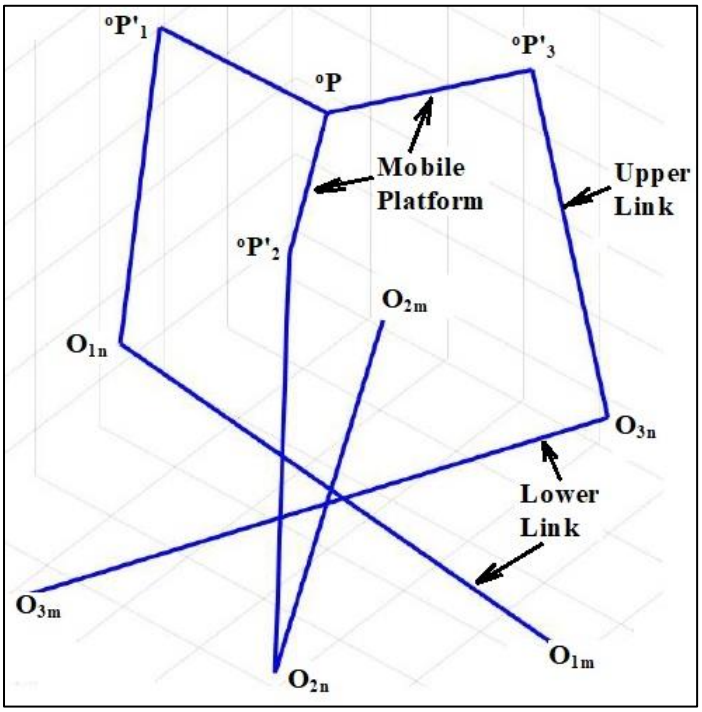

Figure 3-7. SPR mechanism linkage data.

In Table 3-2, rows 1 and 2 give details of the length and mass of the lower link. Rows 3, 4 and 5 show the values of the coordinate points $O_{1\mathrm{m}}$, $O_{2\mathrm{m}}$, $O_{3\mathrm{m}}$ considered with respect to the frame O.

Table 3-2. CAD data of SPR mechanism

S.No.	Unbalanced Linkage	Value	Units
1	Length (Lower Link)	313	Millimeters
2	Mass (Lower Link)	641.6	Grams
3	Point O_{1m}	(0.0, 162.1, -64.3)	X,Y,Z @ fixed frame O
4	Point O_{2m}	(-140.3, -81.1, -64.3)	X,Y,Z @ fixed frame O
5	Point O_{3m}	(140.3, -81.1, -64.3)	X,Y,Z @ fixed frame O
6	Length (Upper Link)	243	Millimeters
7	Mass (Upper Link)	483.5	Grams
8	Point O_{1n}	(-16.8, -149.3, -37.1)	X,Y,Z @ fixed frame O
9	Point O_{2n}	(129.8, 74.9, -37.1)	X,Y,Z @ fixed frame O
10	Point O_{3n}	(-129.8, 74.9, -37.1)	X,Y,Z @ fixed frame O
11	Length (Mobile Platform)	189.7	Millimeters
12	Mass (Mobile Platform)	313	Grams
13	Point ${}^{O}P_1'$	(0.0, -109.5, 202.5)	X,Y,Z @ fixed frame O
14	Point ${}^{O'}P_1'$ (x_1', y_1', z_1')	(0.0, -105.1, 86.1)	X,Y,Z @ local frame M
15	Point ${}^{O}P_2'$	(94.8, 54.8, 202.5)	X,Y,Z @ fixed frame O
16	Point ${}^{O'}P_2'$ (x_2', y_2', z_2')	(91.1, 52.6, 86.1)	X,Y,Z @ local frame M
17	Point ${}^{O}P_3'$	(-94.8, 54.8, 202.5)	X,Y,Z @ fixed frame O
18	Point ${}^{O'}P_3'$ (x_3', y_3', z_3')	(-91.1, 52.6, 86.1)	X,Y,Z @ local frame M
19	Point ${}^{O}P$	(0.0, 0.0, 0.202)	X,Y,Z @ fixed frame O
20	Length l_{ic}	123	Millimeters

The values are extracted using Solidworks CAD model of the SPR. These three points represent the positions of the three revolute joints that connect the servomotors with the lower links, respectively. Figure 3-7 shows the details of these points. Rows 6 and 7 give details of the length and mass of the upper link. Rows 8, 9 and 10 show the values of the coordinate points O_{1n}, O_{2n}, O_{3n} considered with respect to the frame O. These three points represent the positions of the three revolute joints that connect the lower links with the upper links respectively. Rows 11 and 12 give details of the length and mass of the mobile platform. Rows 13, 15 and 17 show the values of the coordinate points ${}^{O}P_1'$, ${}^{O}P_2'$, ${}^{O}P_3'$ considered with respect to the frame O. These three points represent the positions of the three revolute joints that connect the upper links with the mobile platform respectively. Rows 14, 16 and 18 show the values of the coordinate points ${}^{O'}P_1'$, ${}^{O'}P_2'$, ${}^{O'}P_3'$ considered with respect to the local frame M of the mobile platform. The points ${}^{O}P_1'$, ${}^{O}P_2'$, ${}^{O}P_3'$ and the points ${}^{O'}P_1'$, ${}^{O'}P_2'$, ${}^{O'}P_3'$ represent the three revolute joint points on the mobile platform, respectively, while the former points are considered with respect to the frame O and the latter with respect to the local frame M. Row 19 shows the position of the end effector in terms of its coordinate point ${}^{O}P$ considered with respect to the frame O. Row 20 gives the length of COM of the upper link considered from its intersecting point with the lower link.

The INVDYN module performs the inverse kinematics and dynamics and the inputs are represented by defining trajectory path and velocity profile. Aarts et al. (2011) describes the syntax for using the TRAJECT command. The trajectory path is described using five TRAJECT commands at four points (see Appendix D). For point ºP, as shown in figure 3-7, the velocity profile is specified using the TRAJECT. Two velocity profiles were defined, one at low speed and the other at high speed. Low speed in this thesis refers to the time for the end-effector to move

over the distance between the two neighboring TRAJECT points, 0.1 seconds in this case. The high speed in this thesis refers to the time for the end-effector to move over the distance between the two neighboring TRAJECT points, 0.03 seconds in this case.

According to the method of AKP as discussed before, both the lower link and the upper link were modified. Figure 3-8 shows the Spavisual diagram of SPACAR. The lower link was balanced by using equations (3.86), (3.87) & (3.88). Equations (3.87) and (3.88) give the link adjustment using AKP while equation (3.86) gives the value of the modified length of the lower link. The values in these equations were taken using rows 1 and 2 of Table 3-2.

Points $O_{1\mathrm{m}}$, $O_{2\mathrm{m}}$, $O_{3\mathrm{m}}$ as shown in figure 3-7 give the coordinate values. The length of the balanced link was calculated to be 207 mm as shown in equation (3.95) and the AKP link adjustment was calculated as 106 mm. Though the lower link length was modified its mass remains the same as per the AKP.

The upper link was balanced by using equations (3.93) and (3.94). Using equation (3.94), the upper link was balanced using the AKP approach and its value was calculated as $l_{iu} = 162.1 + 81.1 = = 0.243\, m$. Table 3-3 shows the values of SPR geometry modified using the AKP approach. Though the length of the upper link was modified its mass remains the same as per the AKP approach.

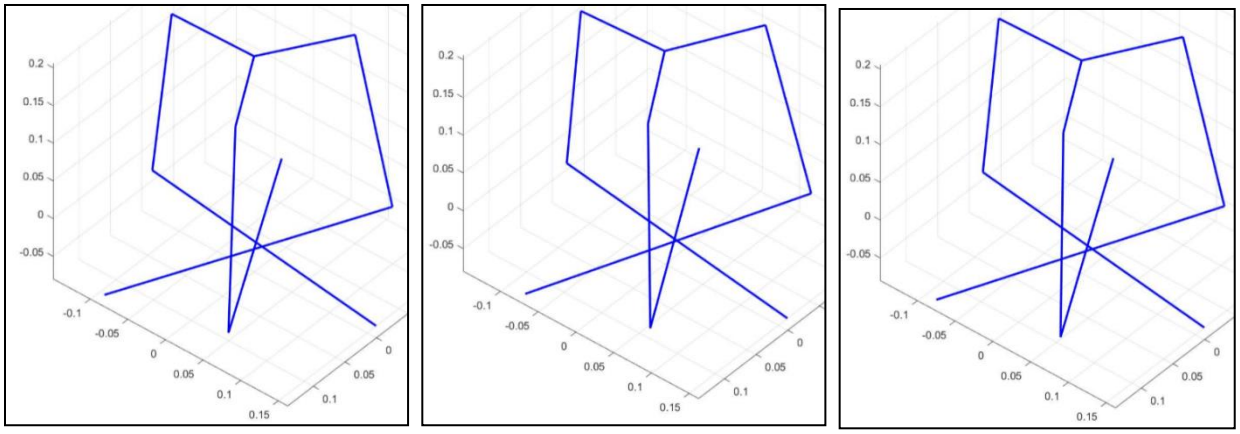

(a) (b) (c)

Figure 3-8. (a) Low speed simulation model position of SPR at time interval t=0 (b) The position of the rotated mechanism at t=0.2s (c) The position of the rotated mechanism at t=0.4s.

In Table 3-3, rows 1 and 2 give details of the length and mass of the lower link. Rows 3, 4 and 5 show the values of the coordinate points $O_{1\mathrm{m}}$, $O_{2\mathrm{m}}$, $O_{3\mathrm{m}}$ considered with respect to the frame O. The values are extracted using Solidworks CAD model of the SPR. These three points represent the positions of the three revolute joints that connect the servomotors with the lower links respectively. Figure 3-7 shows the details of these points. Rows 6 and 7 give details of the length and mass of the upper link which was modified using AKP. Rows 8, 9 and 10 show the values of the coordinate points $O_{1\mathrm{n}}$, $O_{2\mathrm{n}}$, $O_{3\mathrm{n}}$ considered with respect to the frame O. These three points represent the positions of the three revolute joints that connect the lower links with the upper links respectively. Rows 11 and 12 give details of the length and mass of the mobile platform. Rows 13, 14 and 15 show the values of the coordinate points ${}^{O}P_1'$, ${}^{O}P_2'$, ${}^{O}P_3'$ considered with respect to the frame O. These three points represent the positions of the three revolute joints that connect the upper links with the mobile platform, respectively.

Table 3-3. CAD data of force balanced SPR using AKP

S.No.	AKP modified Linkage	Value	Units
1	Length (Lower Link)	207	Millimeters
2	Mass (Lower Link)	641.6	Grams
3	Point O_{1m}	(0.0, 162.1, -64.3)	X,Y,Z @ fixed frame O
4	Point O_{2m}	(-140.3, -81.1, -64.3)	X,Y,Z @ fixed frame O
5	Point O_{3m}	(140.3, -81.1, -64.3)	X,Y,Z @ fixed frame O
6	Length (Upper Link)	243.2	Millimeters
7	Mass (Upper Link)	483.5	Grams
8	Point O_{1n}	(-36.6, -61.9, -33.8)	X,Y,Z @ fixed frame O
9	Point O_{2n}	(71.9, -0.7, -33.8)	X,Y,Z @ fixed frame O
10	Point O_{3n}	(-35.4, 62.7, -33.8)	X,Y,Z @ fixed frame O
11	Length (Mobile Platform)	189.7	Millimeters
12	Mass (Mobile Platform)	313	Grams
13	Point ${}^{O}P_1''$	(8.40, -20.2, 83.5)	X,Y,Z @ fixed frame O
14	Point ${}^{O}P_2''$	(13.3, 17.4, 83.5)	X,Y,Z @ fixed frame O
15	Point ${}^{O}P_3''$	(-21.7, 2.8, 83.5)	X,Y,Z @ fixed frame O

Figure 3-9 shows the SPACAR Spavisual model of the SPR mechanism modified by the AKP approach at various time intervals at low speed.

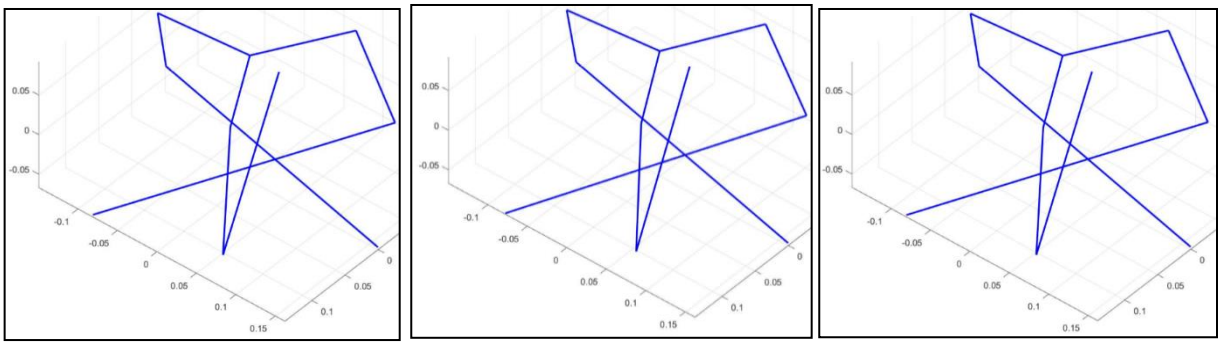

(a) (b) (c)

Figure 3-9. (a) Low speed simulation model of SPR, modified using the AKP approach, at time interval t=0; (b) The position of the rotated mechanism at t=0.2s; (c) The position of the rotated mechanism at t=0.4s.

The reaction forces of the SPR in the X, Y and Z directions are shown in figures 3-10, 3-11 and 3-12, respectively. From figure 3-10, no reaction force in the x-direction is found at both low speed and high speed for the balanced SPR mechanism. It is noted that for the unbalanced SPR mechanism, the reaction force in the x-direction was very small, so the results for both the balanced and unbalanced mechanisms are overlapping in the plot. From figure 3-11 it can be seen that the reaction forces of the balanced SPR are nearly zero at both low and high speeds, but there are significant reaction forces in the y-direction for the unbalanced mechanism. Tables 3-4 and 3-5 shows the values of the reaction forces at different time intervals for both the low speed and high speed. From figure 3-12, it can be seen that the reaction force in the z-direction for the balanced (i.e., in the gravity direction) is nearly zero. It is noted that the reaction force in the z-direction for the unbalanced mechanism is very small, so the two results are overlapping in the plot.

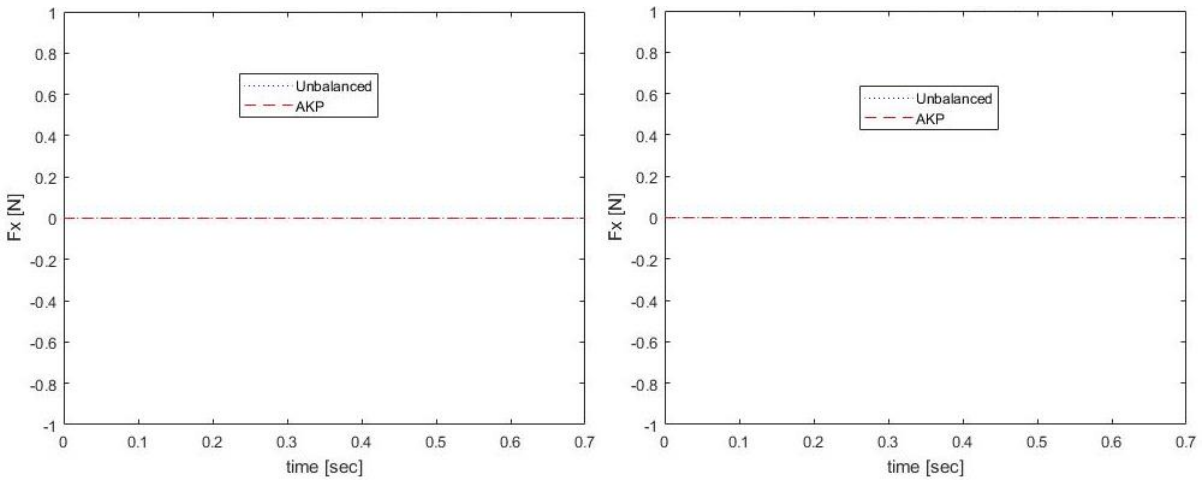

(a) (b)

Figure 3-10. X reaction force of the SPR for unbalanced and AKP-balanced at (a) Low speed (b) High speed.

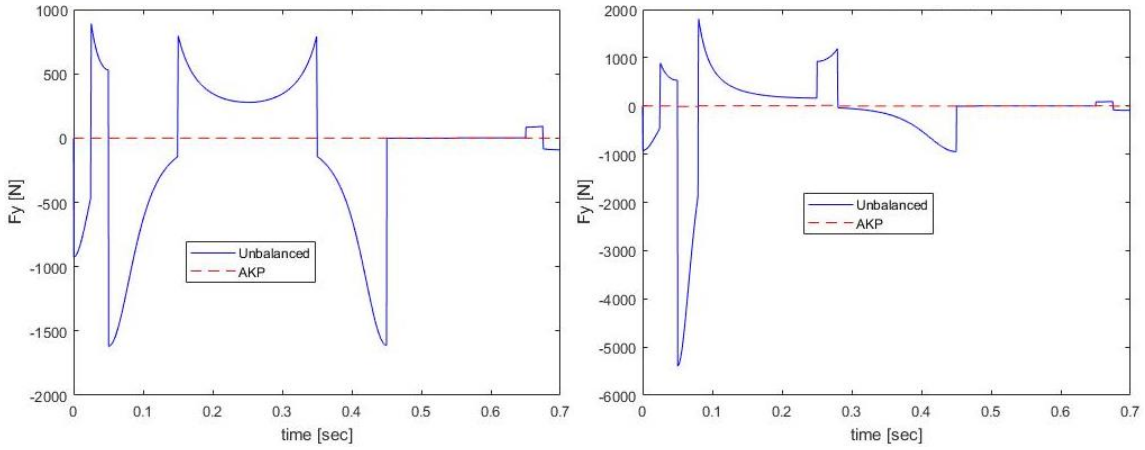

(a) ***(b)***

Figure 3-11. Y reaction force of the SPR for unbalanced and AKP-balanced at (a) Low speed (b) High speed.

Table 3-4. The reaction force in the Y-direction at low speed at various time intervals

time, t [sec]→	t=0.005	t=0.01	t=0.02	t=0.2	t=0.3	t=0.45	t=0.55	t=0.65
Unbalanced, Fy [N]	-898	-823	-587	346	344	-1611	0	2
AKP, Fy [N]	0	0	0	4	4	-4	0	2

Table 3-5. The reaction force in the Y-direction at high speed at various time intervals

time, t [sec]→	t=0.005	t=0.01	t=0.02	t=0.2	t=0.3	t=0.45	t=0.55	t=0.65
Unbalanced, Fy [N]	-898	-823	-587	186	-56	-948	1	1
AKP, Fy [N]	0	0	0	2	-2	-2	0	0

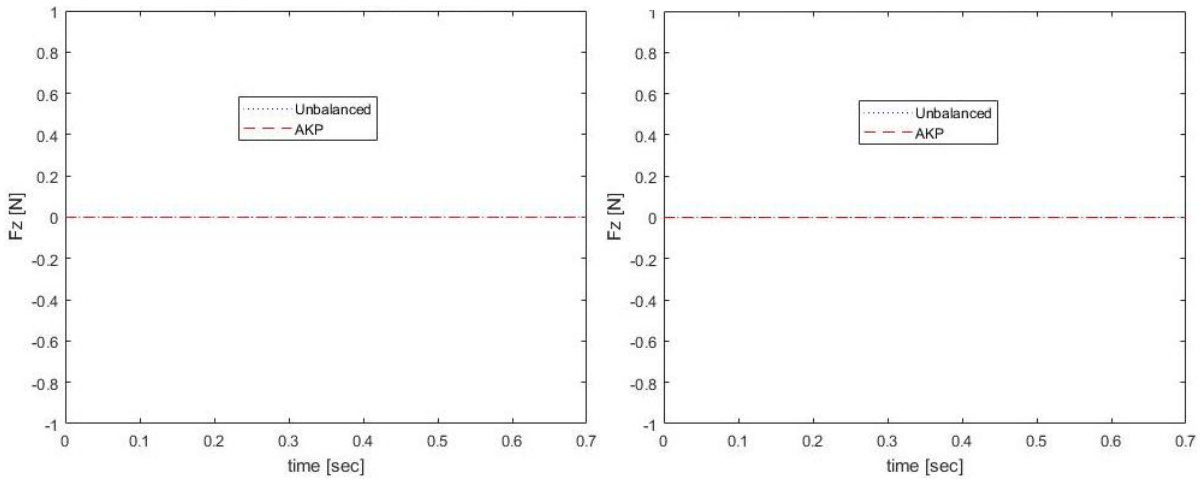

(a) (b)

Figure 3-12. Z reaction force of the SPR for the unbalanced and AKP-balanced at: (a) Low speed (b) High speed.

3.9. Conclusion

The main conclusion of this chapter is that the AKP approach can be extended to force balancing of SPR, and in fact it can be extended to force balancing of any spatial mechanisms, as the derivation of the balancing equations is not restricted by the special structural feature with SPR. The following specific conclusions can be drawn: (1) the total number of the force balancing equations with the AKP approach for the SPR is 18 while the total number of the force balancing equations with the CW approach is 16; (2) the total number of the loop closure equations is 6; (3) force balancing can be achieved by adjusting the lower link and upper link only.

Chapter 4

Dynamic Balancing of SPR using AKP-CW

4.1. Introduction

In this chapter, the AKP will be extended to combine it with the CW in the ACRCM approach (Wijk and Herder, 2008) to dynamic balancing of SPR. Section 4.2 will briefly discuss the idea. Section 4.3 will introduce the general methodology for dynamic balancing of SPR. Section 4.4 will present the principle of dynamic balancing of SPR. Section 4.5 will present the angular momentum of SPR. Section 4.6 will present the principle of the balancing of shaking moment. Section 4.7 will present the equations for moment balancing. Section 4.8 will present the equation for the CW adjustment of the lower link. Section 4.9 will present the equation for the AKP adjustment of the upper link.

4.2. ACRCM for Dynamic Balancing

As reviewed in Section 1.3, one of the AD approaches, ACRCM, includes a gear mechanism and additional actuator with a controller to control the rotation of counterweight added on the mechanism. The counterweight generates the additional moment of inertia to balance shaking moment. The ACRCM approach can perform the full dynamic balancing of mechanisms. On the other hand, the hybrid approach in literature combines two different approaches such as AKP and CW (CW-AKP for short) to perform force balancing of mechanisms (Huang et al., 2010). The idea in this thesis was to combine AKP with the CW part of ACRCM to perform dynamic balancing of SPR.

4.3. Methodology for Deriving the Dynamic Balancing Equation

The combined CW and AKP approach (CW-AKP for short) developed by Huang et al. (2010) is taken as a starting point. This approach is applied to derive the force balance equations by writing the position vectors of the mechanism and its components with respect to the global reference frame. Principle III-F in Section 1.2 is used in deriving the force balancing equations. For the moment balancing equations, the angular momentum of the mechanism along with its components is written with respect to the global reference frame. According to the principle of the angular momentum, the time rate of the change of the angular momentum is equal to the sum of the external moments, where both are considered with respect to the same point. In other words,

$$\sum \mathrm{M}_o = \dot{L_o} \tag{4.1}$$

where $\mathrm{M_o}$ is the sum of the external moment at a reference point O and L_o is the total angular momentum considered at the same reference point (Wu & Gosselin, 2005). The principle III-D in Section 1.2 is used in deriving the moment balancing equations.

4.4. The Principle for Dynamic Balancing of SPR

For the SPR mechanism,

(i) the COM of the mechanism, denoted by r, should remain stationary (Force Balancing)

$$\frac{dr}{dt} = 0 \tag{4.2}$$

(ii) the total angular momentum must remain constant (zero) with respect to a fixed point (Moment Balancing), or

$$\frac{dL_o}{dt} = 0 \tag{4.3}$$

4.5. Angular Momentum of SPR

The angular momentum of the SPR with respect to its center point 'O' and for i=1, 2 & 3

$$L_o = m_p(r_p \times \dot{r}_p) + (L_{il} + m_{il}(r_{il} \times \dot{r}_{il})) + (L_{iu} + m_{iu}(r_{iu} \times \dot{r}_{iu})) - I_i^* \dot{\theta}_i \qquad (4.4)$$

where

- L_o is the total angular momentum of the SPR with respect to point 'O';
- r_p is the position vector of the mobile platform w.r.t 'O';
- L_{il} is the angular momentum of the lower links w.r.t. its COM;
- L_{iu} is the angular momentum of the upper links w.r.t. its COM;
- r_{il} is the position vector of the COM of lower links w.r.t. 'O';
- r_{iu} is the position vector of the COM of upper links w.r.t. 'O';
- I_i^* is the effective inertia of the counterrotations (ACRCM) attached to each servomotor;
- $\dot{\theta}_i$ is the rotational velocity of SPR

Substituting equation (3.27) in Section 3.6.3, equation (3.13) in Section 3.5.2 and equation (3.34) in Section 3.7 to equation (4.4) yields (for i=1, 2 & 3)

$$L_o = term\ \text{I} + \text{term II} + \text{term III} + \text{term IV} + \text{term V} \qquad (4.5)$$

where

$$term\ I = m_p \begin{bmatrix} x + R_{11}x_p + R_{12}y_p + R_{13}z_p \\ y + R_{21}x_p + R_{22}y_p + R_{23}z_p \\ z + R_{31}x_p + R_{32}y_p + R_{33}z_p \end{bmatrix} \text{x} \begin{bmatrix} x_p \frac{d(R_{11})}{dt} + y_p \frac{d(R_{12})}{dt} + z_p \frac{d(R_{13})}{dt} \\ x_p \frac{d(R_{21})}{dt} + y_p \frac{d(R_{22})}{dt} + z_p \frac{d(R_{23})}{dt} \\ x_p \frac{d(R_{31})}{dt} + y_p \frac{d(R_{32})}{dt} + z_p \frac{d(R_{33})}{dt} \end{bmatrix} \qquad (4.6)$$

$$term\ II = m_{il}k_{il}^2\dot{\theta}_i\begin{bmatrix}0\\0\\1\end{bmatrix}+$$

$$m_{il}\begin{bmatrix}x_{io}+x_{ic}(c\theta_i c\delta_i - s\theta_i s\delta_i)-y_{ic}(s\theta_i c\beta_1 c\delta_i + c\theta_i c\beta_1 s\delta_i)+z_{ic}(s\theta_i s\beta_1 c\delta_i + c\theta_i s\beta_1 s\delta_i)\\ y_{io}+x_{ic}(c\theta_i s\delta_i + s\theta_i c\delta_i)-y_{ic}(s\theta_i c\beta_1 s\delta_i - c\theta_i c\beta_1 c\delta_i)+z_{ic}(s\theta_i s\beta_1 s\delta_i - c\theta_i s\beta_1 c\delta_i)\\ z_{io}+y_{ic}s\beta_1+z_{ic}c\beta_1\end{bmatrix}\times$$

$$\begin{bmatrix}x_{ic}(-s\theta_i c\delta_i\dot{\theta}_i - c\theta_i s\delta_i\dot{\theta}_i)-y_{ic}(c\theta_i c\beta_1 c\delta_i\dot{\theta}_i - s\theta_i c\beta_1 s\delta_i\dot{\theta}_i)+z_{ic}(c\theta_i s\beta_1 c\delta_i\dot{\theta}_i - s\theta_i s\beta_1 s\delta_i\dot{\theta}_i)\\ x_{ic}(-s\theta_i s\delta_i\dot{\theta}_i + c\theta_i c\delta_i\dot{\theta}_i)-y_{ic}(c\theta_i c\beta_1 s\delta_i\dot{\theta}_i + s\theta_i c\beta_1 c\delta_i\dot{\theta}_i)+z_{ic}(c\theta_i s\beta_1 s\delta_i\dot{\theta}_i + s\theta_i s\beta_1 c\delta_i\dot{\theta}_i)\\ 0\end{bmatrix}$$

(4.7)

$$term\ III = m_{iu}k_{iu}^2\dot{\theta}_i\begin{bmatrix}0\\0\\1\end{bmatrix} \tag{4.8}$$

$$term\ IV =$$

$$m_{iu}\begin{bmatrix}x_{io}+l_{i1}(s\theta_i s\beta_1 c\delta_i + c\theta_i s\beta_1 s\delta_i)+x_{iuc}c\mu_i - y_{iuc}s\mu_i c\beta_2 + z_{iuc}s\mu_i s\beta_2\\ y_{io}+l_{i1}(s\theta_i s\beta_1 s\delta_i - c\theta_i s\beta_1 c\delta_i)+x_{iuc}s\mu_i + y_{iuc}c\mu_i c\beta_2 - z_{iuc}c\mu_i s\beta_2\\ z_{io}+l_{i1}c\beta_1 + y_{iuc}s\beta_2 + z_{iuc}c\beta_2\end{bmatrix}$$

$$\times\begin{bmatrix}l_{i1}(c\theta_i s\beta_1 c\delta_i\dot{\theta}_i - s\theta_i s\beta_1 s\delta_i\dot{\theta}_i)-x_{iuc}s\mu_i\dot{\mu}_i - y_{iuc}c\mu_i c\beta_2\dot{\mu}_i + z_{iuc}c\mu_i s\beta_2\dot{\mu}_i\\ l_{i1}(c\theta_i s\beta_1 s\delta_i\dot{\theta}_i + s\theta_i s\beta_1 c\delta_i\dot{\theta}_i)+x_{iuc}c\mu_i\dot{\mu}_i - y_{iuc}s\mu_i c\beta_2\dot{\mu}_i + z_{iuc}s\mu_i s\beta_2\dot{\mu}_i\\ 0\end{bmatrix}$$

(4.9)

$$term\ V = I_i^*\dot{\theta}_i\begin{bmatrix}0\\0\\1\end{bmatrix} \tag{4.10}$$

The above equation including all the terms is expanded as

$$L_o = m_p\sum_{i=1}^{3}\begin{bmatrix}(y+R_{21}x_p+R_{22}y_p+R_{23}z_p)(x_p\dot{R}_{31}+y_p\dot{R}_{32}+z_p\dot{R}_{33})\\ (x+R_{11}x_p+R_{12}y_p+R_{13}z_p)(x_p\dot{R}_{31}+y_p\dot{R}_{32}+z_p\dot{R}_{33})\\ (x+R_{11}x_p+R_{12}y_p+R_{13}z_p)(x_p\dot{R}_{21}+y_p\dot{R}_{22}+z_p\dot{R}_{23})\end{bmatrix}$$

$$\begin{bmatrix}-(z+R_{31}x_p+R_{32}y_p+R_{33}z_p)(x_p\dot{R}_{21}+y_p\dot{R}_{22}+z_p\dot{R}_{23})\\ -(z+R_{31}x_p+R_{32}y_p+R_{33}z_p)(x_p\dot{R}_{11}+y_p\dot{R}_{12}+z_p\dot{R}_{13})\\ -(y+R_{21}x_p+R_{22}y_p+R_{23}z_p)(x_p\dot{R}_{11}+y_p\dot{R}_{12}+z_p\dot{R}_{13})\end{bmatrix}$$

$$+\begin{bmatrix} 0 \\ 0 \\ m_{il}k_{il}^2\dot{\theta}_i \end{bmatrix}$$

$$+\sum_{i=1}^{3} m_{il}\begin{bmatrix} 0 \\ 0 \\ ab \end{bmatrix}$$

$$-(z_{io}+y_{ic}s\beta_1+z_{ic}c\beta_1)(x_{ic}(-s\theta_i s\delta_i\dot{\theta}_i+c\theta_i c\delta_i\dot{\theta}_i)-y_{ic}(c\theta_i c\beta_1 s\delta_i\dot{\theta}_i+s\theta_i c\beta_1 c\delta_i\dot{\theta}_i)+z_{ic}(c\theta_i s\beta_1 s\delta_i\dot{\theta}_i+s\theta_i s\beta_1 c\delta_i\dot{\theta}_i))$$
$$-(z_{io}+y_{ic}s\beta_1+z_{ic}c\beta_1)(x_{ic}(-s\theta_i c\delta_i\dot{\theta}_i-c\theta_i s\delta_i\dot{\theta}_i)-y_{ic}(c\theta_i c\beta_1 c\delta_i\dot{\theta}_i-s\theta_i c\beta_1 s\delta_i\dot{\theta}_i)+z_{ic}(c\theta_i s\beta_1 c\delta_i\dot{\theta}_i-s\theta_i s\beta_1 s\delta_i\dot{\theta}_i))$$
$$-cd$$

$$+\begin{bmatrix} 0 \\ 0 \\ m_{iu}k_{iu}^2\dot{\theta}_i \end{bmatrix}$$

$$+\sum_{i=1}^{3} m_{iu}\begin{bmatrix} 0- \\ 0- \\ ef- \end{bmatrix}$$

$$(z_{io}+l_{i1}c\beta_1+y_{iuc}s\beta_2+z_{iuc}c\beta_2)(l_{i1}(c\theta_i s\beta_1 s\delta_i\dot{\theta}_i+s\theta_i s\beta_1 c\delta_i\dot{\theta}_i)+x_{iuc}c\mu_i\dot{\mu}_i-y_{iuc}s\mu_i c\beta_2\dot{\mu}_i+z_{iuc}s\mu_i s\beta_2\dot{\mu}_i)$$
$$(z_{io}+l_{i1}c\beta_1+y_{iuc}s\beta_2+z_{iuc}c\beta_2)(l_{i1}(c\theta_i s\beta_1 c\delta_i\dot{\theta}_i-s\theta_i s\beta_1 s\delta_i\dot{\theta}_i)-x_{iuc}s\mu_i\dot{\mu}_i-y_{iuc}c\mu_i c\beta_2\dot{\mu}_i+z_{iuc}c\mu_i s\beta_2\dot{\mu}_i)$$
$$gh$$

$$-I_{il}^*\dot{\theta}_i\begin{bmatrix} 0 \\ 0 \\ 1 \end{bmatrix}$$

(4.11)

4.6. Moment Balancing

By using equation (4.3) and separating the time-dependent parameters with other geometrical and inertial parameters and equating the terms to zero, we obtain

In X-direction:

$$\dot{R}_{31}yx_p+\dot{R}_{32}yy_p+\dot{R}_{33}yz_p-\dot{R}_{21}zx_p-\dot{R}_{22}zy_p-\dot{R}_{23}zz_p+(\dot{R}_{31}R_{21}-\dot{R}_{21}R_{31})x_p{}^2+(\dot{R}_{31}R_{22}$$
$$-\dot{R}_{21}R_{32}+\dot{R}_{32}R_{21}-\dot{R}_{22}R_{31})x_py_p+(\dot{R}_{31}R_{23}-\dot{R}_{21}R_{33}+\dot{R}_{33}R_{21}-\dot{R}_{23}R_{31})x_pz_p+(\dot{R}_{32}R_{22}$$

$$-\dot{R}_{22}R_{32})y_p{}^2 + (\dot{R}_{32}R_{23} - \dot{R}_{22}R_{33} + \dot{R}_{33}R_{22} - \dot{R}_{23}R_{32})y_p z_p + (\dot{R}_{33}R_{23} - \dot{R}_{23}R_{33})z_p{}^2 - s\theta_i\dot{\theta}_i$$
$$(m_{il}z_{ic}z_{io}c\delta_i - m_{il}x_{ic}z_{io}s\delta_i + m_{il}z_{ic}y_{ic}c\delta_i - m_{il}x_{ic}y_{ic}s\delta_i + m_{iu}c\delta_i l_{i1}z_{io} + m_{iu}c\delta_i l_{i1}y_{iuc}) -$$
$$c\theta_i\dot{\theta}_i(m_{il}(x_{ic}z_{io}c\delta_i + z_{ic}z_{io}s\delta_i + x_{ic}y_{ic}c\delta_i + z_{ic}y_{ic}s\delta_i) + m_{iu}(z_{io}s\delta_i l_{i1} + y_{iuc}s\delta_i l_{i1}))$$
$$-c\mu_i\dot{\mu}_i(m_{iu}x_{iuc}z_{io} + m_{iu}x_{iuc}y_{iuc}) - s\mu_i\dot{\mu}_i(m_{iu}z_{iuc}z_{io} + m_{iu}z_{iuc}y_{iuc}) = 0$$

(4.12)

In Y-direction:

$$\dot{R}_{31}xx_p + \dot{R}_{32}xy_p + \dot{R}_{33}xz_p - \dot{R}_{11}zx_p - \dot{R}_{12}zy_p - \dot{R}_{13}zz_p + \left(\dot{R}_{31}R_{11} - \dot{R}_{11}R_{31}\right)x_p{}^2 +$$
$$\left(\dot{R}_{32}R_{12} - \dot{R}_{12}R_{32}\right)y_p{}^2 + \left(\dot{R}_{33}R_{13} - \dot{R}_{13}R_{33}\right)z_p{}^2 + \left(\dot{R}_{31}R_{12} + \dot{R}_{32}R_{11} - \dot{R}_{11}R_{32} - \dot{R}_{12}R_{31}\right)$$
$$x_p y_p + \left(\dot{R}_{31}R_{13} + \dot{R}_{33}R_{11} - \dot{R}_{11}R_{33} - \dot{R}_{13}R_{31}\right)x_p z_p + \left(\dot{R}_{32}R_{13} + \dot{R}_{33}R_{12} - \dot{R}_{12}R_{33} - \dot{R}_{13}R_{32}\right)$$
$$y_p z_p + s\theta_i\dot{\theta}_i(m_{il}x_{ic}z_{io}c\delta_i + m_{il}z_{ic}z_{io}s\delta_i + m_{il}x_{ic}y_{ic}c\delta_i + m_{il}z_{ic}y_{ic}s\delta_i + m_{iu}s\delta_i z_{io}l_{i1} +$$
$$m_{iu}s\delta_i y_{iuc}l_{i1}) - c\theta_i\dot{\theta}_i(m_{il}(z_{ic}z_{io}c\delta_i - x_{ic}z_{io}s\delta_i + z_{ic}y_{ic}c\delta_i - x_{ic}y_{ic}s\delta_i) + m_{iu}c\delta_i l_{i1}z_{io}$$
$$+m_{iu}c\delta_i l_{i1}y_{iuc}) + s\mu_i\dot{\mu}_i(m_{iu}x_{iuc}z_{io} + m_{iu}x_{iuc}y_{iuc}) - c\mu_i\dot{\mu}_i(m_{iu}z_{iuc}z_{io} + m_{iu}z_{iuc}y_{iuc}) = 0$$

(4.13)

In Z-direction:

$$\dot{R}_{21}xx_p + \dot{R}_{22}xy_p + \dot{R}_{23}xz_p - \dot{R}_{11}yx_p - \dot{R}_{12}yy_p - \dot{R}_{13}yz_p + \left(\dot{R}_{21}R_{11} - \dot{R}_{11}R_{21}\right)x_p{}^2 + (\dot{R}_{22}$$
$$R_{12} - \dot{R}_{12}R_{22})y_p{}^2 + \left(\dot{R}_{23}R_{13} - \dot{R}_{13}R_{23}\right)z_p{}^2 + \left(\dot{R}_{21}R_{13} + \dot{R}_{23}R_{11} - \dot{R}_{13}R_{21} - \dot{R}_{11}R_{23}\right)x_p z_p$$
$$+\left(\dot{R}_{21}R_{12} + \dot{R}_{22}R_{11} - \dot{R}_{12}R_{21} - \dot{R}_{11}R_{22}\right)x_p y_p + \left(\dot{R}_{22}R_{13} + \dot{R}_{23}R_{12} - \dot{R}_{13}R_{22} - \dot{R}_{12}R_{23}\right)y_p z_p$$
$$+s\theta_i\dot{\theta}_i(m_{il}(x_{io}z_{ic}c\delta_i - x_{io}x_{ic}s\delta_i + y_{io}x_{ic}c\delta_i + y_{io}z_{ic}s\delta_i) + m_{iu}x_{io}c\delta_i l_{i1} + m_{iu}y_{io}s\delta_i l_{i1})$$
$$+c\theta_i\dot{\theta}_i(m_{il}(x_{io}x_{ic}c\delta_i + x_{io}z_{ic}s\delta_i - y_{io}z_{ic}c\delta_i + y_{io}x_{ic}s\delta_i) + m_{iu}x_{io}s\delta_i l_{i1} - m_{iu}y_{io}c\delta_i l_{i1})$$
$$+c\mu_i\dot{\mu}_i(m_{iu}x_{io}x_{iuc} - m_{iu}y_{io}z_{iuc})$$
$$+s\mu_i\dot{\mu}_i(m_{iu}x_{io}z_{iuc} + m_{iu}y_{io}x_{iuc}) + s\mu_i\dot{\mu}_i s\theta_i(m_{iu}c\delta_i l_{i1}z_{iuc} + m_{iu}s\delta_i l_{i1}x_{iuc})$$
$$+c\mu_i\dot{\mu}_i c\theta_i(m_{iu}s\delta_i l_{i1}x_{iuc} + m_{iu}c\delta_i l_{i1}z_{iuc}) + c\theta_i\dot{\theta}_i c\mu_i(m_{iu}x_{iuc}s\delta_i l_{i1} + m_{iu}z_{iuc}c\delta_i l_{i1})$$
$$+s\mu_i\dot{\mu}_i c\theta_i(m_{iu}s\delta_i l_{i1}z_{iuc} - m_{iu}c\delta_i l_{i1}x_{iuc}) + c\mu_i\dot{\mu}_i s\theta_i(m_{iu}c\delta_i l_{i1}x_{iuc} - m_{iu}s\delta_i l_{i1}z_{iuc})$$
$$+\dot{\mu}_i(m_{iu}x_{iuc}x_{iuc} + m_{iu}z_{iuc}z_{iuc}) + s\theta_i\dot{\theta}_i c\mu_i(m_{iu}x_{iuc}c\delta_i l_{i1} - m_{iu}z_{iuc}s\delta_i l_{i1})$$
$$+c\theta_i\dot{\theta}_i s\mu_i(m_{iu}z_{iuc}s\delta_i l_{i1} - m_{iu}x_{iuc}c\delta_i l_{i1}) + s\theta_i\dot{\theta}_i s\mu_i(m_{iu}z_{iuc}c\delta_i l_{i1} + m_{iu}x_{iuc}s\delta_i l_{i1})$$

$$+\dot{\theta}_i(m_{il}x_{ic}x_{ic} + m_{il}z_{ic}z_{ic} + +m_{iu}l_{i1}l_{i1} + m_{il}k_{il}^2 + m_{iu}k_{iu}^2 - I_i^*) = 0$$

(4.14)

4.7. Moment Balancing Equations

Separating the coefficients from the time dependent terms, seventeen equations are obtained:

$$m_{il}z_{ic}z_{io}c\delta_i - m_{il}x_{ic}z_{io}s\delta_i + m_{il}z_{ic}y_{ic}c\delta_i - m_{il}x_{ic}y_{ic}s\delta_i + m_{iu}c\delta_i l_{i1}z_{io} + m_{iu}c\delta_i l_{i1}y_{iuc} = 0$$

(4.15)

$$m_{il}x_{ic}z_{io}c\delta_i + m_{il}z_{ic}z_{io}s\delta_i + m_{il}x_{ic}y_{ic}c\delta_i + m_{il}z_{ic}y_{ic}s\delta_i + m_{iu}z_{io}s\delta_i l_{i1} + m_{iu}y_{iuc}s\delta_i l_{i1} = 0$$

(4.16)

$$m_{il}x_{io}z_{ic}c\delta_i - m_{il}x_{io}x_{ic}s\delta_i + m_{il}y_{io}x_{ic}c\delta_i + m_{il}y_{io}z_{ic}s\delta_i + m_{iu}x_{io}c\delta_i l_{i1} + m_{iu}y_{io}s\delta_i l_{i1} = 0$$

(4.17)

$$m_{il}x_{io}x_{ic}c\delta_i + m_{il}x_{io}z_{ic}s\delta_i - m_{il}y_{io}z_{ic}c\delta_i + m_{il}y_{io}x_{ic}s\delta_i + m_{iu}x_{io}s\delta_i l_{i1} - m_{iu}y_{io}c\delta_i l_{i1} = 0$$

(4.18)

$$m_{iu}x_{iuc}z_{io} + m_{iu}x_{iuc}y_{iuc} = 0 \quad (4.19)$$

$$m_{iu}z_{iuc}z_{io} + m_{iu}z_{iuc}y_{iuc} = 0 \quad (4.20)$$

$$m_{iu}x_{io}x_{iuc} - m_{iu}y_{io}z_{iuc} = 0 \quad (4.21)$$

$$m_{iu}x_{io}z_{iuc} + m_{iu}y_{io}x_{iuc} = 0 \quad (4.22)$$

$$m_{iu}s\delta_i l_{i1}x_{iuc} + m_{iu}c\delta_i l_{i1}z_{iuc} = 0 \quad (4.23)$$

$$m_{iu}s\delta_i l_{i1}z_{iuc} - m_{iu}c\delta_i l_{i1}x_{iuc} = 0 \quad (4.24)$$

$$m_{iu}x_{iuc}x_{iuc} + m_{iu}z_{iuc}z_{iuc} = 0 \quad (4.25)$$

$$m_{il}x_{ic}^2 + m_{il}z_{ic}^2 + +m_{iu}l_{il}^2 + m_{il}k_{il}^2 + m_{iu}k_{iu}^2 - I_i^* = 0 \quad (4.26)$$

$$xx_p = xy_p = xz_p = 0 \quad (4.27)$$

$$yx_p = yy_p = yz_p = 0 \quad (4.28)$$

$$zx_p = zy_p = zz_p = 0 \tag{4.29}$$

$$x_p x_p = x_p y_p = x_p z_p = 0 \tag{4.30}$$

$$y_p y_p = y_p z_p = z_p z_p = 0 \tag{4.31}$$

4.8. CW Approach for the Lower Link

In Section 3.7, the force balancing equation used in the modification of the lower link is listed as follows:

Using equation (3.65), the lower link equation is written as

$$l_{11} = \frac{m_{1l} y_{1c} c\beta_1 - m_{1l} z_{1c} s\beta_1}{m_{1u} s\beta_1} \tag{4.32}$$

The length of link adjustment is given by v_{1l}

$$v_{1l} = l_{1l}^{\circ} - \mathrm{l}_{1\mathrm{l}} = l_{1l}^{\circ} - \frac{m_{1l} y_{1c} c\beta_1 - m_{1l} z_{1c} s\beta_1}{m_{1u} s\beta_1} \tag{4.33}$$

Also $v_{1l} = v_{2l} = v_{3l} = v_{il}$ (because of the symmetry of the mechanism) (4.34)

4.9. AKP Approach for the Upper Link

In Section 3.7 it was shown to use the AKP method of adjustment of the link for the upper link and the equations were listed as follows:

Using equation (3.93)

$$l_{1u} = \ l_{2u} = l_{3u} = \frac{y_{1o} - y_{30}}{s\beta_2} \tag{4.35}$$

Using equation (3.94), the upper link length adjustment was given as

$$v_{1u} = v_{2u} = v_{3u} = l_{1u}^{\circ} - \frac{y_{1o} - y_{30}}{s\beta_2}$$

(4.36)

The above equations (4.32), (4.33) & (4.34) give the link mass redistribution based on the CW approach for the lower links while equations (4.35) & (4.36) give the length of the link adjustments using the AKP approach for the upper links.

4.10. Validation

Validation of the equations developed for both force balancing and moment balancing of the SPR was conducted through the simulation by using SPACAR. Information regarding SPACAR and the simulation is explained in detail in section 3.8. The simulation was performed at both low speed and high speed. Data specified in the input file is related to the modified SPR using CW-AKP. The CW added to the SPR is used for force balancing, and this CW is rotated so that it can balance shaking moment as well. Section 4.2 gives information on ACRCM with CW-AKP. The input file data of the SPACAR SPR model is listed in Appendix E.

The initial angles of the unbalanced mechanism were described in Section 3.8. All the units of measurement for length is in millimeter and mass in grams.

Solving for l_{1l} using the force balancing equation (4.32)

$$l_{11} = \frac{m_{1l}y_{1c}(c\beta_1 = 0) - m_{1l}z_{1c}(s\beta_1 = 1)}{m_{1u}s\beta_1} = \frac{641.6 * 156\ (mm)}{483.5} = 207\text{mm}$$

(4.37)

Solving for m_{1l} using the force balancing equation (3.66) from Chapter 3, we have

$$\sqrt{3}m_{2l}x_{2c} - m_{2l}y_{2c}c\beta_1 + m_{2l}z_{2c}s\beta_1 + m_{2u}l_{21}s\beta_1 = 0 \quad (4.38)$$

$$\mathrm{m_{1l}} = (m_{2u}l_{21}s\beta_1)/z_{2c}s\beta_1 = 414\ gms \quad (4.39)$$

The upper link is balanced using equation (4.35) as follows:

$$l_{iu} = 162.1 + 81.1 = 0.243\ m \quad (4.40)$$

The mass and length of the CW (ACRCM) were calculated using the moment balancing equation (4.26) as shown:

$$I_i^* = m_{il}x_{ic}^2 + m_{il}z_{ic}^2 + +m_{iu}l_{il}^2 + m_{il}k_{il}^2 + m_{iu}k_{iu}^2 \quad (4.41)$$

where I_i^* is the moment of inertia of the ACRCM

k_{il} is the radius of gyration of the lower link, $k_{il}^2 = \left(\frac{l_{il}^2}{12}\right)$

k_{iu} is the radius of gyration of the upper link and, $k_{iu}^2 = \left(\frac{l_{iu}^2}{12}\right)$

Inputs to equation (4.40) are taken from rows 1,2 6, 7, 20 of table 4-1

$$I_1^* = I_2^* = I_3^* = 0.0273\ kg/m^2 \quad (4.42)$$

For the gear component (ACRCM) that is a solid disc with radius R_i, thickness t_i, mass m_i^*, inertia I_i^* and made of steel material, the equations are (Wijk, 2008)

$$m_i^* = \rho\pi t_i R_i^2 \quad (4.43)$$

$$I_i^* = \frac{m_i^* R_i^2}{2} \quad (4.44)$$

$$I_i^* = \frac{m_i^{*2}}{2\rho\pi t_i} \tag{4.45}$$

From equations (4.41) and (4.44), consider ti = 0.010 m and density of steel ρ=7800 kg/m^3

$$m_1^* = m_2^* = m_3^* = 3.7\ kg \tag{4.46}$$

From equations (4.42) and (4.45)

$$R_1 = R_2 = R_3 = 0.122 \text{ m} \tag{4.47}$$

Wijk (2008) showed that the gear component with mass, m_i^*, is mounted to the link l* and is calculated using force balancing equation.

$$m_i^* l_i^* = m_{il} l_{il} \tag{4.48}$$

From equations (4.45), (4.47) and using values from rows 1, 2 of table 4-1:

$$l_1^* = l_2^* = l_3^* = 0.023 \text{ m} \tag{4.49}$$

Table 4-1. CAD data of force and moment balanced SPR using CW-AKP

S.No.	CW-AKP mod. Linkage	Value	Remarks
1	Length (Lower Link)	207 mm	Measured using CAD
2	Mass (Lower Link)	414 gms	Measured using CAD
3	Point O_{1m}	(0.0, 162.1, -64.3)	X,Y,Z @ fixed frame O
4	Point O_{2m}	(-140.3, -81.1, -64.3)	X,Y,Z @ fixed frame O
5	Point O_{3m}	(140.3, -81.1, -64.3)	X,Y,Z @ fixed frame O

6	Length (Upper Link)	243 mm	Measured using CAD
7	Mass (Upper Link)	483.5 gms	Measured using CAD
O8	Point O_{1n}	(-52.1, -149.8, -37.6)	X,Y,Z @ fixed frame O
9	Point O_{2n}	(129.8, 74.9, -37.6)	X,Y,Z @ fixed frame O
10	Point O_{3n}	(-129.8, 74.9, -37.6)	X,Y,Z @ fixed frame O
11	Length (Mobile Platform)	189.7 mm	Calculated
12	Mass (Mobile Platform)	313 gms	Measured using CAD
13	Point ${}^{O}P_1'''$	(8.7, -109.5, 90.5)	X,Y,Z @ fixed frame O
14	Point ${}^{O}P_2'''$	(94.8, 54.8, 90.5)	X,Y,Z @ fixed frame O
15	Point ${}^{O}P_3'''$	(-94.8, 54.8, 90.5)	X,Y,Z @ fixed frame O
16	Point @ ACRCM leg-1	(0.2, 162.1, -23.5)	X,Y,Z @ fixed frame O
17	Point @ ACRCM leg-2	(-140.4, -80.9, -23.5)	X,Y,Z @ fixed frame O
18	Point @ ACRCM leg-3	(140.4, -81.1, -23.5)	X,Y,Z @ fixed frame O
19	Length l_{i2}	123 mm	Measured from CAD
20	x_{ic}, y_{ic}, z_{ic} (i=1, 2 & 3)	0.0, -134.05, -80.5	Measured from CAD

In Table 4-1, rows 1 and 2 give details of the length and mass of the lower link. Rows 3, 4 and 5 show the values of the coordinate points O_{1m}, O_{2m}, O_{3m}, considered with respect to the frame O. The values are extracted using Solidworks CAD model of the SPR. These three points represent the positions of the three revolute joints that connect the servomotors with the lower links respectively. Rows 6 and 7 give details of the length and mass of the upper link, which were modified using AKP. Rows 8, 9 and 10 show the values of the coordinate points O_{1n}, O_{2n}, O_{3n},

considered with respect to the frame O. These three points represent the positions of the three revolute joints that connect the lower links with the upper links, respectively. Rows 11 and 12 give details of the length and mass of the mobile platform. Rows 13, 14 and 15 show the values of the coordinate points ${}^{O}P_1'$, ${}^{O}P_2'$, ${}^{O}P_3'$, considered with respect to the frame O. These three points represent the positions of the three revolute joints that connect the upper links with the mobile platform, respectively. Rows 16, 17 and 18 show the values of the coordinate points of counterweights (ACRCMs), considered with respect to the frame O. Row 19 gives the length of COM of upper link, considered from its intersecting point with the lower link. Row 20 shows the coordinate point ${}^{L}C_{il}$ of the COM of the lower link, considered with respect to the frame L.

Table 4-2 lists the calculated values of ACRCM from equations (4.46) and (4.49). Row 1 gives details of the counterweights (ACRCMs). Row 2 gives the distance between the counterweights and the revolute joints, described by points $O_{1\mathrm{m}}$, $O_{2\mathrm{m}}$ and $O_{3\mathrm{m}}$.

Table 4-2. Calculated ACRCM data

S.No.	CW-AKP mod. Linkage	Value	Remarks
1	ACRCM (Lower Link)	3.7 kg	Calculated value
2	Length (ACRCM)	23.5 mm	Calculated value

Figure 4-1 shows the SPACAR Spavisual simulation of the combined model CW-AKP for the SPR mechanism at time intervals when t=0, t=0.2s and t=0.4s. The ACRCM lengths are also visible from the three plots with the extended lengths. The simulation was performed by moving the SPR from one coordinate point to next coordinate point using a specified trajectory command.

A total of the five trajectory commands using four different coordinate points were used in this simulation.

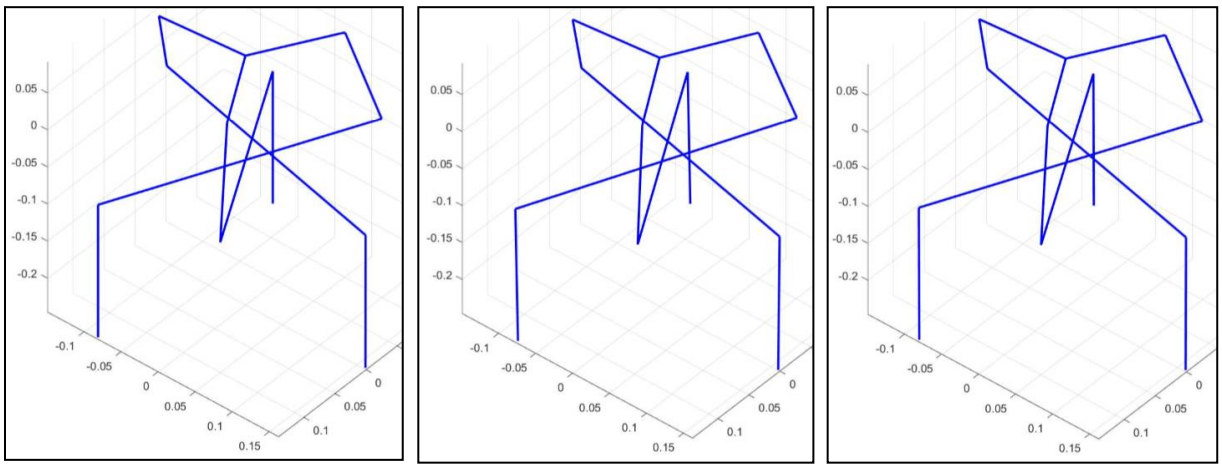

(a) (b) (c)

Figure 4-1. (a) Low speed simulation model position of SPR at time interval t=0; (b) The position of the rotated mechanism at t=0.2s; (c) The position of the rotated mechanism at t=0.4s.

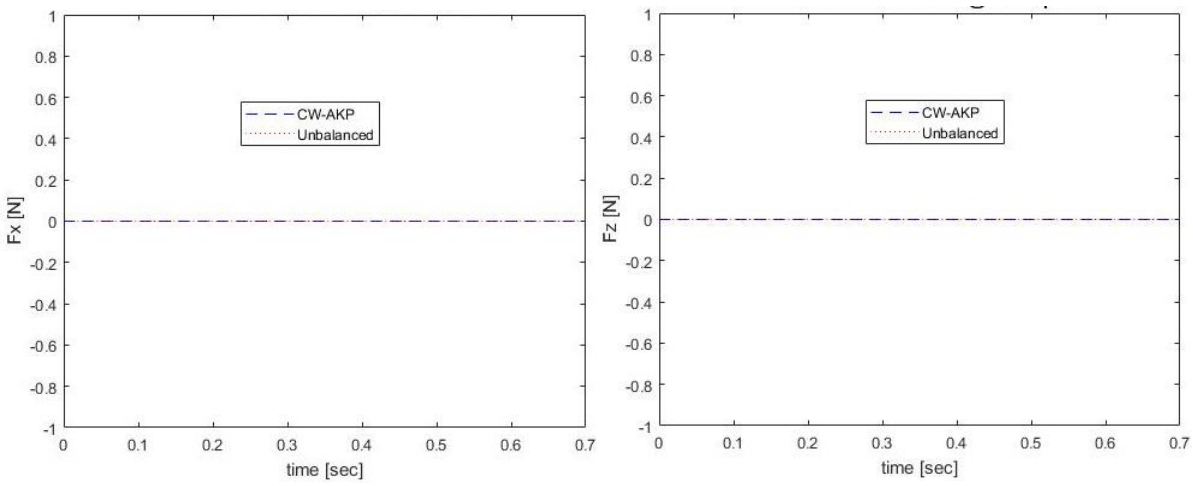

(a) (b)

Figure 4-2. The reaction force of the SPR (unbalanced and dynamically balanced with the CW-AKP approach) at low speed: (a) X-direction (b) Z-direction.

Figure 4-2 shows the reaction force of the SPR in both the x and z directions. In the x- and z-directions, no reaction force exists in the plot. It is noted that for the unbalanced SPR mechanism,

the reaction force in both directions was very small, so the results for both the balanced and unbalanced mechanisms are overlapping in these plots. Even at high speed, the plots in both the x- and z- directions remain the same as compared to the plots at low speed.

Figure 4-3 shows the reaction forces in the y-direction of the SPR at low speed. The reaction force of the dynamical balanced SPR using CW-AKP shows improved performance. Table 4-3 shows the values of the forces at low speed at different time intervals.

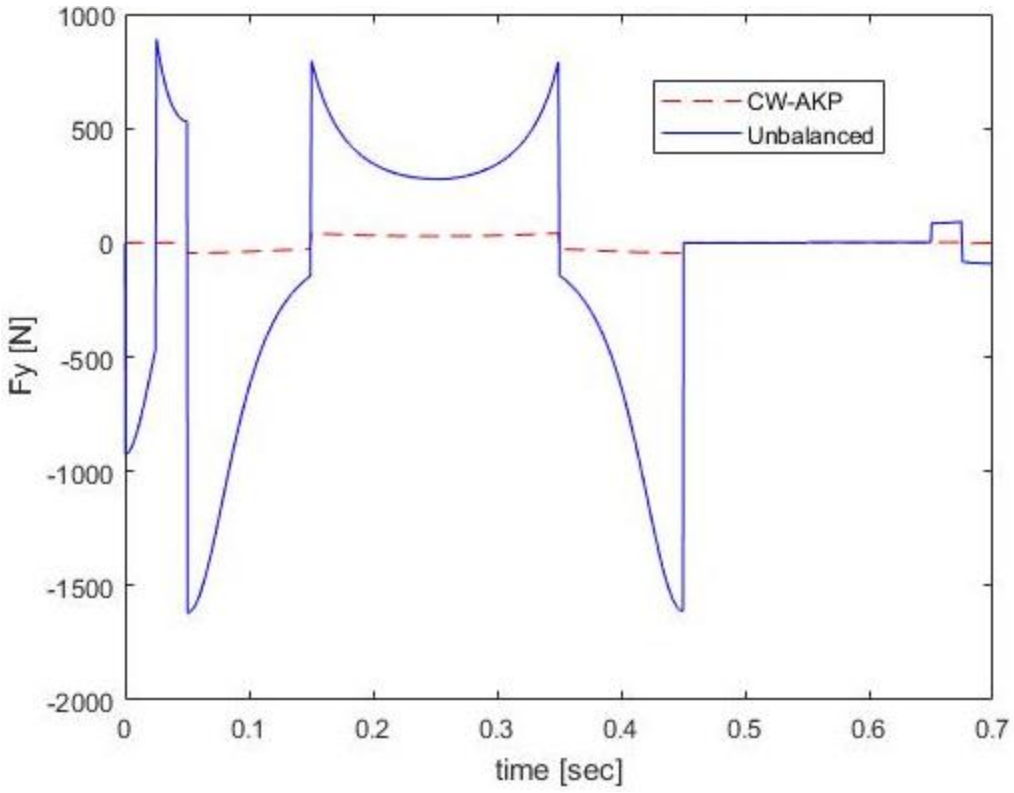

Figure 4-3. The reaction force of the SPR in the Y-direction for both unbalanced and dynamically balanced with CW-AKP at low speed.

Table 4-3. The reaction force in the Y-direction at various time intervals

time, t [sec]→	t=0.01	t=0.025	t=0.05	t=0.2	t=0.3	t=0.45	t=0.55	t=0.65

Unbalanced, Fy [N]	-823	890	-1616	346	344	-1611	-2	2
CW-AKP, Fy [N]	0	0	31	29	31	-45	0	0

In figure 4-4 shaking moment of the SPR is plotted for the unbalanced and CW-AKP balanced SPR. The unbalanced SPR shows wide fluctuations of shaking moment as compared to CW-AKP balanced SPR. The plot showed better performance of CW-AKP approach in terms of fluctuation of the shaking moment. Table 4-4 shows the values of the shaking moment at low speed at different time intervals.

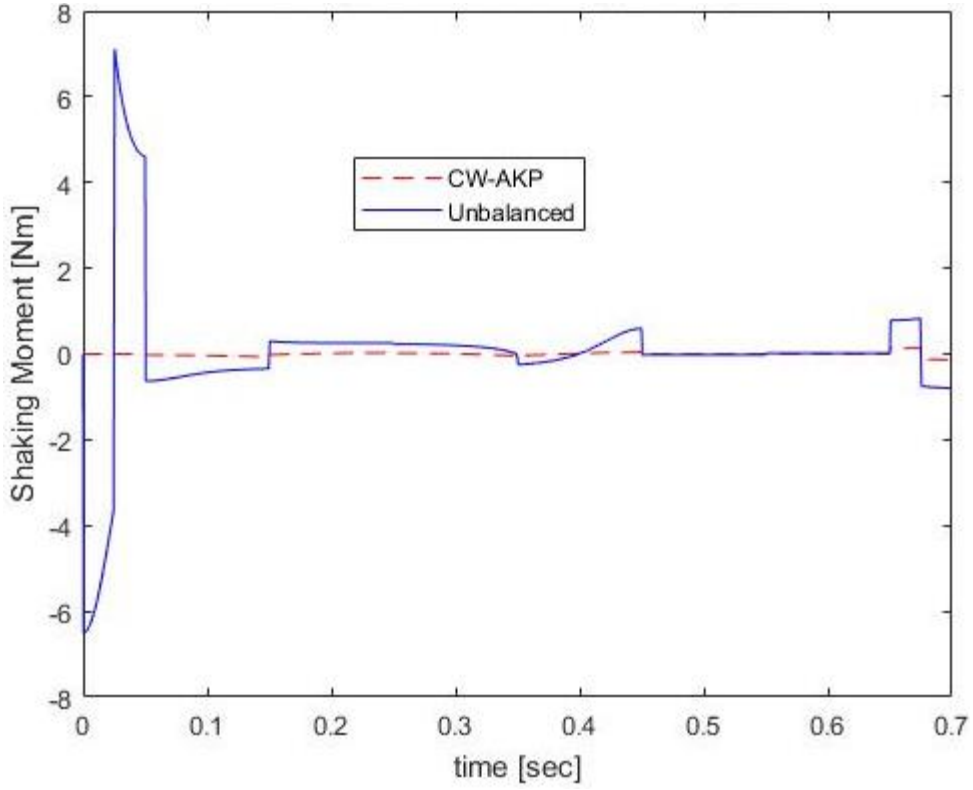

Figure 4-4. Shaking moment of SPR for both unbalanced and dynamically balanced with CW-AKP at low speed.

Table 4-4. The shaking moment at various time intervals

time, t [sec]→	t=0.01	t=0.05	t=0.2	t=0.25	t=0.3	t=0.45	t=0.55	t=0.65
Unbalanced, τ [Nm]	-6	5	0.25	0.25	0.2	0.6	0	0

CW-AKP, τ [Nm]	0	0	0	0	0	0	0	0

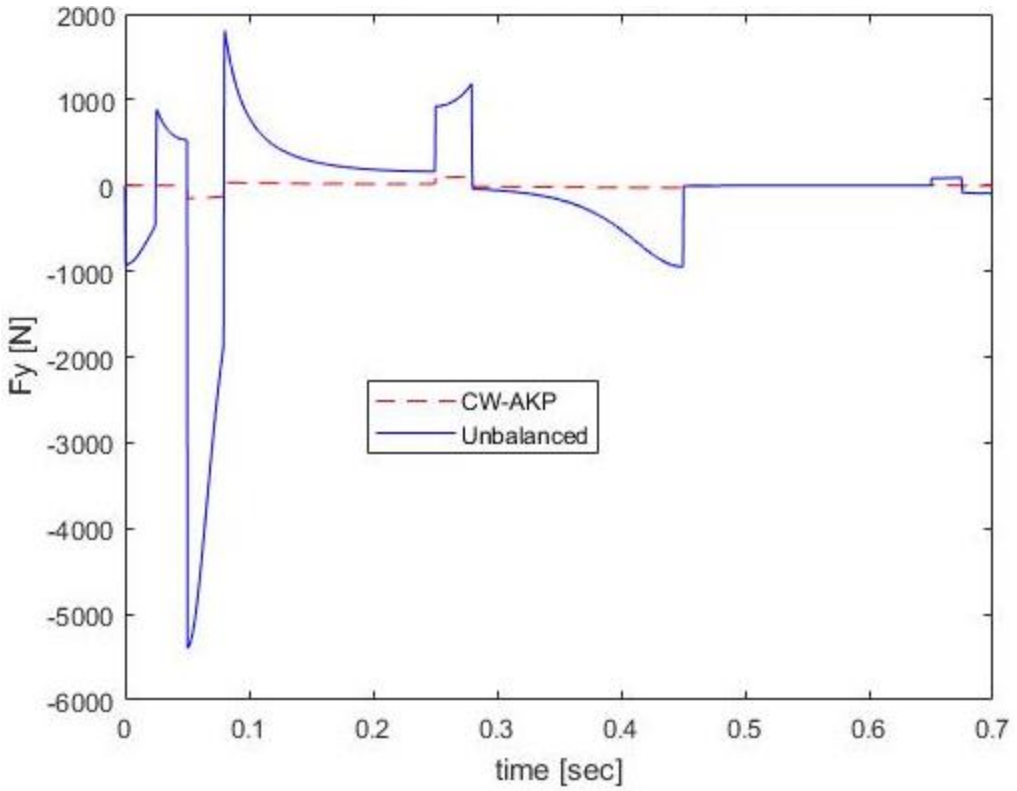

Figure 4-5. The reaction force of the SPR in the Y-direction for both unbalanced and dynamically balanced with CW-AKP at high speed.

Table 4-5. The reaction force in the Y-direction at various time intervals

time, t [sec]→	t=0.01	t=0.025	t=0.05	t=0.2	t=0.28	t=0.45	t=0.55	t=0.65
Unbalanced, Fy [N]	-832	871	-5396	185	1189	-948	1	1
CW-AKP, Fy [N]	0	0	18	95	104	-26	0	0

Figure 4-5 shows the reaction forces of the SPR at high speed in the y-direction. Plots in the figure indicate that the CW-AKP approach has a better performance when SPR is dynamic balanced. Table 4-5 shows the values of the forces at high speed at different time intervals.

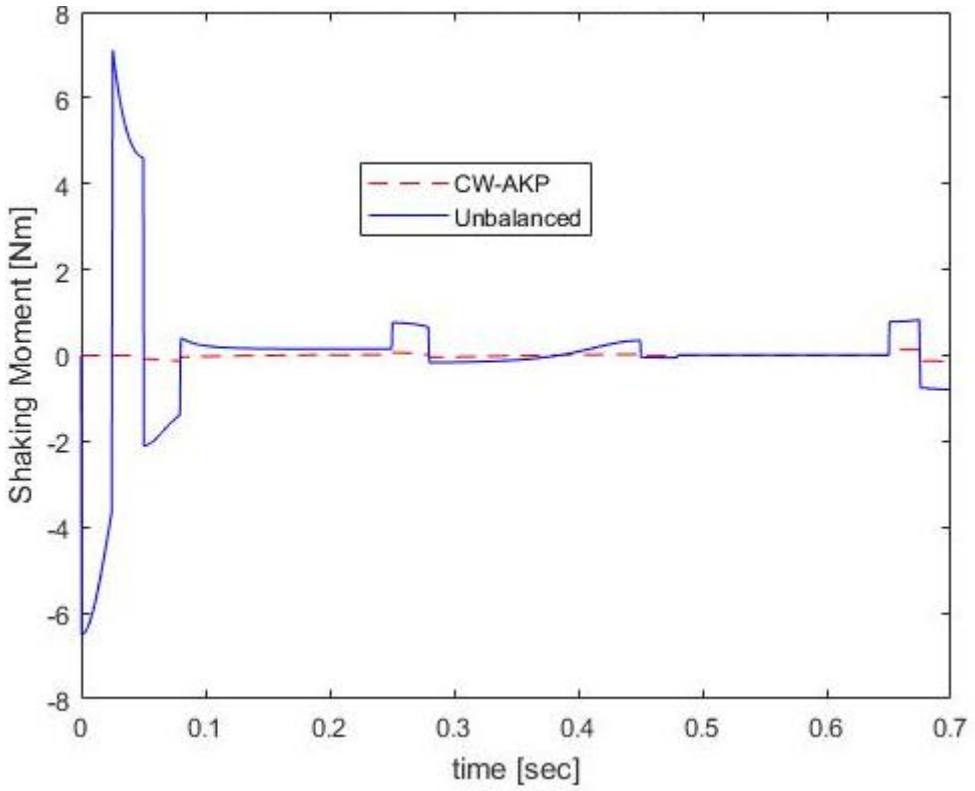

Figure 4-6. Shaking moment of the SPR for both unbalanced and dynamically balanced with CW-AKP at high speed.

In figure 4-6 shaking moment of the SPR at high speed is shown for the unbalanced SPR (which is both force and moment unbalanced) and dynamically balanced SPR with CW-AKP. The unbalanced SPR shows wide fluctuations. The dynamic-balanced SPR shows nearly zero shaking moment, which validates the CW-AKP approach. Table 4-6 shows the values of the shaking moment at high speed at different time intervals.

Table 4-6. The shaking moment at various time intervals

time, t [sec]→	t=0.01	t=.025	t=0.2	t=0.25	t=0.3	t=0.45	t=0.55	t=0.65
Unbalanced, τ [Nm]	-6	7	-0.1	0.7	-0.1	0.3	0	0
CW-AKP, τ [Nm]	0	0	0	0	0	0	0	0

4.11. Conclusion

This chapter presented the work of dynamically balancing SPR with a combined AKP and CW approach, which is further based on the ACRCM approach to dynamic balancing of mechanisms. This new approach is called CW-AKP for short. Specifically, in the CW-AKP approach, the CW was added on the lower link, which serves for both force balancing and moment balancing, and the AKP was applied to the upper link, which serves for force balancing only. As a result for dynamic balancing SPR, there are seventeen moment balancing equations and eighteen force balancing equations. The simulation-based experiment (with SPACAR software) shows that the CW-AKP is effective.

Chapter 5

Optimizing the SPR for Partial Moment Balancing

5.1. Introduction

In this chapter the CW-AKP is extended to optimize the SPR for partial moment balancing or miniaturization of shaking moment. The mathematical expression for shaking moment is derived from writing the angular moment equation at the center point 'O'. The relation between shaking moment and angular momentum is described in Section 4.1. This shaking moment is considered as the objective function for miniaturization. In the optimization process the problem is solved by searching for the variables that minimize the objective function. The CW-AKP developed by Huang (2010) is taken as a starting point. The optimal variables are: the added masses, their locations, and the length of the link of AKP. For the purpose of validation of the work, the simulation by SPACAR software is used.

5.2. Optimization Methodology

- Optimize the force-balanced mechanism for minimalizing shaking moment (also called partially moment balancing).
- Objective function is shaking moment.
- Write the moment equation for the mechanism with respect to a fixed point on the base.
- Objective function, Min F = F(m, l) in terms of shaking moment.
- Constraint equation is the derived force balance equation.
- Optimization variables are mass (m) and link length (l).

5.3. Objective Function

As described in Section 4.3 for shaking moment balance, $\sum \mathrm{M} = \dot{L_o} = 0$, where M was the sum of external moment at a reference point and L_o was the total angular momentum considered at the same reference point. If this shaking moment is not completely balanced but made a minimum, we can use the selected terms of time rate change of the angular momentum equation for optimization. The selection was based on the optimization or decision variables, i.e. link mass and length, and the shaking moment was considered as the objective function to be minimized. A simplified shaking moment equation was used as an objective function in this optimization problem.

From Section 4.5, equation (4.4) describes the angular momentum of the mechanism with respect to point 'O', which is revised here:

$$L_o = m_p(r_p \times \dot{r}_p) + \sum_{i=1}^{3}[(L_{il} + m_{il}(r_{il} \times \dot{r}_{il})) + (L_{iu} + m_{iu}(r_{iu} \times \dot{r}_{iu}))] \quad (5.1)$$

where

- L_{il} is the angular momentum of the lower links w.r.t. its COM.
- L_{iu} is the angular momentum of the upper links w.r.t. its COM.

L_{il} and L_{iu} can be written as

$$L_{il} = m_{il}k_{il}^2\dot{\theta}_{il} \quad (5.2)$$

$$L_{iu} = m_{iu}k_{iu}^2\dot{\theta}_{iu} \quad (5.3)$$

where k_{il} is the radius of gyration of the lower link and where k_{iu} is the radius of gyration of the upper link and

$$k_{il}^2 = \left(\frac{l_{il}^2}{12}\right) \; and \; k_{iu}^2 = \left(\frac{l_{iu}^2}{12}\right) \tag{5.4}$$

Using equations (5.2), (5.3), (5.4), we can write equation (5.1) as

$$L_o = m_p\left(r_p \; x \; \dot{r}_p\right) + \sum_{i=1}^{3}\left(m_{il}(r_{il} \; x \; \dot{r}_{il})\right) + \sum_{i=1}^{3}(m_{iu}(r_{iu} \; x \; \dot{r}_{iu})) + \sum_{i=1}^{3}\left(\frac{m_{il}l_{il}^2\dot{\theta}_{il}}{12}\right) + \sum_{i=1}^{3}\left(\frac{m_{iu}l_{iu}^2\dot{\theta}_{iu}}{12}\right) \tag{5.5}$$

From equation (5.5), the shaking moment in scalar form can be written as

$$\dot{L_o} = m_p r_p^2\ddot{\theta}_p + \sum_{i=1}^{3} m_{il}r_{il}^2\ddot{\theta}_{il} + \sum_{i=1}^{3} m_{iu}r_{iu}^2\ddot{\theta}_{iu} + \sum_{i=1}^{3}\left(\frac{m_{il}l_{il}^2\ddot{\theta}_{il}}{12}\right) + \sum_{i=1}^{3}\left(\frac{m_{iu}l_{iu}^2\ddot{\theta}_{iu}}{12}\right) \tag{5.6}$$

From Appendix-B using the value of r_{il}, substituting the values of $\frac{\beta_1}{2} = 45°$

$$\sum_{i=1}^{3} r_{il} = \frac{l_{il}}{2\sin\left(\frac{\beta_1}{2}\right)} = 0.3536\; l_{il} \tag{5.7}$$

$$\sum_{i=1}^{3} r_{iu} = \frac{l_{iu}}{2\sin\left(\frac{\beta_2}{2}\right)} = 0.3536\; l_{iu} \tag{5.8}$$

Using equations (5.7), (5.8), we can write equation (5.6) as

$$\dot{L_o} = m_p r_p^2\ddot{\theta}_p + \sum_{i=1}^{3} 0.125 m_{il}l_{il}^2\ddot{\theta}_{il} + \sum_{i=1}^{3} 0.125 m_{iu}l_{iu}^2\ddot{\theta}_{iu} + \sum_{i=1}^{3}\left(\frac{m_{il}l_{il}^2\ddot{\theta}_{il}}{12}\right) + \sum_{i=1}^{3}\left(\frac{m_{iu}l_{iu}^2\ddot{\theta}_{iu}}{12}\right) \tag{5.9}$$

As the optimization variables are mass and length of the link, only the last four terms of equation (5.9) are considered, as they contain the mass and length of links.

The Objective Function can be simplified and written as (Acevedo et al. 2012):

$$f = \sum_{i=1}^{3}(0.208\, m_{il} l_{il}^2) + \sum_{i=1}^{3}(0.208\, m_{iu} l_{iu}^2) \tag{5.10}$$

5.4. Constraint Equations

The force balancing equations derived in Chapter 3 are used as the constraint equation for optimization. Equations (3.86) and (3.92) describe the constraint equations selected for this optimization problem.

$$m_{il} y_{ic} c\beta_1 - m_{il} z_{ic} s\beta_1 - m_{iu} l_{i1} s\beta_1 = 0 \tag{5.11}$$

$$l_{3u} s\beta_2 = (y_{1o} - y_{30}) \tag{5.12}$$

Using equation (3.28) from Chapter 3, the total mass of SPR in terms of its components and for i= 1, 2 & 3

$$M = m_p + m_{il} + m_{iu} \Rightarrow \; m_{iu} = M - m_p - m_{il} \tag{5.13}$$

From Table 3-2 in Section 3.8, substituting the values of M and m_p

$$m_{iu} = 1.125 - m_{il} \tag{5.14}$$

From section 3.8, substituting the values of z_{ic} = half length of lower link = 157 mm and $\beta_1 = 90°$ into equation (5.11) and further simplifying it with equation (5.15) gives the constraint equation (g1), as shown later in section 5.5. From table 3-2 from rows 3 and 5, substituting the

values of $y_{10} = 162.1$ $y_{30} = -81.1$ and $\beta_1 = 90°$ into equation (5.12) gives the constraint equation (g2), as shown later in section 5.5. Substituting equation (5.14) into equation (5.10), m_{iu} is eliminated and the number of variables in the objective function is reduced to three. The optimization problem using the three variables is formulated later in section 5.5.

5.5. Optimization Problem Formulation

Substituting all values as described in Section 5.4 and data from Table 3-2 in Section 3.8 the problem is formulated as

Minimize $f(m_{il}, l_{il}, l_{iu}) = 0.208 m_{il} l_{il}^2 + 0.234 l_{iu}^2 - 0.208 m_{il} l_{iu}^2$

$$f = \sum_{i=1}^{3} (0.208\, m_{il} l_{il}^2) + \sum_{i=1}^{3} (1.125 - m_{il})\, 0.208\, l_{iu}^2$$

Subject to

$h1: 0$

$g1: 0.157 m_{il} + 1.125 l_{il} - m_{il} l_{il} = 0$

$g2: l_{iu} - 0.243 = 0$ (5.15)

5.6. Solving using MATLAB Toolbox

For solving the optimization problems, MATLAB optimization toolbox functions or solvers were used for maxima or minima solutions. These problems involve writing the objective and the constraint functions. These problems are solvable when the functions representing it are continuous, discontinuous or stochastic. In MATLAB toolbox, 'fmincon' command was used as an optimizing function for solving the problem. The 'fmincon' function uses four different

algorithms, of which the sequential quadratic programming (SQP) algorithm was used here. SQP is one of the best algorithms available in Matlab as it has fast convergence rate and has a strong theoretical basis. By following the syntax, the problem was formulated. The syntax also has options to calculate the Hessian of the Lagrangian (User's, M. G. O. T., 2012).

Using equation 5.16 as described in Section 5.5 the optimization problem was solved using 'fmincon' syntax. Using equation (5.16), two *.m files were written, one as the objective function and one as the constraint equations. The objective function is smof.m file while the constraint equations are csteq.m file. The complete syntax of 'fmincon' command used is found in the appendix E. Using SQP solver the optimized results were found to be $m_{il} = 475.6\ gms$, $l_{il} = 115$ mm and $m_{iu} = 243.3\ mm$. The results were verified for local minima using different starting points and using interior-point solver. The results showed that the value of the 'exitflag' using fmincon was the one which represents that the first order optimality conditions were satisfied. The minimum shaking moment value was found to be 0.0093 Nm. Appendix F lists the complete optimization program including the objective function, the constraint equations, 'fmincon' function syntax and the results calculated.

5.7. Validation

Validation was carried out using the SPACAR simulation. Appendix G lists the input program file that was used in the simulation. The input file is similar to the file used in Section 4.11. The input dynamic data for specifying the trajectories and nodes data remain the same for all simulations. The initial angles of the unbalanced mechanism were described in Section 3.8. Table 3-2 in Section

3.8 specifies the input data. All units of measurement for length are in millimeter and mass in grams.

Using the optimized values for mass $m_{il} = 475.6\ gms$ and length $l_{il} = 115\ mm$ for the balanced lower link, the CW that is a solid disc with radius R_i, thickness t_i =0.010 m, mass m_i^*, inertia I_i^* and made of steel material with density 7800 kg/m^3 were calculated using the equations (4.40), (4.41) (4.42, (4.43), (4.44) and (4.47). Table 5-1 lists the calculated values of CW from the above equations. The mass of the upper link remains unchanged for the optimization.

$$m_{ic}^* = 2.5\ kg \tag{5.16}$$

$$R_i = 100\ mm \tag{5.17}$$

$$l_{ic}^* = 22.2\ mm \tag{5.18}$$

Table 5-1. Data of the optimized SPR

S.No.	CW-AKP mod. Linkage	Value	Remarks
1	CW	2.5 kg	From optimization & equ. (4.40)
2	CW Location	22.2 mm	From optimization & equ. (4.47)
3	Length of Upper Link	243.3 mm	From Optimization

The simulation was performed using the trajectory path described by the five points and by using the TRAJECT command to describe the path in SPACAR.

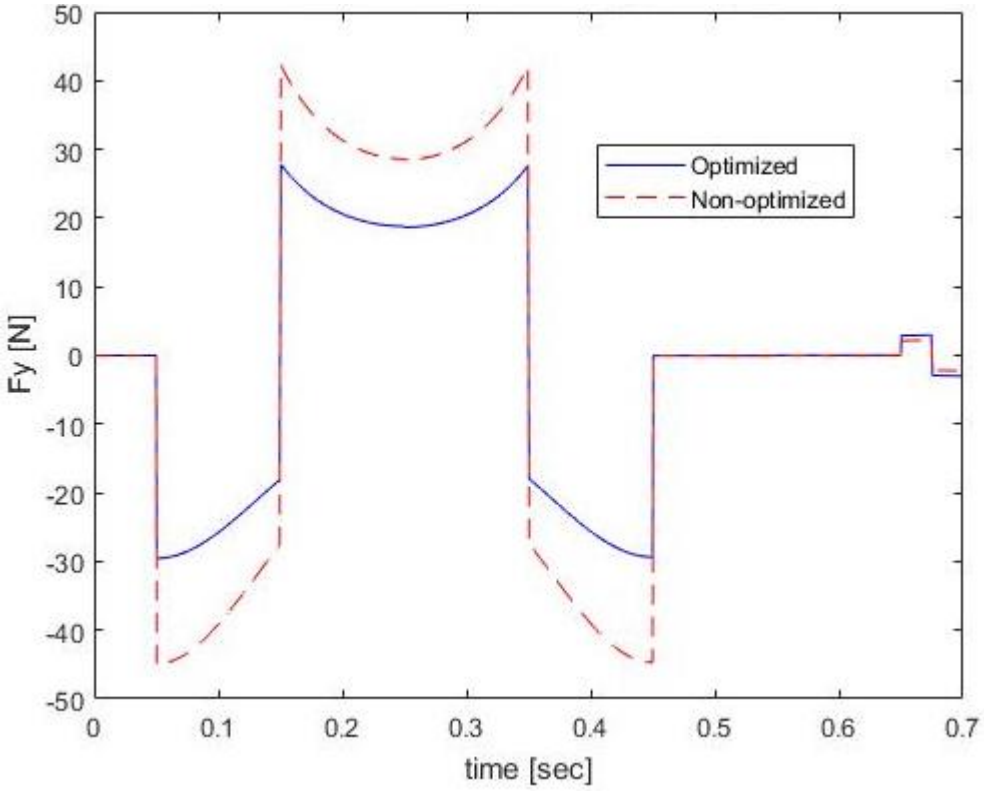

Figure 5-1. The reaction force of the SPR in the Y-direction for optimized and non-optimized, dynamically balanced with CW-AKP at low speed.

Figure 5-1 shows the reaction forces in the y-direction of the SPR at low speed. The comparison plot shows that the forces are reduced for the optimized linkage using CW-AKP. Table 5-2 shows the values of the forces of the SPR at low speed at different time intervals.

Table 5-2. The reaction force in the Y-direction at various time intervals

time, t [sec]→	t=0.01	t=0.05	t=0.2	t=0.25	t=0.3	t=0.45	t=0.55	t=0.65
Optimized, Fy [N]	0	0	21	18	20	-30	0	0
Non-Optimized, Fy [N]	0	0	31	28	31	-44	0	0

Figure 5-2 shows the shaking moment of the SPR at low speed. Table 5-3 shows the values of the shaking moment at low speed at different time intervals.

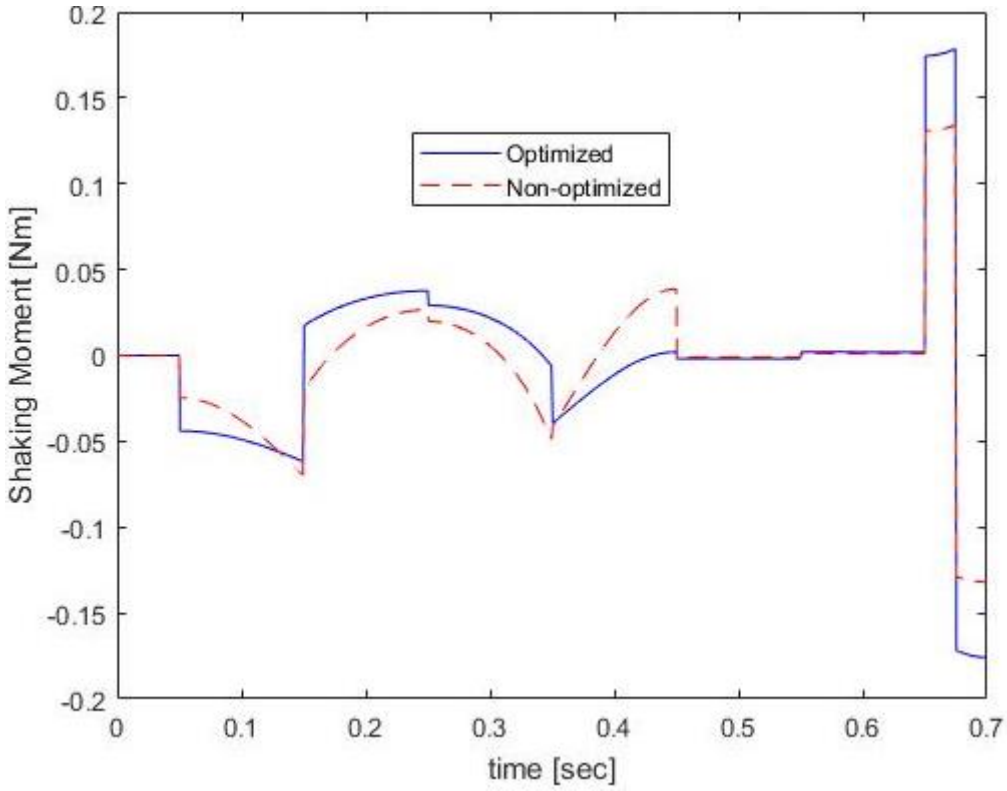

Figure 5-2. Shaking moment of optimized and non-optimized, dynamically balanced SPR with CW-AKP at low speed.

Table 5-3. The shaking moment at various time intervals

time, t [sec]→	t=0.01	t=0.05	t=0.2	t=0.25	t=0.3	t=0.45	t=0.55	t=0.65
Optimized, τ [Nm]	0	0	0.03	0.03	0.02	0	0	0
Non-Optimized, τ [Nm]	0	0	0.01	0.02	0	0.03	0	0

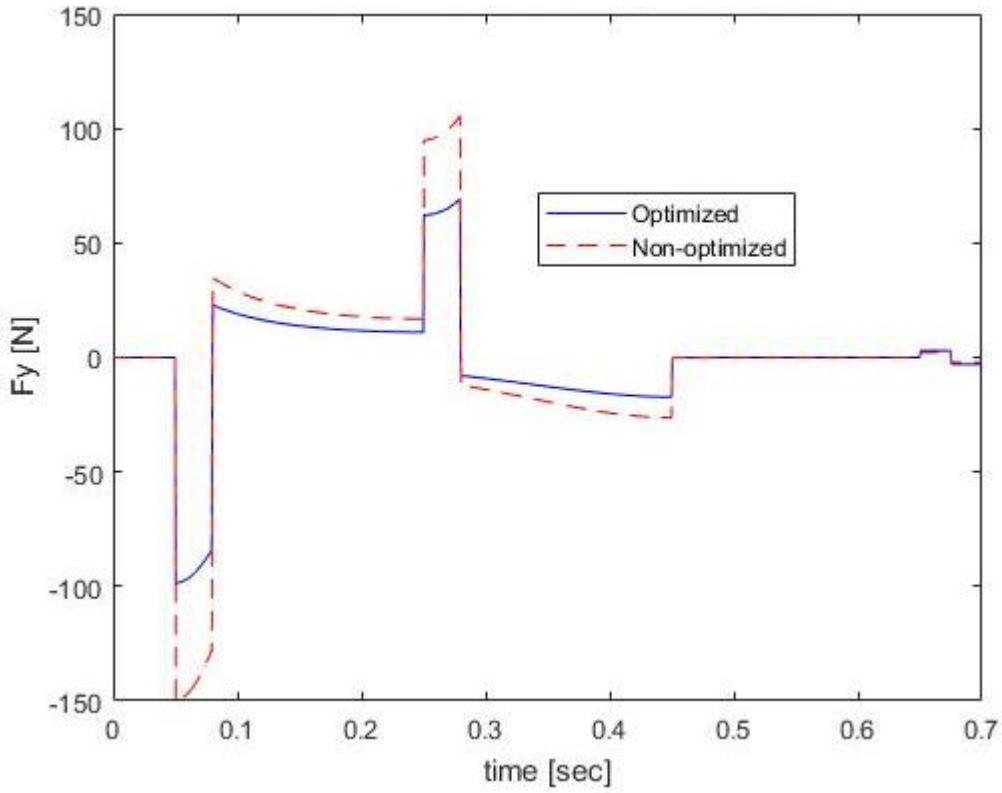

Figure 5-3. The reaction force of the SPR in the Y-direction for optimized and non-optimized, dynamically balanced with CW-AKP at high speed.

Figure 5-3 shows the reaction forces in the y-direction of the SPR at high speed. Similar to the low speed the comparison plot shows reduced forces for the optimized linkage. Table 5-4 shows the values of the forces of the SPR at high speed at different time intervals. Figure 5-4 shows the shaking force in the y-direction of the SPR at high speed. Table 5-5 shows the values of the shaking moment of the SPR at high speed at different time intervals.

Table 5-4. The reaction force in the Y-direction at various time intervals

time, t [sec]→	t=0.01	t=0.05	t=0.2	t=0.27	t=0.3	t=0.45	t=0.55	t=0.65
Optimized, Fy [N]	0	0	12	65	-9	-17	0	0
Non-Optimized, Fy [N]	0	0	18	100	-14	-26	0	0

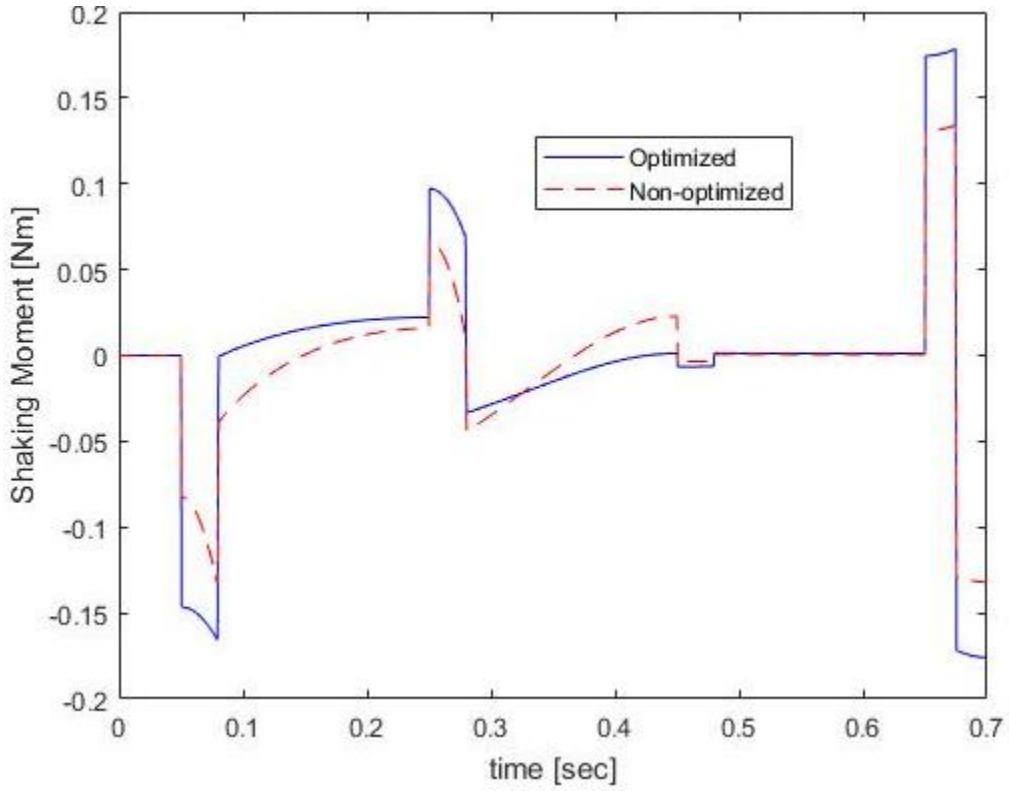

Figure 5-4. Shaking moment of optimized and non-optimized, dynamically balanced SPR with CW-AKP at high speed.

Table 5-5. The shaking moment at various time intervals

time, t [sec]→	t=0.01	t=0.05	t=0.2	t=0.25	t=0.3	t=0.45	t=0.55	t=0.65
Optimized, τ [Nm]	0	0	0.02	0.09	-0.03	0	0	0
Non-Optimized, τ [Nm]	0	0	0.01	0.06	-0.03	0.02	0	0

5.8. Conclusion

The chapter presented an approximate approach to partially balancing the shaking moment of SPR while at the same time the SPR is fully force balanced. To each leg, there are three decision or optimization variables, namely the length of the upper link, the CW and its location. The optimization problem model is that the shaking moment of SPR was taken as an objective function,

and the force balancing equation is the constraint equation. The objective function is a quadratic form by approximation. This approach is shown to be effective based on the simulation.

Chapter 6

Conclusion and Future Work

6.1. Overview and Conclusions

The primary objective of this thesis was to extend the AKP approach to balancing of spatial robotic mechanisms. The spherical parallel robotic mechanism was chosen as a study vehicle. In Section 1.5 the research objectives and Section 1.6 the research methodology were explained. The three objectives as proposed have been achieved.

In Chapter 3, it was shown that the AKP approach was extended to force balance the SPR using the force balancing principle III. A total of the eighteen balancing equations were derived. Using the loop-closure equations relates the lower link and the upper link in terms of its coordinates, rotation matrix, its parameters and time-dependent variables. For the SPR mechanism the lower link and the upper link were modified using the AKP approach. The simulation has confirmed the effectiveness of the extended AKP approach for complete force balancing of the SPR.

The dynamic balancing equations of the SPR using a combined approach of AKP and CW was derived in Chapter 4. The mechanism was dynamic balanced by force balancing first and then moment balancing. Specifically, the SPR can be forced balanced using the AKP approach for the upper links and the CW approach for the lower links. Then it can be moment balanced by using an active counter-rotating counter mass (ACRCM) with a servomotor to rotate it for the lower links. Its mass acts as counterweights during force balancing and ACRCM acts as balancer during moment balancing and using this method is advantageous. A total of the seventeen-moment

balance equations was derived. The simulation with SPACAR has confirmed the effectiveness of this approach to complete dynamic balancing of the SPR.

The third objective of this thesis was to extend the CW-AKP approach in the partial moment balancing of mechanisms with the goal that the shaking moment was made as a minimum. In Chapter 5, the work towards this objective was described, and the problem was modelled as an optimization problem and solved using the optimization toolbox in MATLAB. From the simulation, 12% reduction in shaking moment was achieved.

6.2. Contributions

There are several contributions in the area of balancing of mechanisms. First, the AKP approach has been shown to be applicable to spherical parallel robotic mechanisms. Since SPRs and general spatial mechanisms are similar in that bodies in them exercise a spatial motion, the AKP approach is applicable to general spatial mechanisms. Second, the new approach to dynamic balancing of mechanisms is developed, which combines AKP and ACRCM. The benefit of this approach is that the torque fluctuation on the actuator is reduced in comparison with the ACRCM approach due to the replacement of CW by AKP. Finally, the combined AKP and CW approach for fully force balancing of mechanisms is extended to partial moment balancing for SPRs.

6.3. Future Work

One of the problems with the combined AKP and ACRCM approach is the need of additional transmission and control systems that control the rotation of the CW. It is worthwhile to study whether AKP may contribute to the so-called inherent balancing of mechanisms, the moment

balancing in this case. The nature of AKP is similar to the concept of the inherent balancing (Wijk, 2014). So it is feasible to see how much AKP can contribute to moment balancing of mechanisms. Another idea surrounding AKP is to make AKP active in such a way that the translation actuator is put in place to change the length of the link, which is a foundation for the balancing of machines with consideration of loading. It is noted that the load effect to balancing of machines is important especially to the so-called soft machine or soft robot. The definition of soft robots is referred to the paper (Chen et al., 2017).

References

Aarts, R. G. K. M., Meijaard, J. P., & Jonker, J. B. (2011). SPACAR User Manual. *University of Twente, Enschede, The Netherlands, Report No. WA-1299*.

Acevedo, M., Ceccarelli, M., & Carbone, G. (2012). Application of counter-rotary counterweights to the dynamic balancing of a spatial parallel manipulator. In *Applied Mechanics and Materials* (Vol. 162, pp. 224-233). Trans Tech Publications.

Arakelian, V., Samsonyan, A., & Arakelyan, N. (2015, October). Optimum Shaking Force Balancing of Planar 3-RRR Parallel Manipulators by means of an Adaptive Counterweight System. In *Proceedings of the 14th IFToMM World Congress* (pp. 305-309).

Bai, S. (2010). Optimum design of spherical parallel manipulators for a prescribed workspace. *Mechanism and Machine Theory*, *45*(2), 200-211.

Bai, S., Hansen, M. R., & Angeles, J. (2009). A robust forward-displacement analysis of spherical parallel robots. *Mechanism and Machine Theory*, *44*(12), 2204-2216.

Basu, D., & Ghosal, A. (1997). Singularity analysis of platform-type multi-loop spatial mechanisms. Mechanism and Machine Theory, 32(3), 375-389.

Bonev, I. A. (2002). Geometric analysis of parallel mechanisms. Canada: Université Laval.

Berkof, R. S., & Lowen, G. (1969). A new method for completely force balancing simple linkages. Journal of Engineering for Industry, 91(1), 21-26.

Boisclair, J., Richard, P-L., Laliberte, T., & Gosselin, C. (2017). Gravity compensation of Robotic Manipulators Using Cylindrical Halbach Arrays. In IEEE/ASME Transactions on Mechatronics, 22 (1), 457-464, February. doi: 10.1109/TMECH.2016.2614386.

Chen, A., Yin, R.X., Cao, L., Yuan, C.W., Ding, H.K. and Zhang, W.J. 2017."Soft Robotics: Definition and Research Issues." In IEEE International Conference on Mechatronics and Machine Vision in Practice, Auckland, New Zealand, November 21-23, 2017.

Chiang, C. H. Kinematics of spherical mechanisms (1988). Cambridge University Press, Cambridge). Optimal selection of precision points for function synthesis of spherical 4R linkage, 2189, 149-149.

Craig, J. J. (2005). Introduction to robotics: mechanics and control (Vol. 3, pp. 48-70). Upper Saddle River, NJ, USA; Pearson/Prentice Hall.

De Jong, J. J., & Herder, J. L. (2015). A comparison between five principle strategies for adapting shaking force balance during varying payload. In Proceedings of the 14th IFToMM World Congress. Taipei, Taiwan. doi: 10.6567/IFToMM.WC.OS2.043.

Gao, F., Qian, Z. Q., Wang, X. J., Bi, Z. M., & Zhang, W. J. (2015, June). A novel approach to embodiment design of a robotic system for maximum workspace. In Industrial Electronics and Applications (ICIEA), 2015 IEEE 10th Conference on (pp. 539-544). IEEE.

Gosselin, C. M., & Hamel, J. F. (1994, May). The agile eye: a high-performance three-degree-of-freedom camera-orienting device. In Robotics and Automation, 1994. Proceedings, 1994 IEEE International Conference on (pp. 781-786). IEEE.

Gosselin, C. M., Pierre, E. S., & Gagne, M. (1996). On the development of the agile eye. IEEE Robotics & Automation Magazine, 3(4), 29-37.

Gosselin, C. (2008). Gravity compensation, static balancing and dynamic balancing of parallel mechanisms. In *Smart Devices and Machines for Advanced Manufacturing* (pp. 27-48). Springer, London.

Hamlin, G. J., & Sanderson, A. C. (1994). A novel concentric multi-link spherical joint with parallel robotics applications. In Robotics and Automation, 1994. Proceedings, IEEE International Conference on (1267-1272) IEEE. May.

Herder, J. (2001). Energy-free Systems. Theory, conception, and design of statically balanced spring mechanisms (Doctoral Dissertation), Delft University of Technology, Netherlands.

Huang, J., Ouyang, P. R., Cheng, L., & Zhang, W. J. (2010). A Hybrid Approach to Force Balancing of Robotic Mechanisms. In Proceedings of the ASME 2010 International Mechanical Engineering Congress & Exposition (IMECE 2010) (pp. 735-744). January.

Innocenti, C., & Parenti-Castelli, V. (1993). Echelon form solution of direct kinematics for the general fully-parallel spherical wrist. *Mechanism and Machine Theory*, *28*(4), 553-561.

Jonker, J. B. (2007). Dynamics of machines: A finite element approach.

Kochev, I. S. (1992). Active balancing of the frame shaking moment in high speed planar machines. Mechanism and Machine Theory, 27(1), 53-58.

Lowen, G. G., Tepper, F. R., & Berkof, R. S. (1983). Balancing of linkages—an update. Mechanism and Machine Theory, 18(3), 213-220.

Nahon, M. A., & Angeles, J. (1989, May). Force optimization in redundantly-actuated closed kinematic chains. In Robotics and Automation, 1989. Proceedings, 1989 IEEE International Conference on (pp. 951-956). IEEE.

Ouyang, P. R. (2002). Force Balancing Design and Trajectory Tracking Control of Real-time Controllable Mechanisms, Master Thesis, University of Saskatchewan.

Ouyang, P. R., Zhang, W. J., & Wu, F. X. (2002). Nonlinear PD control for trajectory tracking with consideration of the design for control methodology. In Robotics and Automation, 2002. Proceedings. ICRA'02. IEEE International Conference on (Vol. 4, pp. 4126-4131). IEEE.

Ouyang, P. R., & Zhang, W. J. (2005). Force balancing of robotic mechanisms based on adjustment of kinematic parameters. Journal of Mechanical Design, 127(3), 433-440.

Ouyang, P. R., Zhang, W. J., & Huang, J. (2016). Synthesizing of Parallel Robots Using Adjusting Kinematic Parameters Method. In Dynamic Balancing of Mechanisms and Synthesizing of Parallel Robots (pp. 143-172). Springer International Publishing.

Polyanin, A. D., & Manzhirov, A. V. (2006). Handbook of mathematics for engineers and scientists. CRC Press.

Spiegel, M. R., & Liu, J. (1999). *Schaum's mathematical handbook of formulas and tables* (Vol. 1000). New York: McGraw-Hill.

Sun, Z., Zhang, B., Huang, J., & Zhang, W. J. (2010). On a mechatronics approach to balancing of robotic mechanisms: redundant servo motor. In Proceedings of International Conference on Advanced Mechatronics (ICAM2010) (pp. 4-6).

Sun, Z., Zhang, B., Cheng, L., & Zhang, W. J. (2011). Application of the redundant servomotor approach to design of path generator with dynamic performance improvement. Mechanism and Machine Theory, 46(11), 1784-1795.

Talbourdet, G. L., & Shepler, P. R. (1941). Mathematical solution of 4-bar linkages—IV, balancing of linkages. Machine Design, 13, 73-77.

Tepper, F.R., & Lowen, G. G., (1972). General theorems concerning full force balancing of planar linkages by internal mass redistribution. Journal of Engineering for Industry. 94B (3), 789-796.

User's, M. G. O. T. (2012). Guide (2012). MATLAB Global Optimization Toolbox User's Guide.

Wang, J., & Gosselin, C. M. (1999). Static balancing of spatial three-degree-of-freedom parallel mechanisms. *Mechanism and Machine Theory*, *34*(3), 437-452.

Wang, Z. H. (2000). Mechatronic design to real-time controllable mechanical systems: force balancing and trajectory tracking. M. Sc. thesis, University of Saskatchewan.

Wijk, V., & Herder, J. L. (2008, April). Dynamic balancing of mechanisms by using an actively driven counter-rotary counter-mass for low mass and low inertia. In Proceedings of the Second International Workshop on Fundamental Issues and Future Research Directions for Parallel Mechanisms and Manipulators, Montpellier (pp. 241-251).

Wijk, V. (2008). Towards low mass and low inertia dynamic balancing of mechanisms (MSc. thesis. TU Delft).

Wijk, V. (2014). Methodology for analysis and synthesis of inherently force and moment-balanced mechanisms-theory and applications (Doctoral Dissertation), University of Twente, Netherlands.

Wikipedia contributors. (2019, July 1). Denavit–Hartenberg parameters. In Wikipedia, The Free Encyclopedia. Retrieved 03:10, July 28, 2019, from https://en.wikipedia.org/w/index.php?title=Denavit%E2%80%93Hartenberg_parameters&oldid=904298170

Wu, Y., & Gosselin, C. (2005). Design of reactionless 3-DOF and 6-DOF parallel manipulators using parallelepiped mechanisms. IEEE Transactions on Robotics, 21(5), 821-833.

Zhang, W. J. (1994). An integrated environment for CAD/CAM of mechanical systems (Doctoral Dissertation), Delft University of Technology, Netherlands.

Zhang, W. J., Ouyang, P.R., Gupta, M.M., Sun, Z.H. (2010). A novel hybridization design principle for intelligent mechatronics systems. ICAM 2010, Japan.

Zhang, W.J., Ouyang, P.R., Sun, Z.H., (2010). A novel hybridization design principle for intelligent mechatronics systems, Proceedings of International Conference on Advanced Mechatronics (ICAM2010), 2010, Osaka, Japan, October 4-6.

Zhang, L., Jin, Z. L., & Li, S. Z. (2014). Kinematics analysis and design of a novel spherical orthogonal 3-RRR parallel mechanism. *J. Chem. Pharm. Res*, *6*(7), 2470-2476.

Appendix A. LIV Technique or Method

Linearly independent vectors (LIV) method was proposed by Berkof & Lowen (1969) for force-balancing a four and six-bar planar linkage. The four-bar linkage is shown in Figure A1. The force balancing principle is based on the total center of mass (COM) of the mechanism is made stationary. The force balance conditions are derived by writing the position vectors of the mechanism and its links and the kinematic closed-loop relation of the mechanism. By equating the time dependent terms to zero, the condition equations are formed. The equations of time-dependent term are condition equations. The shaking forces are balanced by adding CWs on links i.e. by mass redistribution. In this method all the joints of the mechanism contain revolute joints only (Tepper & Lowen, 1972).

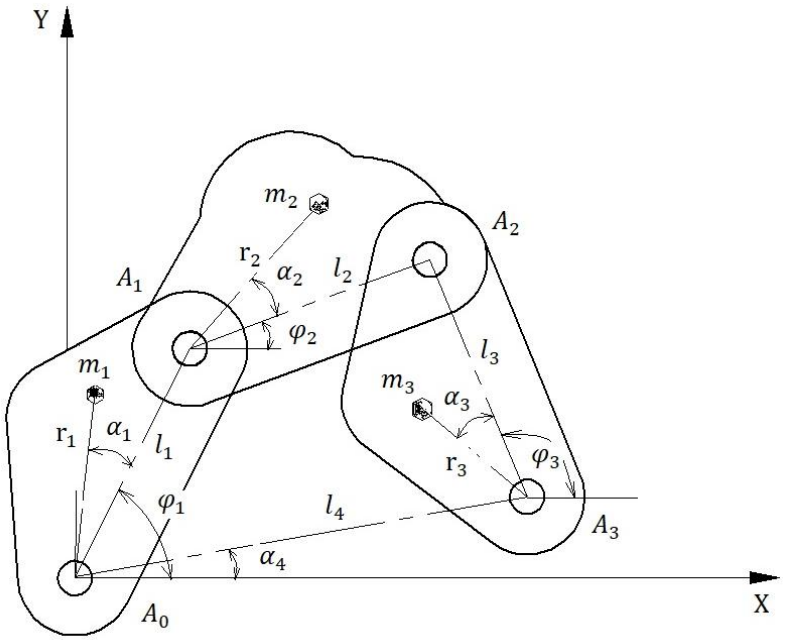

Figure A-1. Mechanism with four links and arbitrary COM locations.

The equation for a mechanism's COM by the position vector rv is:

$$\boldsymbol{r_v} = \frac{1}{M}\sum_{i=1}^{3} m_i \boldsymbol{r_i} \qquad \text{(A-1)}$$

where mi is the mass of link i, ri is the position vector of COM of link i, and M is the total mass of the mechanism.

The position vectors for the individual links can be written as

$$\boldsymbol{r_1} = r_1 e^{i(\varphi_1+\alpha_1)} \quad \text{(A-2)}$$

$$\boldsymbol{r_2} = l_1 e^{i\varphi_1} + r_2 e^{i(\varphi_2+\alpha_2)} \quad \text{(A-3)}$$

$$\boldsymbol{r_3} = l_4 e^{i\varphi_4} + r_3 e^{i(\varphi_3+\alpha_3)} \quad \text{(A-4)}$$

The kinematic closed-loop equation using unit vectors $e^{i\varphi_1}$, $e^{i\varphi_2}$, $e^{i\varphi_3}$ and $e^{i\varphi_4}$ for the four-bar link is written as:

$$l_1 e^{i\varphi_1} + l_2 e^{i\varphi_2} - l_3 e^{i\varphi_3} - l_4 e^{i\varphi_4} = 0 \quad \text{(A-5)}$$

From equation (A-5), substituting for $e^{i\varphi_2}$ in equation A-1 and making the time dependent terms i.e. $e^{i\varphi_1}$ and $e^{i\varphi_3}$ equal to zero, we have

$$\boldsymbol{r_v} = \frac{1}{M}(m_3 l_2 + m_2 r_2 e^{i\propto_2})\frac{l_4}{l_2} e^{i\alpha_4} \quad \text{(A-6)}$$

$$m_1 r_1 e^{i\alpha_1} + m_2 l_1 - m_2 \frac{l_1}{l_2} r_2 e^{i\alpha_2} = 0 \quad \text{(A-7)}$$

$$m_3 r_3 e^{i\alpha_3} + m_2 \frac{l_3}{l_2} r_2 e^{i\alpha_2} = 0 \quad \text{(A-8)}$$

Equation A-6 shows that the total COM of the mechanism is made stationary. Equations A-7 and A-8 are two force balance condition equations derived for the four-bar closed loop linkage. For the six-bar linkage, three equations are derived as the condition equations. Using the force balance condition equations on a four-bar linkage, two of its links are modified while the configurations of the other two links remain unchanged. Of the two, one is moving link while the other is the mechanism's base. On a six-bar linkage, three of its links must be modified using CW.

Appendix B. Spherical Link Length and Its Chord

Let s_1 be the spherical length of link-i, b_1 is its chord length; r is its radius and β_1 be the link angle (Chiang, 1988; Polyanin & Manzhirov, 2006).

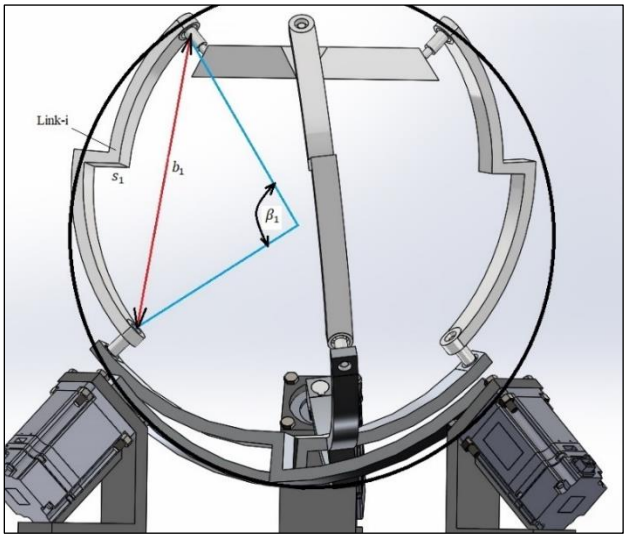

Figure A-2. Spherical link length, its chord and radius.

From the above figure, the length of the arc is given by:

$$\boldsymbol{s}_1 = r\boldsymbol{\beta}_1 \qquad \text{(A-9)}$$

Where $\boldsymbol{\beta}_1$ is in radians and the lengths are in similar units.

From the figure, we can also write

$$\sin\left(\frac{\boldsymbol{\beta}_1}{2}\right) = \frac{\left(\frac{b_1}{2}\right)}{r} \qquad \text{(A-10)}$$

From equations (A-1) & (A-2), substituting for r in equation A-1

$$b_1 = \boldsymbol{s}_1 \frac{\sin\left(\frac{\boldsymbol{\beta}_1}{2}\right)}{\left(\frac{\boldsymbol{\beta}_1}{2}\right)} \qquad \text{(A-11)}$$

Equation A-3 shows the relationship between the spherical length of the link in terms of its chord and radius.

Appendix C. Denavit-Hartenberg (D-H) notation

Mechanism's link i is denoted kinematically using D-H method (Craig, 2005) that describes the four parameters as shown in figure C-1. The geometrical parameters of the general link are:

$\mathbf{a_i}$ = mutual perpendicular distance from axis(i) to axis(i+1) i.e. link length

$\boldsymbol{\alpha_i}$ = link twist from axis(i) to axis(i+1)

$\mathbf{d_i}$ = link offset from axis a(i-1) to axis a(i) along axis Z_i

$\boldsymbol{\Theta_i}$ = joint angle from axis(i-1) to axis(i)

$\mathbf{a_i}$ and $\boldsymbol{\alpha_i}$ describes the link while $\mathbf{d_i}$ and $\boldsymbol{\Theta_i}$ describes the link's relation to its adjoining link.

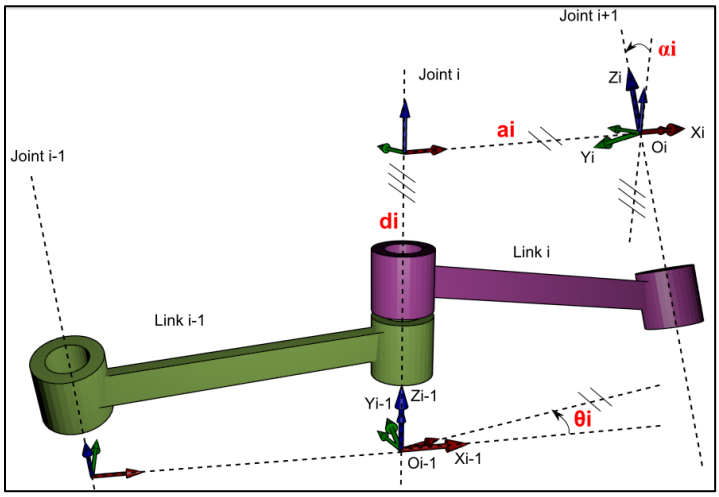

Figure C-1. D-H notation (Wikipedia, 2019).

Appendix D. Force Balancing Program for SPACAR/MATLAB

D.1. *.dat file representing unbalanced data at low speed

```
HINGE 1 1 2      0 1 0
BEAM 4 3 2 4 5   0 1 0
HINGE 2 5 6      0 1 0
BEAM 5 4 6 7 8   0 1 0
HINGE 3 8 9      1 0 1
BEAM 6 7 9 10 11 0 1 0
BEAM 7 10 11 12 13 0 1 0
HINGE 8 13 14 1 0 1
BEAM 9 12 14 15 16 0 1 0
HINGE 10 16 17 0 1 0
BEAM 11 15 17 18 19 0 1 0
HINGE 12 19 20 0 1 0
BEAM 13 10 11 21 22 0 1 0
HINGE 14 22 23 1 0 1
BEAM 15 21 23 24 25 0 1 0
HINGE 16 25 26 0 1 0
BEAM 17 24 26 27 28 0 1 0
HINGE 18 28 29 0 1 0

X 3   0.0     0.1621 -0.0643
X 4  -0.0168 -0.1493 -0.0371
X 7   0.0    -0.1095  0.2025
X 10  0.0     0.0     0.2055
X 12  0.0948  0.0548  0.2025
X 15  0.1298  0.0749 -0.0371
X 18 -0.1403 -0.0811 -0.0643
X 21 -0.0948  0.0548  0.2025
X 24 -0.1298  0.0749 -0.0371
X 27  0.1403 -0.0811 -0.0643

FIX 1
FIX 3
INPUTX 10 1
INPUTX 10 2
INPUTX 10 3
RLSE 1 1
RLSE 2 1
RLSE 3 1

END
HALT
```

```
XM 3 1.25
XM 20 1.25
XM 29 1.25
EM 4 2.05
EM 5 1.99
EM 6 1.72
EM 7 1.72
EM 9 1.99
EM 11 2.05
EM 13 1.72
EM 15 1.99
EM 17 2.05

END
HALT

TRAJECT 1
TRANS 10 0.0 0.0 0.202
TRTIME 0.05 100
TRAJECT 2
TRANS 10 0.0002 -0.0001 0.2016
TRVMAX 10 0.1
TRFRONT 10 0.0
TRM 10 0.015
TRTIME 0.2 400
TRAJECT 3
TRANS 10 0.0002 0.0 0.2016
TRVMAX 10 0.1
TRFRONT 10 0.0
TRM 10 0.015
TRTIME 0.2 400
TRAJECT 4
TRANS 10 -0.0001 0.0 0.2014
TRVMAX 10 0.1
TRFRONT 10 0.0
TRM 10 0.015
TRTIME 0.2 400
TRAJECT 5
TRANS 10 0.0 0.0 0.2020
TRTIME 0.05 100

NOMS 1 1 1
NOMS 2 2 1
NOMS 3 3 1
NOMS 4 8 1
NOMS 5 10 1
```

```
NOMS 6 12 1
NOMS 7 14 1
NOMS 8 16 1
NOMS 9 18 1

REFE 1 1 1
REFE 2 2 1
REFE 3 3 1
REFE 4 8 1
REFE 5 10 1
REFE 6 12 1
REFE 7 14 1
REFE 8 16 1
REFE 9 18 1
REFEP 10 1 1
REFEP 11 2 1
REFEP 12 3 1
REFEP 13 8 1
REFEP 14 10 1
REFEP 15 12 1
REFEP 16 14 1
REFEP 17 16 1
REFEP 18 18 1
REFEDP 19 1 1
REFEDP 20 2 1
REFEDP 21 3 1
REFEDP 22 8 1
REFEDP 23 10 1
REFEDP 24 12 1
REFEDP 25 14 1
REFEDP 26 16 1
REFEDP 27 18 1
REFX 28 10 1
REFX 29 10 2
REFX 30 10 3
REFX 31 10 1
REFX 32 10 2
REFX 33 10 3

END
END

VISUALIZATION
BEAMVIS 0.01 0.01
HINGEVIS 1 0.01 0.03
HINGEVIS 2 0.01 0.03
```

```
HINGEVIS 3 0.01 0.03
LIGHT 1
TRANSPARENCY 0.6
TRAJECT 1
TRAJECTNODE 10
```

D.2. *.dat file representing AKP-balanced data at low speed

```
HINGE 1 1 2      0 1 0
BEAM 4 3 2 4 5   0 1 0
HINGE 2 5 6      0 1 0
BEAM 5 4 6 7 8   0 1 0
HINGE 3 8 9      1 0 1
BEAM 6 7 9 10 11 0 1 0
BEAM 7 10 11 12 13 0 1 0
HINGE 8 13 14 1 0 1
BEAM 9 12 14 15 16 0 1 0
HINGE 10 16 17 0 1 0
BEAM 11 15 17 18 19 0 1 0
HINGE 12 19 20 0 1 0
BEAM 13 10 11 21 22 0 1 0
HINGE 14 22 23 1 0 1
BEAM 15 21 23 24 25 0 1 0
HINGE 16 25 26 0 1 0
BEAM 17 24 26 27 28 0 1 0
HINGE 18 28 29 0 1 0

X 3 0.000 0.1621 -0.0643
X 4 -0.0318 -0.0492 -0.0211
X 7 0.0537 -0.0359 0.2007
X 10 0.0 0.0 0.2007
X 12 0.0043 0.0645 0.2007
X 15 0.0585 -0.0029 -0.0121
X 18 -0.1404 -0.0809 -0.0643
X 21 -0.0579 -0.0285 0.2007
X 24 -0.0267 0.0521 -0.0211
X 27 0.1404 -0.0811 -0.0643
FIX 1
FIX 3
INPUTX 10 1
INPUTX 10 2
INPUTX 10 3
RLSE 1 1
RLSE 2 1
RLSE 3 1

END
```

```
HALT

XM 3 1.25
XM 20 1.25
XM 29 1.25
EM 4 2.05
EM 5 3.93
EM 6 1.72
EM 7 1.72
EM 9 3.93
EM 11 2.05
EM 13 1.72
EM 15 3.93
EM 17 2.05

END
HALT

TRAJECT 1
TRANS 10 0.0 0.0 0.2007
TRTIME 0.05 100
TRAJECT 2
TRANS 10 0.0002 -0.0001 0.2005
TRVMAX 10 0.1
TRFRONT 10 0.0
TRM 10 0.015
TRTIME 0.2 400
TRAJECT 3
TRANS 10 0.0002 0.0 0.2005
TRVMAX 10 0.1
TRFRONT 10 0.0
TRM 10 0.015
TRTIME 0.2 400
TRAJECT 4
TRANS 10 -0.0001 0.0 0.2003
TRVMAX 10 0.1
TRFRONT 10 0.0
TRM 10 0.015
TRTIME 0.2 400
TRAJECT 5
TRANS 10 0.0 0.0 0.2007
TRTIME 0.05 100

NOMS 1 1 1
NOMS 2 2 1
NOMS 3 3 1
```

```
NOMS 4 8 1
NOMS 5 10 1
NOMS 6 12 1
NOMS 7 14 1
NOMS 8 16 1
NOMS 9 18 1

REFE 1 1 1
REFE 2 2 1
REFE 3 3 1
REFE 4 8 1
REFE 5 10 1
REFE 6 12 1
REFE 7 14 1
REFE 8 16 1
REFE 9 18 1
REFEP 10 1 1
REFEP 11 2 1
REFEP 12 3 1
REFEP 13 8 1
REFEP 14 10 1
REFEP 15 12 1
REFEP 16 14 1
REFEP 17 16 1
REFEP 18 18 1
REFEDP 19 1 1
REFEDP 20 2 1
REFEDP 21 3 1
REFEDP 22 8 1
REFEDP 23 10 1
REFEDP 24 12 1
REFEDP 25 14 1
REFEDP 26 16 1
REFEDP 27 18 1
REFX 28 10 1
REFX 29 10 2
REFX 30 10 3
REFX 31 10 1
REFX 32 10 2
REFX 33 10 3

END
END

VISUALIZATION
BEAMVIS 0.01 0.01
```

```
HINGEVIS 1 0.01 0.03
HINGEVIS 2 0.01 0.03
HINGEVIS 3 0.01 0.03
LIGHT 1
TRANSPARENCY 0.6
TRAJECT 1
TRAJECTNODE 10
```

D.3. *.dat file representing unbalanced SPR data at high speed

```
HINGE 1 1 2      0 1 0
BEAM 4 3 2 4 5   0 1 0
HINGE 2 5 6      0 1 0
BEAM 5 4 6 7 8   0 1 0
HINGE 3 8 9      1 0 1
BEAM 6 7 9 10 11 0 1 0
BEAM 7 10 11 12 13 0 1 0
HINGE 8 13 14 1 0 1
BEAM 9 12 14 15 16 0 1 0
HINGE 10 16 17 0 1 0
BEAM 11 15 17 18 19 0 1 0
HINGE 12 19 20 0 1 0
BEAM 13 10 11 21 22 0 1 0
HINGE 14 22 23 1 0 1
BEAM 15 21 23 24 25 0 1 0
HINGE 16 25 26 0 1 0
BEAM 17 24 26 27 28 0 1 0
HINGE 18 28 29 0 1 0

X 3   0.0     0.1621 -0.0643
X 4  -0.0168 -0.1493 -0.0371
X 7   0.0    -0.1095  0.2025
X 10  0.0     0.0     0.2055
X 12  0.0948  0.0548  0.2025
X 15  0.1298  0.0749 -0.0371
X 18 -0.1403 -0.0811 -0.0643
X 21 -0.0948  0.0548  0.2025
X 24 -0.1298  0.0749 -0.0371
X 27  0.1403 -0.0811 -0.0643

FIX 1
FIX 3
INPUTX 10 1
INPUTX 10 2
INPUTX 10 3
RLSE 1 1
RLSE 2 1
```

```
RLSE 3 1

END
HALT

XM 3 1.25
XM 20 1.25
XM 29 1.25
EM 4 2.05
EM 5 1.99
EM 6 1.72
EM 7 1.72
EM 9 1.99
EM 11 2.05
EM 13 1.72
EM 15 1.99
EM 17 2.05

END
HALT

TRAJECT 1
TRANS 10 0.0 0.0 0.202
TRTIME 0.05 100
TRAJECT 2
TRANS 10 0.0002 -0.0001 0.2016
TRVMAX 10 0.03
TRFRONT 10 0.0
TRM 10 0.015
TRTIME 0.2 400
TRAJECT 3
TRANS 10 0.0002 0.0 0.2016
TRVMAX 10 0.03
TRFRONT 10 0.0
TRM 10 0.015
TRTIME 0.2 400
TRAJECT 4
TRANS 10 -0.0001 0.0 0.2014
TRVMAX 10 0.03
TRFRONT 10 0.0
TRM 10 0.015
TRTIME 0.2 400
TRAJECT 5
TRANS 10 0.0 0.0 0.2020
TRTIME 0.05 100
```

```
NOMS 1 1 1
NOMS 2 2 1
NOMS 3 3 1
NOMS 4 8 1
NOMS 5 10 1
NOMS 6 12 1
NOMS 7 14 1
NOMS 8 16 1
NOMS 9 18 1

REFE 1 1 1
REFE 2 2 1
REFE 3 3 1
REFE 4 8 1
REFE 5 10 1
REFE 6 12 1
REFE 7 14 1
REFE 8 16 1
REFE 9 18 1
REFEP 10 1 1
REFEP 11 2 1
REFEP 12 3 1
REFEP 13 8 1
REFEP 14 10 1
REFEP 15 12 1
REFEP 16 14 1
REFEP 17 16 1
REFEP 18 18 1
REFEDP 19 1 1
REFEDP 20 2 1
REFEDP 21 3 1
REFEDP 22 8 1
REFEDP 23 10 1
REFEDP 24 12 1
REFEDP 25 14 1
REFEDP 26 16 1
REFEDP 27 18 1
REFX 28 10 1
REFX 29 10 2
REFX 30 10 3
REFX 31 10 1
REFX 32 10 2
REFX 33 10 3

END
END
```

VISUALIZATION
BEAMVIS 0.01 0.01
HINGEVIS 1 0.01 0.03
HINGEVIS 2 0.01 0.03
HINGEVIS 3 0.01 0.03
LIGHT 1
TRANSPARENCY 0.6
TRAJECT 1
TRAJECTNODE 10

D.4. *.dat file representing AKP-balanced data at high speed

HINGE 1 1 2 0 1 0
BEAM 4 3 2 4 5 0 1 0
HINGE 2 5 6 0 1 0
BEAM 5 4 6 7 8 0 1 0
HINGE 3 8 9 1 0 1
BEAM 6 7 9 10 11 0 1 0
BEAM 7 10 11 12 13 0 1 0
HINGE 8 13 14 1 0 1
BEAM 9 12 14 15 16 0 1 0
HINGE 10 16 17 0 1 0
BEAM 11 15 17 18 19 0 1 0
HINGE 12 19 20 0 1 0
BEAM 13 10 11 21 22 0 1 0
HINGE 14 22 23 1 0 1
BEAM 15 21 23 24 25 0 1 0
HINGE 16 25 26 0 1 0
BEAM 17 24 26 27 28 0 1 0
HINGE 18 28 29 0 1 0

X 3 0.000 0.1621 -0.0643
X 4 -0.0318 -0.0492 -0.0211
X 7 0.0537 -0.0359 0.2007
X 10 0.0 0.0 0.2007
X 12 0.0043 0.0645 0.2007
X 15 0.0585 -0.0029 -0.0121
X 18 -0.1404 -0.0809 -0.0643
X 21 -0.0579 -0.0285 0.2007
X 24 -0.0267 0.0521 -0.0211
X 27 0.1404 -0.0811 -0.0643

FIX 1
FIX 3
INPUTX 10 1
INPUTX 10 2

```
INPUTX 10 3
RLSE 1 1
RLSE 2 1
RLSE 3 1

END
HALT

XM 3 1.25
XM 20 1.25
XM 29 1.25
EM 4 2.05
EM 5 3.93
EM 6 1.72
EM 7 1.72
EM 9 3.93
EM 11 2.05
EM 13 1.72
EM 15 3.93
EM 17 2.05

END
HALT

TRAJECT 1
TRANS 10 0.0 0.0 0.2007
TRTIME 0.05 100
TRAJECT 2
TRANS 10 0.0002 -0.0001 0.2005
TRVMAX 10 0.03
TRFRONT 10 0.0
TRM 10 0.015
TRTIME 0.2 400
TRAJECT 3
TRANS 10 0.0002 0.0 0.2005
TRVMAX 10 0.03
TRFRONT 10 0.0
TRM 10 0.015
TRTIME 0.2 400
TRAJECT 4
TRANS 10 -0.0001 0.0 0.2003
TRVMAX 10 0.03
TRFRONT 10 0.0
TRM 10 0.015
TRTIME 0.2 400
TRAJECT 5
```

```
TRANS 10 0.0 0.0 0.2007
TRTIME 0.05 100

NOMS 1 1 1
NOMS 2 2 1
NOMS 3 3 1
NOMS 4 8 1
NOMS 5 10 1
NOMS 6 12 1
NOMS 7 14 1
NOMS 8 16 1
NOMS 9 18 1

REFE 1 1 1
REFE 2 2 1
REFE 3 3 1
REFE 4 8 1
REFE 5 10 1
REFE 6 12 1
REFE 7 14 1
REFE 8 16 1
REFE 9 18 1
REFEP 10 1 1
REFEP 11 2 1
REFEP 12 3 1
REFEP 13 8 1
REFEP 14 10 1
REFEP 15 12 1
REFEP 16 14 1
REFEP 17 16 1
REFEP 18 18 1
REFEDP 19 1 1
REFEDP 20 2 1
REFEDP 21 3 1
REFEDP 22 8 1
REFEDP 23 10 1
REFEDP 24 12 1
REFEDP 25 14 1
REFEDP 26 16 1
REFEDP 27 18 1
REFX 28 10 1
REFX 29 10 2
REFX 30 10 3
REFX 31 10 1
REFX 32 10 2
REFX 33 10 3
```

```
END
END

VISUALIZATION
BEAMVIS 0.01 0.01
HINGEVIS 1 0.01 0.03
HINGEVIS 2 0.01 0.03
HINGEVIS 3 0.01 0.03
LIGHT 1
TRANSPARENCY 0.6
TRAJECT 1
TRAJECTNODE 10
```

Appendix E. Dynamic Balancing Program for SPACAR/MATLAB

E.1. *.dat file representing balanced SPR using CW-AKP at low speed

```
HINGE 1 1 2      0 1 0
BEAM 4 3 2 4 5   0 1 0
HINGE 2 5 6      0 1 0
BEAM 5 4 6 7 8   0 1 0
HINGE 3 8 9      1 0 1
BEAM 6 7 9 10 11 0 1 0
BEAM 7 10 11 12 13 0 1 0
HINGE 8 13 14 1 0 1
BEAM 9 12 14 15 16 0 1 0
HINGE 10 16 17 0 1 0
BEAM 11 15 17 18 19 0 1 0
HINGE 12 19 20 0 1 0
BEAM 13 10 11 21 22 0 1 0
HINGE 14 22 23 1 0 1
BEAM 15 21 23 24 25 0 1 0
HINGE 16 25 26 0 1 0
BEAM 17 24 26 27 28 0 1 0
HINGE 18 28 29 0 1 0
BEAM 19 3 2 30 31 0 1 0
HINGE 20 31 32 0 -1 0
BEAM 21 18 19 33 34 0 1 0
HINGE 22 34 35 0 -1 0
BEAM 23 27 28 36 37 0 1 0
HINGE 24 37 38 0 -1 0

X 3 0.000 0.1621 -0.0643
X 4 -0.0521 -0.1498 -0.0376
X 7 0.0087 -0.1095 0.0905
X 10 0.0 0.0 0.0905
X 12 0.0948 0.0548 0.0905
X 15 0.1298 0.0749 -0.0376
X 18 -0.1404 -0.0809 -0.0643
X 21 -0.0948 0.0548 0.0905
X 24 -0.1298 0.0749 -0.0376
X 27 0.1404 -0.0811 -0.0643
X 30 0.0002 0.1621 -0.0235
X 33 -0.1404 -0.0809 -0.0235
X 36 0.1404 -0.0811 -0.0235

FIX 1
FIX 3
INPUTX 10 1
```

```
INPUTX 10 2
INPUTX 10 3
RLSE 1 1
RLSE 2 1
RLSE 3 1

END
HALT

XM 3 0.5294
XM 20 0.5294
XM 29 0.5294
EM 4 0.69
EM 5 3.93
EM 6 1.72
EM 7 1.72
EM 9 3.93
EM 11 0.69
EM 13 1.72
EM 15 3.93
EM 17 0.69

END
HALT

TRAJECT 1
TRANS 10 0.0 0.0 0.0905
TRTIME 0.05 100
TRAJECT 2
TRANS 10 0.0002 -0.0001 0.0903
TRVMAX 10 0.1
TRFRONT 10 0.0
TRM 10 0.015
TRTIME 0.2 400
TRAJECT 3
TRANS 10 0.0002 0.0 0.0903
TRVMAX 10 0.1
TRFRONT 10 0.0
TRM 10 0.015
TRTIME 0.2 400
TRAJECT 4
TRANS 10 -0.0001 0.0 0.0901
TRVMAX 10 0.1
TRFRONT 10 0.0
TRM 10 0.015
TRTIME 0.2 400
```

TRAJECT 5
TRANS 10 0.0 0.0 0.0905
TRTIME 0.05 100

NOMS 1 1 1
NOMS 2 2 1
NOMS 3 3 1
NOMS 4 8 1
NOMS 5 10 1
NOMS 6 12 1
NOMS 7 14 1
NOMS 8 16 1
NOMS 9 18 1

REFE 1 1 1
REFE 2 2 1
REFE 3 3 1
REFE 4 8 1
REFE 5 10 1
REFE 6 12 1
REFE 7 14 1
REFE 8 16 1
REFE 9 18 1
REFEP 10 1 1
REFEP 11 2 1
REFEP 12 3 1
REFEP 13 8 1
REFEP 14 10 1
REFEP 15 12 1
REFEP 16 14 1
REFEP 17 16 1
REFEP 18 18 1
REFEDP 19 1 1
REFEDP 20 2 1
REFEDP 21 3 1
REFEDP 22 8 1
REFEDP 23 10 1
REFEDP 24 12 1
REFEDP 25 14 1
REFEDP 26 16 1
REFEDP 27 18 1
REFX 28 10 1
REFX 29 10 2
REFX 30 10 3
REFX 31 10 1
REFX 32 10 2

```
REFX 33 10 3

END
END

VISUALIZATION
BEAMVIS 0.01 0.01
HINGEVIS 1 0.01 0.03
HINGEVIS 2 0.01 0.03
HINGEVIS 3 0.01 0.03
LIGHT 1
TRANSPARENCY 0.6
TRAJECT 1
TRAJECTNODE 10
```

E.2. *.dat file representing optimized SPR using CW-AKP at high speed

With respect to *.dat file at low speed, the dynamic data of traject function as described below will be replaced for high speed *.dat file with all other data remaining the same

```
TRAJECT 1
TRANS 10 0.0 0.0 0.0905
TRTIME 0.05 100
TRAJECT 2
TRANS 10 0.0002 -0.0001 0.0903
TRVMAX 10 0.03
TRFRONT 10 0.0
TRM 10 0.015
TRTIME 0.2 400
TRAJECT 3
TRANS 10 0.0002 0.0 0.0903
TRVMAX 10 0.03
TRFRONT 10 0.0
TRM 10 0.015
TRTIME 0.2 400
TRAJECT 4
TRANS 10 -0.0001 0.0 0.0901
TRVMAX 10 0.03
TRFRONT 10 0.0
TRM 10 0.015
TRTIME 0.2 400
TRAJECT 5
TRANS 10 0.0 0.0 0.0905
TRTIME 0.05 100
```

Appendix F. Optimization program using MATLAB toolbox

F.1. smof.m Objective function

```
function fm = smof(x)
fm=0.208*x(1)*x(2)*x(2)+0.234*x(3)*x(3)-0.208*x(1)*x(3)*x(3);
end
```

%x(1)= m_{il}

%x(2)= l_{il}

%x(3)= l_{iu}

F.2. csteq.m Constraint Equations

```
function [c,ceq] = csteq(x)
c=0;
ceq=[0.157*x(1)+1.125*x(2)-x(1)*x(2);x(3)-.243];
end
```

F.3. 'fmincon' Function

```
options=optimoptions('fmincon','Algorithm','SQP','Display','Iter')
Starting Point used = [0.001; 0.002; 0.002]
% Other starting points used for checking for global solution =
                    [0.009; 0.009; 0.009], [0.1; 0.2; 0.2], [0.1; 0.1; 0.1], [0.7; 0.7; 0.7]
[xfinal,fval,exitflag,output]=fmincon(@smof,[0.01;0.02;0.02],[],[],[],[],[],[],@csteq,options)
```

F.4. 'fmincon' Results

Iter	Func-count	Fval	Feasibility	Step Length	Norm of step	First-order optimality
0	4	9.360000e-05	2.230e-01	1.000e+00	0.000e+00	9.277e-03
1	8	1.372635e-02	5.444e-05	1.000e+00	2.240e-01	1.193e-01
2	12	1.357929e-02	1.970e-05	1.000e+00	1.209e-02	1.205e-02
3	16	1.284752e-02	5.169e-04	1.000e+00	6.037e-02	1.191e-02
4	21	9.753581e-03	2.867e-03	1.000e+00	2.883e-01	6.457e-03
5	27	9.307071e-03	6.266e-04	7.000e-01	1.161e-01	9.258e-03

6	31	9.283563e-03	1.028e-05	1.000e+00	6.496e-03	2.431e-04
7	35	9.283922e-03	6.801e-09	1.000e+00	1.261e-04	1.512e-05
8	39	9.283922e-03	1.945e-10	1.000e+00	2.335e-05	4.348e-07

Local minimum found that satisfies the constraints.

Optimization completed because the objective function is non-decreasing in feasible directions, to within the value of the optimality tolerance, and constraints are satisfied to within the value of the constraint tolerance.

<stopping criteria details>

x = 0.4756 -0.1150 0.2430

fval = 0.0093

exitflag = 1

output =

struct with fields:

iterations: 8

funcCount: 39

algorithm: 'sqp'

message: '↲Local minimum found that satisfies the constraints.↲↲Optimization completed because the objective function is non-decreasing in ↲feasible directions, to within the value of the optimality tolerance,↲and constraints are satisfied to within the value of the constraint tolerance.↲↲<stopping criteria details>↲↲Optimization completed: The relative first-order optimality measure, 4.348227e-07,↲is less than options.OptimalityTolerance = 1.000000e-06, and the relative maximum constraint↲violation, 1.945151e-10, is less than options.

ConstraintTolerance = 1.000000e-06.

constrviolation: 1.9452e-10

stepsize: 2.3354e-05

lssteplength: 1

firstorderopt: 4.3482e-07

Appendix G. Optimized SPR Program for SPACAR/MATLAB

G.1. *.dat file representing optimized SPR using CW-AKP at low speed

```
HINGE 1 1 2      0 1 0
BEAM 4 3 2 4 5   0 1 0
HINGE 2 5 6      0 1 0
BEAM 5 4 6 7 8   0 1 0
HINGE 3 8 9      1 0 1
BEAM 6 7 9 10 11 0 1 0
BEAM 7 10 11 12 13 0 1 0
HINGE 8 13 14 1 0 1
BEAM 9 12 14 15 16 0 1 0
HINGE 10 16 17 0 1 0
BEAM 11 15 17 18 19 0 1 0
HINGE 12 19 20 0 1 0
BEAM 13 10 11 21 22 0 1 0
HINGE 14 22 23 1 0 1
BEAM 15 21 23 24 25 0 1 0
HINGE 16 25 26 0 1 0
BEAM 17 24 26 27 28 0 1 0
HINGE 18 28 29 0 1 0
BEAM 19 3 2 30 31 0 1 0
HINGE 20 31 32 0 -1 0
BEAM 21 18 19 33 34 0 1 0
HINGE 22 34 35 0 -1 0
BEAM 23 27 28 36 37 0 1 0
HINGE 24 37 38 0 -1 0

X 3 0.000 0.1621 -0.0643
X 4 -0.0521 -0.1498 -0.0376
X 7 0.0087 -0.1095 0.0905
X 10 0.0 0.0 0.0905
X 12 0.0948 0.0548 0.0905
X 15 0.1298 0.0749 -0.0376
X 18 -0.1404 -0.0809 -0.0643
X 21 -0.0948 0.0548 0.0905
X 24 -0.1298 0.0749 -0.0376
X 27 0.1404 -0.0811 -0.0643
X 30 0.0002 0.1621 -0.0222
X 33 -0.1404 -0.0809 -0.0222
X 36 0.1404 -0.0811 -0.0222

FIX 1
FIX 3
INPUTX 10 1
```

```
INPUTX 10 2
INPUTX 10 3
RLSE 1 1
RLSE 2 1
RLSE 3 1

END
HALT

XM 3 0.3198
XM 20 0.3198
XM 29 0.3198
EM 4 1.24
EM 5 3.93
EM 6 1.72
EM 7 1.72
EM 9 3.93
EM 11 1.24
EM 13 1.72
EM 15 3.93
EM 17 1.24

END
HALT

TRAJECT 1
TRANS 10 0.0 0.0 0.0905
TRTIME 0.05 100
TRAJECT 2
TRANS 10 0.0002 -0.0001 0.0903
TRVMAX 10 0.1
TRFRONT 10 0.0
TRM 10 0.015
TRTIME 0.2 400
TRAJECT 3
TRANS 10 0.0002 0.0 0.0903
TRVMAX 10 0.1
TRFRONT 10 0.0
TRM 10 0.015
TRTIME 0.2 400
TRAJECT 4
TRANS 10 -0.0001 0.0 0.0901
TRVMAX 10 0.1
TRFRONT 10 0.0
TRM 10 0.015
TRTIME 0.2 400
```

```
TRAJECT 5
TRANS 10 0.0 0.0 0.0905
TRTIME 0.05 100

NOMS 1 1 1
NOMS 2 2 1
NOMS 3 3 1
NOMS 4 8 1
NOMS 5 10 1
NOMS 6 12 1
NOMS 7 14 1
NOMS 8 16 1
NOMS 9 18 1

REFE 1 1 1
REFE 2 2 1
REFE 3 3 1
REFE 4 8 1
REFE 5 10 1
REFE 6 12 1
REFE 7 14 1
REFE 8 16 1
REFE 9 18 1
REFEP 10 1 1
REFEP 11 2 1
REFEP 12 3 1
REFEP 13 8 1
REFEP 14 10 1
REFEP 15 12 1
REFEP 16 14 1
REFEP 17 16 1
REFEP 18 18 1
REFEDP 19 1 1
REFEDP 20 2 1
REFEDP 21 3 1
REFEDP 22 8 1
REFEDP 23 10 1
REFEDP 24 12 1
REFEDP 25 14 1
REFEDP 26 16 1
REFEDP 27 18 1
REFX 28 10 1
REFX 29 10 2
REFX 30 10 3
REFX 31 10 1
REFX 32 10 2
```

```
REFX 33 10 3

END
END

VISUALIZATION
BEAMVIS 0.01 0.01
HINGEVIS 1 0.01 0.03
HINGEVIS 2 0.01 0.03
HINGEVIS 3 0.01 0.03
LIGHT 1
TRANSPARENCY 0.6
TRAJECT 1
TRAJECTNODE 10
```

G.2. *.dat file representing optimized SPR using CW-AKP at high speed

With respect to *.dat file at low speed, the dynamic data of traject function as described below will be replaced for high speed *.dat file with all other data remaining the same

```
TRAJECT 1
TRANS 10 0.0 0.0 0.0905
TRTIME 0.05 100
TRAJECT 2
TRANS 10 0.0002 -0.0001 0.0903
TRVMAX 10 0.03
TRFRONT 10 0.0
TRM 10 0.015
TRTIME 0.2 400
TRAJECT 3
TRANS 10 0.0002 0.0 0.0903
TRVMAX 10 0.03
TRFRONT 10 0.0
TRM 10 0.015
TRTIME 0.2 400
TRAJECT 4
TRANS 10 -0.0001 0.0 0.0901
TRVMAX 10 0.03
TRFRONT 10 0.0
TRM 10 0.015
TRTIME 0.2 400
TRAJECT 5
TRANS 10 0.0 0.0 0.0905
TRTIME 0.05 100
```